Pancreatic ß-Cell Identity and Metabolic Consequences following Anti-Inflammatory Therapy in Type 2 Diabetes

Inauguraldissertation

zur

Erlangung der Würde eines Doktors der Philosophie

vorgelegt der

Philosophisch-Naturwissenschaftlichen Fakultät

der Universität Basel

von

Thierry Michael Nordmann

aus Zürich (ZH) und Basel (BS)

Basel, 2016

Originaldokument gespeichert auf dem Dokumentenserver der Universität Basel

edoc.unibas.ch

Genehmigt von der Philosophisch-Naturwissenschaftlichen Fakultät
auf Antrag von

Prof. Dr. Marc Y. Donath
Prof. Dr. Christoph Hess

Basel, den 23.02.2016

Prof. Dr. Jörg Schibler
Dekan der Philosophisch-Naturwissenschaftlichen Fakultät

Abstract

Type 2 diabetes mellitus (T2DM) is a metabolic disorder, characterized by the inability of the insulin secreting β-cells to compensate for insulin resistance. Increasing evidence points towards a role of the immune system in this development. Furthermore, ß-cell dedifferentiation has recently been proposed as a mechanism underlying β-cell failure in T2DM. Therefore we investigated whether cytokines may induce ß-cell dedifferentiation and whether anti-inflammatory drugs, alone or in combination, may improve insulin secretion.

We observed that IL-1ß drives ß-cell dedifferentiation in both human and mouse pancreatic islets. Interestingly, ß-cell identity maintaining transcription factor FoxO1 was downregulated upon IL-1ß exposure. To test the relevance of IL-1ß induced dedifferentiation in vivo, 3 animal models of T2DM were investigated for the presence of ß-cell dedifferentiation and the impact of IL-1ß antagonism. All 3 models showed signs of islet-inflammation and ß-cell dedifferentiation. However, IL-1ß antagonism failed to restore reduced expression of key ß-cell identity markers, while partially improving glycemia. Thus, while IL-1ß triggers dedifferentiation and dysfunction in vitro, glycemic improvement through IL-1ß antagonism appears not to be related to ß-cell redifferentiation in vivo. In addition, while separate treatment of anti-IL-1ß, anti-TNFα and NF-κB suppressing salicylate showed favorable effects on glycemia, our data do not show a meaningful additive effect of IL-1ß inhibition together with TNFα antagonism or with salicylate.

Finally, focusing on the adaptive side of inflammation, we tested whether the physiological, exercise-induced and muscle-derived IL–6 is regulated by the IL–1 system. In a double blind, crossover study in humans, we could show that the beneficial effect of muscle-induced IL–6 is not meaningfully affected by IL–1 antagonism.

Abstract **iii**
List of abbreviations **vii**
Introduction **1**
Insulin and glucose homeostasis 1
Insulin biosynthesis 1
Glucose sensing and insulin secretion in pancreatic ß-cells 1
Peripheral insulin signaling 3
Cellular glucose transporters 5
Insulin resistance 6
Pathophysiology 6
NF-κB inhibition, salsalate and insulin resistance 8
TNFα inhibition and insulin resistance 10
ß-cell failure 10
ß-cell loss 11
ß-cell dedifferentiation 12
ß cell dedifferentiation and glucotoxicity 14
ß-cell dedifferentiation and oxidative stress 14
ß cell dedifferentiation and free fatty acids 15
ß cell dedifferentiation and inflammation 16
ß-cell dysfunction 17
IL-1ß and type 2 diabetes mellitus 17
IL-1ß inhibition in type 2 diabetic patients 20
The physiologic role of IL-1ß 20
IL-6 and type 2 diabetes mellitus 22
Figure legends 23
Figures 24
Aims of the Thesis **26**
Methods **27**
Animal Experiments 27
Mouse islet isolation 27
Human pancreatic islets 28
Glucose tolerance tests 29
Insulin tolerance tests 29
Ex-vivo insulin signaling test 29

Hormone measurements 30
Glucose-induced insulin secretion assay 30
Oxygen consumption assay 30
Immunohistochemical staining 31
RNA extraction and qPCR 31
Western Blot 32
HbA1c 33
Statistical analysis 33
I. The Role of IL-1ß in Pancreatic ß-Cell Dedifferentiation 34
Abstract 34
Introduction 34
Results 36
Type 2 diabetic, human pancreatic islets contain more CD45+ immune cells than non-diabetic subjects 36
In vitro cytokine induced dedifferentiation is most prominently triggered by IL-1ß in mouse and human islets 37
FoxO1 is downregulated in vitro in response to IL-1ß in mouse and human islets 37
In vitro free fatty acid induced dedifferentiation is partially dependent on IL-1ß 38
In vivo IL-1ß antagonism ameliorates diabetic phenotype without affecting ß-cell dedifferentiation 39
Discussion 40
Figure legends 44
Figures 47
II. Combinatorial Anti-Inflammatory Treatment Strategies for Type 2 Diabetes Mellitus 55
Salicylate & IL-1ß antagonism 55
Diet induced obesity / streptozotocin model 55
Diet induced obesity model 57
TNFα inhibition & IL-1ß antagonism 59
Diet induced obesity / streptozotocin model 59
Diet induced obesity model 61
Discussion 62

Figure legends 68
Figures 72
III. Muscle-derived IL-6 is not regulated by IL-1 during exercise 81
Abstract 82
Introduction 83
Materials and Methods 84
Study design 84
Study participants 84
Treatment Assignment and Blinding 84
Study procedure 85
Study endpoints 86
Sample collection and analytic procedure 86
MIN6B1 cell cultures 86
Statistical analysis 87
Results 89
Participant flow 89
Baseline characteristics 89
IL-6 89
IL-8, hs-CRP, MCP-1 89
Glucose 90
Cortisol 90
Creatine kinase 91
Fatigue, processing and emotional tests 91
Biological activity of injected Anakinra 92
Discussion 93
Acknowledgements 95
Figure legends 96
Figures 98
Tables 100
Supporting information 102
Acknowledgments 103
References 104

List of abbreviations

ATP	Adenosine triphosphate
cAMP	cyclic adenosine mono-phosphate
CREB	cAMP response element-binding protein
CRP	C-reactive protein
CRTC2	CREB-regulated transcription coactivator 2
DD	Death domain
ER	Endoplasmatic reticulum
FFA	Free-fatty acids
FLIP	FLICE-like inhibitory protein
FoxO1	Forkhead box protein O1
Gck	Glucokinase
GFßR1	Transforming growth factor receptor 1
GIP	Gastric Inhibiting Protein
GLP-1	Glucagon Like Peptide-1
GLUT	Glucose transporters
GP	Glycoprotein
GSIS	Glucose stimulated insulin secretion
GSK3b	Glycogen synthase kinase 3b
HbA1c	Hemoglobin A1c
HOMA	Homeostasis model assessment
i.v.	Intravenous
IAPP	Islet amyloid polypeptide
IFN	Interferon
IKKß	IkappaB kinase ß
IKKβ	Inhibitor of NF-κB-kinase subunit β
IL	Interleukin
IL-1R1/2	Interleukin-1 receptor 1/2
IL-1Ra	Interleukin-1 receptor antagonist
IL-1RacP	Interleuin-1 receptor accessory protein
ipGTT	Intraperitoneal glucose tolerance test
IR	Insulin receptor
IRAK4	Interleukin-1 receptor-associated kinase 4
IRS	Insulin receptor substrate
ITT	Insulin tolerance test
JAK	Janus kinase
JNK	C-Jun N-terminal kinases
LDL	Low density lipoprotein
MAfA/B	V-Maf Avian Musculoaponeurotic Fibrosarcoma Oncogene Homolog A/B
MAPK	Mitogen associated protein kinase
MAPK	Mitogen-activated protein kinase
MCP-1	Monocyte chemoattractant protein-1

mTORC1/2	Mammalian target of Rapamycin complex 1/2
MyD88	Myeloid differentiation primary response gene 88
NF-κB	Nuclear factor kappa-light-chain-enhancer of activated B cells
Ngn3	Neurogenin 3
NIDDM	Non-insulin dependent diabetes mellitus
NLR	NOD-like receptor
NLRP3	NACHT, LRR and PYD domains-containing protein 3
OC	Prohormone convertase
Oct-4	Octamer-binding transcription factor
oGTT	Oral glucose tolerance test
PAMP	Pathogen-associated molecular patterns
Pax4/6	Paired Box 4/6
PDK-1/2	3-phosphoinositide-dependant protein kinase 1/2
Pdx1	Pancreatic duodenal homebox 1
PI3K	Phosphatidylinositide-3-kinase
PIP_3	Phosphatidylinositol-triphosphate
PP	Pancreatic polypeptide
PPx	Partial pancreatectomy
PRR	Pathogen recognition receptors
PTB	Phosphotyrosine binding
PTP	Protein-tyrosine phosphatase
ROS	Reactive oxygen species
SAA	Serum amyloid 1
SGLT1/2	Sodium-glucose linked transporter
SH2	Src Homology 2
STAT	Signal transducers and activators of transcription
T2DM	Type 2 diabetes mellitus
TAB	Tank binding
TAK1/2	Transforming growth factor activating kinase ½
TGFß	Transforming growth factor ß
TIR	Toll/Interleukin-1 receptor 1
TLR	Toll-like receptor
TNFα	Tumor Necrosis Factor α
TRAF6	Tumor necrosis factor receptor associated factor 6

Introduction

Type 2 diabetes is a metabolic disorder, characterized by the presence of both insulin resistance and pancreatic ß-cell dysfunction.

In the following, I will first review the physiologic role of insulin as well as the consequences and pathogenic mechanisms of insulin resistance, with a focus on the potentially targetable role of TNFα and NF-κB. Next, the literature of pancreatic ß-cell failure in type 2 diabetes will be discussed, focusing on both the physiologic and pathogenic role of IL-1ß. Finally, the association of IL-6 in the pathogenesis of type 2 diabetes will be evaluated.

Insulin and glucose homeostasis

Insulin biosynthesis

Insulin is a 5.8 kDa peptide hormone synthesized and stored in pancreatic ß-cells and secreted in response to rising blood glucose levels. Within vertebrates, the primary protein structure of insulin is highly conserved, emphasizing the importance of this hormone. In fact, it is a key regulator of metabolism and influences energy homeostasis of almost all organs in our body.

Pancreatic ß-cells initially synthesize pre-proinsulin, a 104 amino acids long polypeptide containing an N-terminal signal peptide, that guides it into the endoplasmatic reticulum (ER) where it is cleaved, yielding proinsulin. Proinsulin is further processed, transported to the Golgi where it enters secretory vesicles. Inside these vesicles, proinsulin is yet again cleaved into the active insulin hormone and C-peptide, a connective-peptide formerly connecting the A- and B-chain of proinsulin [1]. Interestingly, also other hormones are stored within these secretory molecules, amylin being the most prominent, due to its potential pathogenic role upon aggregation.

Glucose sensing and insulin secretion in pancreatic ß-cells

The events leading to insulin secretion are coupled to the glucose sensing mechanisms of pancreatic ß-cells. Glucose can enter the highly vascularized pancreatic ß-cells via

specific glucose-transporters (Gluts) located on the cell membrane. There are 14 Gluts currently identified, with Glut2 in rodents and Glut1 in humans being the main ß-cell glucose transporters [2]. However, the debate whether Glut2 is important in human pancreatic ß-cells is ongoing, as other researchers have shown a functional role of Glut2 in human pancreatic-cells [3]. Once glucose has entered the ß-cells, it is phosphorylated by the (relatively) ß-cell specific hexokinase IV ("glucokinase") at its 6-phosphate position, rendering it incapable of leaving the cell again. In contrast to Glut 1 and 2, glucokinase is expressed similarly in both human and rodent ß-cells, and is assumed to be the rate limiting enzyme of glucose utilization [2]. Furthermore, glucokinase is also expressed in hepatocytes, enterocytes and neurons [4, 5]. Two characteristic and distinct properties of glucokinase, compared to other hexokinases, make it the ideal enzyme for ß-cell glucose sensing: 1. Lower affinity (Km=6mmol/l), and 2. Lack of feedback inhibition by its product, 6P-Glucose. Both properties allow the ß-cells to maintain a continuous glucose transport across the cell border at physiological glucose levels.

Following glycolysis, pyruvate is generated and further oxidized within the mitochondria via Acetyl-CoA to produce adenosine triphosphate (ATP). Strikingly, unlike other cells in which pyruvate can also generate ATP through anaerobic glycolysis, ß-cells can only metabolize pyruvate through oxidative phosphorylation due to the lack of lactate dehydrogenase, the enzyme shunting pyruvate into anaerobic glycolysis [1]. With increasing levels of ATP, the ATP-sensitive K^+ channel closes, causing cell depolarization and subsequent opening of voltage-dependent Ca^{2+}-channels and Ca^{2+} influx. Intracellular Ca^{2+} leads to the exocytosis of insulin-containing vesicles, the final step of glucose-induced insulin secretion (Fig. 1). Interestingly, upon food ingestion, insulin is released in a biphasic manner consisting of an immediate but transient peak followed by a second, more sustained secretion pattern over time.

In 1964, the observation was made, that oral glucose uptake induces higher blood-insulin levels than the equivalent intravenous (i.v.) administration, an effect termed incretin effect [6]. Ten years later, hormones called Gastric Inhibiting Protein (GIP) and Glucagon Like Peptide-1 (GLP-1), released after oral nutrient ingestion by entero-endocrine cells, were identified and shown to augment glucose-dependent insulin secretion, explaining the above-described incretin effect [7, 8]. By now, the

classical incretin hormones GLP-1 and GIP became very popular, due to their therapeutic implications in T2DM and obesity as well as their emerging beneficial role following bariatric surgery. In addition, a long observed phenomenon of improved glucose control after exercise seems to be mediated by incretins, since muscle-released interleukin-6 (IL-6) was shown to stimulate GLP-1 secretion from intestinal L-cells and pancreatic α-cells, thereby stimulating insulin secretion in a so-called “entero-endocrine loop” [9].

In addition to glucose and incretins, various other stimuli such as amino acids, fatty acids and even cytokines have been shown to directly or indirectly (via incretins or via the nervous system) augment insulin secretion [10, 11].

Peripheral insulin signaling

Insulin secreted by pancreatic ß-cells is rapidly transported to the peripheral organs, where binding to the insulin receptor (IR) and downstream effects occur. IR is a glycoprotein consisting of 2 extracellular α-subunits and 2 transmembrane ß-subunits. Upon insulin binding to one α-subunit of the receptor heterotertramer (α2ß2), the tyrosine kinase of the intracellular domain of the ß-subunit becomes activated by autophosphorylation. In parallel, the insulin receptor interacts with different substrate adaptors, such as the insulin receptor substrate (IRS) family, through a phosphotyrosine binding (PTB) module that facilitates IRS phosphorylation. As a result, phosphorylation of key tyrosine residues create docking sites for downstream signaling molecules with Src Homology 2 (SH2) domains [12]. Many signaling pathways are activated further downstream, among them both the Ras/mitogen associated protein kinase (MAPK) and phosphatidylinositide-3-kinase (PI3K)/AKT pathway [13]. While the RAS/MAPK mediates the effect of insulin on mitogenesis and cell growth, the activation of PI3K/AKT transmits the effects of insulin on metabolism and cell survival.

The activation of AKT is initiated by the catalytic subunit of the lipid kinase PI3K (p110), phosphorylating phosphatidylinositol (4,5) bisphosphate into phosphatidylinositol-triphosphate (PIP_3), which further activates the 3-phosphoinositide-dependant protein kinase 1 (PDK1). PDK1 then phosphorylates the activating threonine residue 308 of AKT. Activated AKT has a plethora of

downstream targets: i) glycogen synthesis activation (via glycogen synthase kinase 3b (GSK3b) and glycogen synthase), ii) protein synthesis promotion (via mTORC1), iii) glucose uptake (via Glut4 translocation) and iiii) hepatic gluconeogenesis inhibition (via cAMP response element-binding protein (CREB)-regulated transcription coactivator 2 (CRTC2)). However, the most important signaling pathway downstream of AKT, controlling metabolism and survival, is the AKT/FOXO1 pathway. Foxo1, a member of the forkhead/winged helix transcription factors, was first identified as an AKT substrate in insulin signaling [14]. Importantly, when located within the nucleus of insulin sensitive tissues it promotes the pathways required during the fasting state (e.g. gluconeogenesis). Upon insulin signaling, FoxO1 is phosphorylated in an AKT-dependent manner, translocates into the cytoplasm, and is thereby deactivated. Many peripheral effects of insulin are mediated by the inhibition of Foxo1 [15].

Another AKT activating signal is derived through PDK2, a complex molecule consisting of the Rapamycin insensitive, mammalian target of Rapamycin 2 (mTORC2) and Rictor, that phosphorylates the activating serine-residue 473 of AKT.

The main effect following insulin signaling after postprandial secretion is to signal, that high enough energy levels have been reached. As a response, all energy-producing, catabolic processes are reduced, while energy consuming, anabolic processes are intensified. What sounds rather simple is an absolute necessity for life, as all cells would succumb without proper energy supply enabling maintenance of ongoing homeostatic processes. At the same time, it is worth mentioning, that not all cells in our body, react to and depend on insulin. While the insulin-dependent tissues (liver, muscle and adipose tissue) heavily rely on insulin in the regulation of their energy source and metabolic state, the so-called insulin-independent tissues (brain, kidney and red blood cells) are able to control their energy source in the absence of insulin. From an evolutionary perspective very smart: in times of low energy supply, insulin levels are low, shifting the bulk of glucose into insulin-independent and vital organs such as the brain and red blood cells, without which, life would not be possible. At a molecular level, this dependency on insulin is mostly based on the type of glucose transporters expressed on the cell, further described below.

Cellular glucose transporters

The majority of glucose enters the cell either via a family of membranous, energy-independent, bidirectional, diffusion based glucose transporters (protein symbol Glut; gene symbol SLC2A) or via active, sodium-dependent glucose co-transporters (protein symbol SGLT; gene symbol SCL5A) [12]. To date, 14 Glut and 6 SGLT have been identified in humans [12, 16]. Since discussing all glucose transporters would go beyond the scope of this introduction, only Glut1, 2 and 4 will be discussed briefly, as they are essential for further understanding.

Glut1 is the most studied glucose-transporter and ubiquitously expressed in all tissues, making it responsible for basal glucose uptake. Of all tissues, Glut1 has the highest expression levels in the nervous system and erythrocytes, being the only significantly expressed glucose transporter in the latter [17]. It has an extremely high affinity for glucose, with a Km value around 1-3mM resulting in maximal glucose uptake at all physiological glucose concentrations and most importantly, is not acutely regulated by insulin [18].

Glut2 is mainly expressed on (rodent) pancreatic ß-cells, hepatocytes, kidney and the small intestine. In contrast to Glut1, its affinity to glucose is very low, with a Km-value around 17mM, making sure that glucose is transported in a linear manner throughout a wide range of extracellular glucose levels. This is especially important in ß-cells, acting as a sensor of blood glucose.

Glut4, mainly expressed in muscle and adipose tissue, is the most important mediator of insulin-dependent glucose uptake. It is indispensible for overall glucose homeostasis. In contrast to other Gluts, the majority of Glut4 is almost completely excluded from the plasma membrane, stored in a sophisticated vesicular complex within the cytoplasm [19]. Upon insulin signaling, these vesicles move to the plasma membrane resulting in a rapid increase of the transporter number, and thereby inducing glucose uptake and clearance of circulating blood glucose.

Insulin resistance

Pathophysiology

Insulin resistance is defined as the diminished quantitative and qualitative response of a target cell to the normal actions of insulin. It is highly associated with obesity, usually the first step in the pathogenesis of non-overt type 2 diabetes and a fundamental aspect of the metabolic syndrome. With all of the vital functions insulin has, it is conceivable that insulin resistance has major and life-threatening pathogenic consequences.

During insulin resistance, the well-coordinated and regulated metabolic pathways are disturbed. The liver does not stop gluconeogenesis, maintains glycogenolysis and hence further increases glucose production during inadequate high blood glucose levels. The muscle and adipose tissue are not adequately increasing their Glut4-dependent glucose uptake, continue glycogenolysis and remain in their catabolic state. Furthermore, insulin-dependent lipid synthesis and storage in adipose tissue is not initiated, increasing other harmful circulating factors within the blood stream, such as free-fatty acids. From an evolutionary point of view, the body's ability to store nutrient-derived energy for times of starvation is necessary and was crucial for survival. Nowadays, food is omnipresent and food intake has become more pleasure than necessity. In parallel, physical activity is decreasing. As a consequence, evolutionary metabolic strategies in today's society have lead to an obesity epidemic. According to the World Health Organization (WHO), in 2014 more than 1.9 billion adults are overweight, of which 600 million are obese [20].

On a cellular level, advances have been made in understanding the biological equivalents of insulin resistance. The most discussed mechanisms are: i) decreased expression/translation of proteins involved in glucose transport and insulin signaling pathways [21], ii) decreased phosphorylation activity of activating phosphorylation sites within the insulin signaling pathway [22], iii) increased phosphorylation of inhibitory phosphorylation sites within the insulin signaling pathway [23], and iiii) increased expression/translation of proteases cleaving insulin signaling molecules [24]. The consequence of altered signaling is, that the response of the tissue to insulin is diminished, ultimately leading to the loss of glucose homeostasis. In order to compensate for the loss of insulin signaling, the pancreatic ß-cells augment insulin

production and secretion, causing the typical hyperinsulinemic state seen in insulin resistant individuals. However, there is also evidence, that elevated insulin itself causes insulin-resistance. Whether the increasing amount of insulin is cause or consequence of insulin resistance remains controversial [21].

Due to the fact that weight gain and obesity are major risk factors for insulin resistance and T2DM, the focus to unravel the etiology causing both diseases was put on the quality and quantity of food intake. In 1985, Fraze and colleagues showed that both fasting and postprandial free-fatty acids (FFA) were significantly elevated in non-insulin dependent diabetes mellitus (NIDDM), leading to the hypothesis that FFA induce insulin resistance [25], a phenomenon termed lipotoxicity.

In parallel, research also intensified to understand the role of adipose tissue in obesity and insulin resistance. In 1993, Hotamisligil and colleagues showed that the pro-inflammatory cytokine Tumor Necrosis Factor α (TNFα), a cytokine produced within adipose tissue, induced insulin resistance, thereby for the first time creating a link between obesity, insulin resistance and inflammation [26]. The concept of adipose tissue being an active, cytokine and chemokine secreting organ rather than just a passive depot for energy storage was revolutionary and rapidly gained popularity within the research community. To this day, factors secreted from adipose tissue, now termed adipo/cytokines, have been identified far beyond TNFα and include leptin, IL-6, resistin, monocyte chemoattractant protein-1 (MCP-1), serum amyloid 1 (SAA) and many more [27].

Further supporting the concept of obesity-driven inflammation, Weisberg and colleagues showed in 2003 that macrophages infiltrate the adipose tissue during obesity [28]. Strikingly, evidence showing that insulin resistance is an inflammatory condition was already present in 1978, when Micossi and colleagues demonstrated a glucose-lowering effect of salicylates, which were only much later recognized to be potent inhibitors of the nuclear factor kappa-light-chain-enhancer of activated B cells (NF-κB) pathway [29, 30]. Even FFA induced insulin resistance was shown to be partly mediated by inflammation, by inducing the toll-like receptor (TLR) 4 pathway, a process suggested to require the hepatokine Fetuin-A [31, 32]

By now the concept of inflammation-induced insulin resistance is well-accepted and various cells of the innate (macrophages, neutrophils, mast cells) and adaptive (T- and

B-cells) immune system are known to infiltrate the adipose tissue during obesity ultimately leading to a pro-inflammatory environment [33]. The current hypothesis of adipose tissue insulin resistance is obesity driven adipocyte hypertrophy and lipid overload, leading to the secretion of chemotactic factors, such as MCP-1 through the activation of pathogen-associated molecular patterns (PAMPs), endoplasmatic reticulum (ER) stress and/or adipocyte necrosis [34-36]. Immune cells, mainly pro-inflammatory macrophages, are then recruited to the site of action and lead to local and systemic inflammation, characterized by the production of inflammatory cytokines, mainly TNFα, IL-1ß and IL-6, causing insulin resistance in adipocytes [37]. Due to the fact, that cytokine levels are not as high but are longer lasting in comparison to an acute infection, obesity induced inflammation is referred to as low-grade, chronic inflammation. Similar changes also occur in other insulin-sensitive tissues, such as the liver and muscle.

Intracellularly, inflammation induced insulin-resistance is mainly characterized by the activation of c-Jun N-terminal kinases (JNK) and the NF-κB pathway [27]. While JNK leads to insulin-resistance via counter regulatory serine-residue phosphorylation in IRS-1, the transcription factor NF-κB leads to the production of pro-inflammatory cytokines IL-1ß, TNFα and IL-6 causing insulin resistance. TNFα has been shown to cause insulin resistance through several mechanisms, such as phosphorylation of inhibitory serine residue 307 (S307) in IRS-1 and up-regulation of inhibitory protein-tyrosine phosphatase (PTP) 1B [38]. Most importantly, both NF-κB and TNFα inhibition have been shown to improve glucose homeostasis in mice and humans, further discussed below [26, 29, 39].

NF-κB inhibition, salsalate and insulin resistance

Almost 40 years ago, Micossi and colleagues reported a reduction in fasting serum glucose levels after 3 days of high-dose aspirin (10g/d) in diabetic and non-diabetic patients [30]. Since concomitant insulin levels were higher, the glucose lowering effect of aspirin were attributed to an aspirin-induced insulin secretion mechanism. Only 31 years later, in 2001, Shoelson and colleagues demonstrated that salicylates, the active compound of aspirin, improve glycemia in mice by ameliorating insulin resistance. Surprisingly salicylate did so not by prostaglandin inhibition but rather

through the inhibition of IkappaB kinase ß (IKKß) and the subsequent, pro-inflammatory NF-κB pathway inhibition [29]. Since aspirin has several associated adverse events (platelet aggregation inhibition, gastrointestinal bleeding) a different pro-drug called salsalate was used. Salsalate, a dimer of non-acetylated salicylate does not inhibit platelet aggregation or cause increased gastrointestinal bleeding. Due to its anti-inflammatory effects, it was already used for treating arthritic disorders in the 1970s and its safety therefore already assessed [40].

After the initial elucidating study in 2001, many preclinical studies in rodents followed, confirming the potential benefits of salsalate-treatment in type 2 diabetes [41, 42]. Basic research also provided further mechanism, of salsalate induced improvement of glucose homeostasis, such as downregulation of cortisol production, activation of brown-adipose tissue and 5' AMP-activated protein kinase (AMPK) activation, even though the contribution of the latter remains controversial, since salsalate treatment improved glucose homeostasis even in AMPK knockout mice [43-45]. In parallel, clinical trials were conducted. In the initial, proof-of concept study, 20 young, obese and non-diabetic subjects received 4g salsalate (or placebo) per day. After 4 weeks, subjects receiving salsalate had significantly lower glycated hemoglobin levels, improved fasting glucose and similar insulin levels, resulting in an improvement of homeostasis model assessment (HOMA) for insulin resistance [39]. Importantly, C-reactive protein (CRP) levels were also reduced, emphasizing the anti-inflammatory nature of the drug. Further studies followed, providing additional evidence for the beneficial effect on glucose metabolism in non-diabetic and diabetic subjects, a summary of which is described in a recent review by M. Donath [46]. A caveat concerning salsalate treatment remains, as an increase in low density lipoprotein (LDL)-cholesterol levels and urinary albumin secretion have been observed during treatment. In addition, salsalate was prescribed 3 times daily and may cause compliance issues. A meta-analysis in 2013, including 34 randomized controlled trials and 17 self-control studies investigating the role of salicylates in type 2 diabetes, revealed that while all doses reduce glycated hemoglobin, only high doses (>3g/day) resulted in reduced fasting blood glucose, an increase of plasma fasting insulin and less cardiovascular complications [47]. Overall the overwhelming body of evidence clearly shows the potential of salsalate as an anti-inflammatory treatment of insulin resistance and type 2 diabetes.

TNFα inhibition and insulin resistance

After the revolutionary study by Hotamisligil and colleagues in 1993 linking insulin resistance to TNFα and therefore to inflammation, many preclinical studies in rodents followed. Evidence clearly suggests, that TNFα positively correlates with insulin resistance, and in vitro exposure of adipocytes to TNFα show the characteristics of an insulin resistant state [48]. Furthermore, genetic models lacking TNFα or its receptor show a clear improvement in insulin resistance and glucose homeostasis over time [26, 49]. Surprisingly, while chronic pharmacological inhibition of TNFα was shown to reduce the complications of type 2 diabetes, e.g. diabetic nephropathy, literature showing improved glucose homeostasis after long-term pharmacological inhibition of TNFα in type 2 diabetic rodent models is lacking.

In parallel, the role of TNFα in insulin resistance in humans was tested in various clinical studies. The first three clinical trials did not show an effect on insulin sensitivity. However these results must be interpreted cautiously, due to the small study size (n=7) and only short term TNFα antagonism (48 hours or 4 weeks) [50-52]. In 2011, a slightly larger study with 40 obese, non-diabetic subjects, demonstrated a significant decrease in fasting blood glucose. However, fasting insulin levels and HOMA for insulin resistance did not improve in comparison to placebo treatment [53]. On the other hand, large cohort studies of anti-TNFα treated patients suffering from rheumatoid arthritis or psoriasis have provided evidence for improved glycemia in patients also suffering from type 2 diabetes [54, 55]. Nevertheless, the beneficial effect on glycemia could also be the indirect consequence of an improvement in the underlying disease and result from less pain and higher physical activity. In summary, clear results from proper, prospective and randomized, controlled studies as to whether TNFα antagonism directly improves insulin sensitivity are still lacking.

ß-cell failure

While the central role of pancreatic ß-cells was undisputed in T1DM, the dogma until the late 90s concerning T2DM was that insulin resistance is the primary driver of the disease. This schematic thinking persisted until around the turn of the millennium, even though evidence existed much earlier, showing the importance of ß-cell dysfunction in the development of T2DM. In 1986, O'Rahilly and colleagues

discovered a familial type of T2DM in whom ß-cell dysfunction rather than insulin resistance caused the disease [56]. In 1999, the first longitudinal study was published, showing a decline in insulin secretion in Pima Indians (the population with the highest prevalence of T2DM in the world), causing the transition from normoglycemia to a hyperglycemic state [57]. Yet T2DM was still believed to be a disease primarily caused by insulin resistance, and insulin secretion defects were believed to occur only at a later stage. Several major findings were necessary in establishing the central role of pancreatic ß-cells. In 2003, three independent research groups showed that ß-cell mass is reduced in human type 2 diabetic patients, as opposed to an increase of ß-cell mass in non-diabetic, obese patients [58-60]. Later on, in 2007, 5 genome-wide association studies, tried to elucidate the genetic basis of T2DM, a disease believed to be a "genetic nightmare" due to its heterogeneity. Surprisingly, most identified genetic variants affected ß-cell function, insulin secretion and obesity rather than insulin resistance genes [61-64]. Of note, only in 2014, a genetic variant of an insulin resistance gene associated with T2DM was discovered [65]. Finally, an analysis by Tabák and colleagues from the Whitehall II study, a huge prospective cohort study including 10,308 British civil servants aged 35 to 55, revealed that 2 years before diagnosis, ß-cell function starts declining rapidly, correlating with the sudden and dramatic increase in fasting blood glucose levels [66].

By now, the central role of pancreatic ß-cells in the pathogenesis of T2DM is well accepted. We now know, that even though insulin resistance is a heavy burden on glucose metabolism, ß-cells are able to compensate to a certain degree, by producing more insulin and therefore maintaining nearly euglycemic levels. Overt disease however, only occurs when ß-cell dysfunction emerges.

Researchers all around the world are still trying to identify the reasons for the ß-cell decline and dysfunction leading to overt T2DM. Due to didactic reasons I would like to discuss the features of ß-cell loss and ß-cell dysfunction separately, being aware of the fact that these 2 phenomena go hand in hand.

ß-cell loss

As mentioned above, in 2003 several research groups showed that ß-cell mass is reduced in human type 2 diabetic patients [58-60]. This conclusion relies on the

analysis performed by immune-histological insulin staining of formaldehyde preserved and paraffin embedded pancreatic sections. In general, the pancreas is a difficult organ to study histologically, due to its proteolytic enzymes causing rapid tissue degradation upon damage. 2 of the 3 studies used pancreatic tissue, obtained 2-12 hours post-mortem. The third study used pancreatic sections from patients undergoing partial or total pancreatectomy for a variety of reasons such as pancreatic cancer or pancreatitis, clearly a potentially biased setting [60]. In order to make a statement on ß-cell mass, one should know the total volume of the pancreas, data only one of the 3 studies provided. Fortunately, the observation of reduced ß-cell mass was backed up by studies in various type 2 diabetic rodent models [67, 68]. Yet, the real and in-situ dynamics of ß-cell mass from normoglycemia to glucose intolerance and to overt diabetes yet remain to be investigated. The current gold standard of ß-cell mass analysis however, still is histology, which can only be done ex vivo. Hopefully, future research in the field of in vivo, non-invasive imaging techniques will soon give us a clear and better understanding of ß-cell dynamics before, during and after disease manifestation.

What causes the loss of ß-cell mass is still a matter of debate. In the initial human studies, Butler and colleagues showed an increase in apoptosis, while Sakuraba and colleagues proposed a correlation to ß-amyloid deposits and oxidative stress related substances. Hence, until recently, the loss of ß-cell mass reduction was postulated to be mainly due to increased apoptosis and insufficient proliferation. In 2012, Talchai and colleagues proposed a new mechanism called ß-cell dedifferentiation [69].

ß-cell dedifferentiation

In order to understand the concept of dedifferentiated ß-cells, we have to understand how cells differentiate to become ß-cells.

Derived from the endoderm, multipotent progenitor cells divide rapidly to form the epithelial network of the pancreas, giving rise to both the exocrine and endocrine pancreas. Within the endocrine pancreas, cells further differentiate into α (glucagon expressing), ß (insulin producing), δ (somatostatin secreting) and PP (pancreatic polypeptide making) cells. In the following, I will focus on the main transcription factors and signals needed for pancreatic ß-cell development, adapted from a nice

review by Bernardo and colleagues [70]. Early on in development the transcription factor Pdx1 (pancreatic duodenal homebox 1) is important, giving a crucially needed signal for pancreatic development of the endoderm. Within this Pdx1+ population, Ngn3 (Neurogenin 3), Oct-4 (octamer-binding transcription factor 4), Nanog and NeuroD1/ß2 are co-expressed, specifying the endocrine lineage. Within this lineage Nkx6.1 (NK6 Homeobox 1), MafA (V-Maf Avian Musculoaponeurotic Fibrosarcoma Oncogene Homolog A), Pax4 (Paired Box 4) and Pdx1 (in a second wave of expression) among others, push ß-cell formation, while Pax6 (Paired Box 6) and Arx (Aristaless Related Homeobox) expression determine α-cell development. Many of the above mentioned transcription factors are only transiently expressed during development. Fully differentiated ß-cells, lose the TF-expression of Ngn3, Nanog and Oct4, maintain expression of Nkx6.1, MafA and Pdx1 and start expressing FoxO1 as well as other non-TF genes like Ins1/2, Glut2 and glucokinase (Gck).

ß-cell dedifferentiation is a potentially reversible loss of identity and reversion to a more primitive, progenitor-like condition. This loss of identity is characterized by a dysfunctional ß-cell, lacking the expression of genes normally expressed in mature ß-cells such as Ins, Glut2 and Gck among others discussed above and eventually leading to the inability to produce insulin. Since dedifferentiated ß-cells lack insulin staining in histological analysis, the dedifferentiation theory also fits the current dogma of ß-cell loss. However, the reversibility distinguishes dedifferentiation from apoptosis. Proof of reversion into an undifferentiated state was presented in Talchai's original paper, where dedifferentiated ß-cells reverted to progenitor-like cells expressing Ngn3 and other developmental markers. Furthermore, that ß-cell loss can be of transient nature was shown in several human studies and case reports, in which intensive, exogenous insulin therapy lead to an increase of endogenously produced insulin by potentially redifferentiated ß-cells under less stress [71]. This phenomenon was also documented in rodent diabetes models, with histological confirmation of re-differentiated ß-cells [72]. In fact, most mouse models of type 2 diabetes show signs of ß-cell dedifferentiation [73, 74]. The proof for the existence of dedifferentiation in humans however, remains scarce. Only in 2013, Guo and colleagues published the first well-documented evidence for ß-cell dedifferentiation in human T2DM by showing that relative gene expression of the transcription factors MafA, MafB, Pdx1 and Nkx6.1 and key ß-cell genes Insulin, Glut1, Glut2 and GLP-1 receptor were

reduced in human islets in comparison with normal subjects [73]. By Western blotting and immunohistochemistry they also demonstrated a reduction of MafA, MafB, Nkx6.1 and Pdx1 at protein level. Even reversion into a more primitive, progenitor-like cell type was present, with increased expression levels of Oct-4. Interestingly, FoxO1, the transcription factor proposed by Talchai and colleagues as being the key transcription factor maintaining ß-cell identity, was expressed at similar levels in both diabetic and non-diabetic subjects.

As mentioned before, one of the most interesting facts about the theory of dedifferentiation is, that it leads to a reversible "ß-cell loss", rather than a permanent disappearance due to apoptosis. Meaning that by means of redifferentiation, insulin secretion and glycemic control could be restored. Dedifferentiating ß-cells as a mechanism of the apparent ß-cell loss has rapidly gained popularity within the field. Rather than occurring at once, the process of dedifferentiation is a continuum of alterations within the ß-cells (Fig. 2). While the characteristics of a dedifferentiated ß-cell are increasingly understood, the cause leading to dedifferentiation remains to be elucidated and many mechanisms have been proposed, which will be discussed below.

ß cell dedifferentiation and glucotoxicity

In partial pancreatectomized (PPx) rats, glucose levels are elevated and the remaining ß-cells are confronted with the maintenance of glucose homeostasis. Under these circumstances, pancreatic islets were isolated and gene expression showed clear signs of dedifferentiation (lower Ins1/2, Glut2, Gck, MafA, Pdx1 and Nkx6.1 expression) and dysfunction (altered GSIS) [74, 75]. These changes were largely prevented by phlorizin (an SGLT1/2 inhibitor, blood glucose lowering) treatment after PPx, proving that hyperglycemia was responsible for the changes after PPx [74]. There is strong evidence, that high glucose levels are harmful via reactive oxygen species (ROS), causing oxidative stress.

ß-cell dedifferentiation and oxidative stress

Oxidative stress is caused by prolonged or increased exposure of ROS. ROS is a general term for reactive molecules containing oxygen, including hydrogen peroxide

(H_2O_2), superoxide ($\cdot O_2^{-}$) hydroxyl radicals ($\cdot OH$), peroxynitrite ($ONOO^{-}$) and many more. One should remember, that ROS is constantly being produced endogenously as a side product of O_2 involving physiologic processes, such as oxidative phosphorylation, and not necessarily pathogenic. In support, at physiologic levels, ROS has been shown to be an important factor in GSIS, acting as a second messenger [76]. However, in order to keep ROS at physiologic levels, a balance is needed and several enzymes exist that are able to "disarm" ROS, such as superoxide dismutase for superoxide as well as catalase and glutathione peroxidase for hydrogen peroxide. In a pathologic setting, the physiologic role of ROS is overruled by its potential harm. Upon chronic hyperglycemia, the glycolytic capacity of the islets are overwhelmed, causing glucose to be shunted into other pathways, leading to the accumulation of ROS [77]. Probably due to the important physiologic role of ROS in ß-cells, pancreatic islets are amongst the tissues with the lowest levels of anti-oxidant enzymes expression and activity [78, 79]. This means, that pancreatic islets are very susceptible to oxidative stress. Indeed elevated levels of oxidative stress markers have been documented in type 2 diabetic human patients and rodent models [59, 80]. Furthermore, exposure of human and mouse islets to mediators of oxidative stress have led to a dedifferentiated state [73, 81]. In addition, by overexpression of anti-oxidant enzymes in the ß-cells of db/db (leptin-receptor deficient) mice, dedifferentiation of ß-cells and dysfunction was prevented [82]. On the other hand, trials in humans, using dietary supplementation with anti-oxidant factors yielded mixed results and no overall clear effects on ß-cells [83, 84].

ß cell dedifferentiation and free fatty acids

Several studies have shown, that saturated FFA, such as palmitate and stearate are able to downregulate important transcription factors upon chronic exposure of human and rodent ß-cells in vitro [85, 86]. Eguchi and colleagues demonstrated, that FFA induced a dedifferentiation-like effect in vivo in mice, in a TLR4/MyD88 dependent pathway, including macrophage recruitment [87]. The importance of palmitate and TLR4 was further strengthened by the identification of Fetuin-A and its suggested important role in palmitate inducing damage in islets [88]. However, whether palmitate-induced damage is reversible by FFA withdrawal and whether exposed ß-cells convert to a progenitor-like phenotype remain unknown. Also, palmitate at the

concentrations used in vitro, has been shown to induce a strong apoptotic response. In summary, further research is needed as to whether FFA induced ß-cell dysfunction is due to dedifferentiation or permanent ß-cell loss.

ß cell dedifferentiation and inflammation

Already in 1993, Pipeleers and colleagues noticed that IL-1 treatment of purified rat ß-cells caused a massive reduction in insulin synthesis without affecting viability [89]. When culturing these probably dedifferentiated ß-cells for 3 days without the cytokine, synthesis of insulin was restored. In 2000, the same group showed that treating rat ß-cells with IL-1ß for 24 hours resulted in reduced Glut2 and Pdx1 protein levels, along with impaired glucose-induced insulin synthesis [90]. Subsequently, “big-data”, micro-array based gene expression studies were performed, mostly focusing on the effect of combinatorial cytokine stress (IL-1ß+IFNγ +TNFα) in which inflammation induced downregulation of important ß-cell genes were confirmed [91, 92]. Both NF-κB for IL-1ß and STAT-1 for IFNγ were identified as “master regulators” in causing inflammation induced dedifferentiation, previously proposed to occur only in type 1 diabetes [91, 93].

Another family of cytokine suggested to be involved in ß-cell dedifferentiation is transforming growth factor (TGF) ß. In a very thorough and comprehensive in vitro study, Blum and colleagues identified an inhibitor of TGFß receptor 1 (TGFßR1), that was able to restore the mature, ß-cell specific gene expression signature in dedifferentiated ß-cells, occurring either through 7 days of culture, cytokine stress or in vivo dedifferentiation [94]. Of note, the phenomenon of dedifferentiating ß-cell after several days in vitro culture is a known fact and only recently been linked to a pro-inflammatory environment [95]. Blum and colleagues also showed, that even in healthy and fully mature ß-cells, inhibition of TGFßR1 resulted in increased expression of ß-cell specific identity markers clearly highlighting the importance of the TGFß-pathway and ß-cell differentiation. However, pharmacological redifferentiation of ß-cells did not fully restore the impairment of glucose-induced insulin secretion, proving that the capacity to adequately respond to high glucose levels requires more than “just” mature β cell gene expression and marks the difference between ß-cell dedifferentiation and ß-cell dysfunction.

While inflammation induced dedifferentiation has been studied in vitro, the mechanisms and relevance in vivo have never been assessed. Even more, whether anti-inflammatory treatments revert ß-cell dedifferentiation in vivo has so far never been studied.

ß-cell dysfunction

Many mechanism were proposed to cause ß-cell dysfunction, including, glucotoxicity, lipotoxicity, oxidative stress, ER-stress, ß-Amyloid deposits, and cytokine-induced dysfunction. The relative contribution of each one remains unclear and probably all are important under individually different lifestyle and genetic conditions. In 2007, Donath and colleagues were able improve glycemia in type 2 diabetic patients through IL-1 antagonism by improving ß-cell function rather than modulating insulin resistance and for the first time, linking inflammation with ß-cell dysfunction in T2DM [96]. Interestingly, all the above-mentioned underlying mechanisms of ß-cell dysfunction were shown to induce inflammation. By now, an overwhelming body of evidence has accumulated, supporting the role on inflammation in T2DM. The most prominent cytokine in its pathogenesis is IL-1ß.

IL-1ß and type 2 diabetes mellitus

IL-1ß is a 17.5kDa small, pro-inflammatory cytokine, first purified in 1977 by Charles Dinarello. It is the most prominent member of the by now large IL-1 family and is mainly produced by pro-inflammatory macrophages. IL-1ß is a tightly regulated cytokine, controlled at multiple levels, from expression to secretion. Expressed as prohormone pro-IL-1ß, enzymatic cleavage through the protease caspase-1 converts it into the active IL-1ß, after which the cytokine leaves the cell trough a still unknown, unconventional secretion mechanism. In summary, both pro-IL-1ß expression and caspase-1 activation need to be present for IL-1ß to be secreted. The expression of pro-IL-1ß is mainly driven through the NF-κB pathway, but also other pathways result in pro-IL1ß expression. The activation of caspase-1, requires a caspase-1 activating platform, the most prominent being NLRP3 (NACHT, LRR and PYD domains-containing protein 3), a complex of multiple proteins called the

inflammasome. NLRP3 itself belongs to the family of pathogen recognition receptors (PRRs), more specifically to the intra-cellular NOD-like receptors (NLRs) family, and is one of only 5 PRRs known to form an inflammasome. Even though NLRP3 is a receptor, unlike other NLRs, its exact ligands are still unknown. Rather than binding to a specific pathogen-associated molecular pattern such as foreign DNA or RNA, NLRP3 seems to act as a sensor for danger signals, explaining why its activation occurs upon so many different signals, such as particulate compounds, low ATP levels, potassium efflux and ROS.

The IL-1ß signaling pathway has become increasingly complex, and a short summary based on a review from Weber and colleagues is provided [97]. Secreted IL-1ß binds to a target cell via the IL-1 receptor 1 (IL-1R1), consisting of an intracellular TIR (Toll/IL-1R) domain and an extracellular immunoglobulin-like domain. IL-1R1/IL-1 rapidly forms a complex together with IL-1RacP (IL-1 receptor accessory protein), a co-receptor mandatory for triggering downstream signaling. Upon activation, the myeloid differentiation primary response gene 88 (MyD88) signaling cascade is initiated, a highly conserved signaling pathway downstream of many PRRs such as TLRs. The cytosolic TIR domain of IL1-R1 interacts with the TIR domain of MyD88. Further downstream, the death domain (DD) of MyD88 binds to the DD of IRAK4 (IL-1R-associated kinase 4), which further recruits and phosphorylates IRAK1, thereby leading to the formation and activation of the "Myddosome", consisting of MyD88/IRAK4/1. Phosphorylated IRAK1 activates TRAF6 (TNF receptor associated factor 6), forming a 2D-lattice and leads to the activation of a membrane bound kinase complex TAK1 (TGFß activated kinase)/TAB1/2 which then dissociates from the membrane. Activated TAK activates downstream signaling pathways NF-κB (via IκB-kinase β (IKKβ) activation), and MAPK (p38 and c-Jun N-terminal kinase (JNK)), ultimately leading to the production of pro-inflammatory cytokines, particularly IL-ß, IL-6, TNFα and MCP-1. Of note, a second IL-1R2 exists, which binds IL-1ß but lacks the cytosolic signaling components, and acts as a decoy receptor. Together with IL-1 receptor antagonist (IL-1Ra), a competitive ligand binding molecule which does not activate IL-1R1, as well as naturally occurring extracelluary secreted receptor domains (sIL-1R1, sIL-1R2), IL-1R2 provide intrinsic mechanisms for negative IL-1 signaling regulation.

Over the years, many functions of IL-1ß have been reported, such as stimulating chemokine production, inducing cytokine production, ROS formation, causing a rise in body temperature and more. The deleterious role of IL-1ß in pancreatic islets was extensively investigated since the 1990's [89, 91, 98]. However, these experimental in vitro experiments were thought to reproduce inflammatory conditions of type 1 diabetes, mimicking the consequences of lymphocyte infiltrations and pancreatic islet inflammation, explaining why most of these experiments were performed with IL-1ß/IFN-γ cytokine mixtures. The first proof for the role of IL-1ß in pancreatic islets of type 2 diabetic models was in 2002, when Maedler and colleagues were able to show, that hyperglycemia alone was able to induce ß-cell intrinsic IL-1ß secretion and causing ß-cell dysfunction [99]. Furthermore, all other mechanisms proposed to induce ß-cell dysfunction, have since been linked to IL-1ß. FFA binds TLR2 and TLR4 possibly via Fetuin-A, eliciting an NF-κB pathway response in pancreatic islets and macrophages [31, 100]. Chemically induced ER stress in ß-cells, leads to the expression of pro-IL-1ß, the assembly of the NLRP3-inflammasom and hence to an IL-1ß induced ß-cell dysfunction [101]. Intra-islet amyloid deposition, consisting of aggregated islet amyloid polypeptide (IAPP) also activates the inflammasome. The presence of IAPP has been documented since 1901 and due to its increasing accumulation over life, the dogma of "degenerative, type 2 diabetes" was born [102]. IAPP is expressed as a pre-prohormone, and stored in vesicles as pro-IAPP together with pro-insulin. Both pro-hormones are further processed by the same endoproteases called prohormone convertase (PC) 1/2/3, and equimolar amounts of IAPP are released together with insulin upon exocytosis [103]. Furthermore, expression of IAPP and insulin are controlled by similar factors, due to their similarity of promoter elements, explaining why the upreglation of insulin also causes more IAPP production [104]. As other amyloidogenic proteins, human IAPP has a strong tendency to aggregate, which is prevented under physiologic conditions by various mechanisms. Surprisingly, mouse IAPP does not aggregate. With increasing age and highly-associated with type 2 diabetes, human IAPP aggregate, become insoluble and form islet-amyloid deposits, called amylin, initially thought to be the consequence of T2DM. In 2010, Masters and colleagues showed, that IAPP in its different aggregation states, is able to induce mature IL-1ß secretion in macrophages, and therefore linking inflammation with intra-islet amyloid [105]. Furthermore, ß-cell expression of the human, amyloidogenic form of IAPP (hIAPP) in mice, led to an

increase of intra-islet IL-1b. This observation was supported in 2014, as clodronate-induced macrophage depletion led to reduced intra-islet IL-1ß and improved glucose homeostasis in hIAPP transgenic mice [106].

IL-1ß inhibition in type 2 diabetic patients

Even though evidence showing the role of IL-1ß in type 2 diabetes was accumulating, the ultimate proof-of-concept study was published in 2007. Donath and colleagues were able to show that IL-1Ra treatment over 13 weeks resulted in a significant reduction of HbA1c, improved insulin secretion and reduction of systemic inflammatory parameters (leucocytes and CRP) in type 2 diabetic patients [96]. In a follow-up study after cessation of treatment, these changes were sustained 39 weeks later, demonstrating the important role of inflammation in the disease [107]. Since the half-life of IL-1Ra is relatively short, the drug had to be administered subcutaneously and once daily, leading to malcompliance. Therefore pharmaceutical firms have developed humanized, anti-IL-1ß antibodies with a half-life of 3 weeks, allowing for monthly injections. Numerous studies have since then been conducted with both IL-1Ra and anti-IL-1ß antibodies, all showing a beneficial effect on glucose homeostasis, recently summarized in a paper published by M. Donath [46, 108-110]. Furthermore, a recent study has shown that by mounting an immune response against IL-1ß by vaccination, endogenous and neutralizing antibodies can be generated also leading to glycemic improvement and circumventing the necessity of continuous antibody injection [111]. A multi-center RCT is currently ongoing, assessing the effect of IL-1ß inhibition on glucose homeostasis as a secondary endpoint. With first results expected in 2017, we will soon know, whether targeting IL-1ß is a valid alternative to current anti-diabetic treatments on a population wide basis.

The physiologic role of IL-1ß

Strikingly, pancreatic ß-cell expresses the highest levels of IL-1R1 when compared to any other tissue in our body [100]. Keeping the detrimental role of IL-1ß in type 2 diabetes in mind, evolutions distribution of the IL-1R1 receptor is challenging. When critically looking at previous literature on IL-1ß and pancreatic ß-cells, several papers

exist, potentially explaining a possible physiologic role of IL-1ß. As early as 1988, a study revealed that rat pancreatic islets acutely exposed to IL-1ß increased glucose-induced insulin secretion [112]. Surprisingly, when chronically (>6 hours) exposed to IL-1ß, glucose induced insulin secretion was inhibited. This finding was confirmed in 2012, proving that low-dose (<2ng/ml) stimulates, and high dose (>10ng/ml) IL-1ß inhibits glucose induced insulin secretion [113]. As already noted by Paracelsus, "sola dosis facit venenum" (English: the dose makes the poison) and IL-1ß seems to have a physiological, beneficial role when acting acutely and at low doses, but is detrimental in a chronic setting, such as in type 2 diabetes. These findings led to the theory of bimodal effect of IL-1ß on insulin secretion. Another clue came from the fact that anti-IL-1ß treatment in type 2 diabetic patients using gevokizumab, decreased 3-month HbA1c values only at intermediate doses but not at the highest dose [108], although other mechanisms than bimodal action such as pharmacokinetics and immune complex formation may have played a role as well. Speculating that a specific amount of IL-1ß is needed for the above-mentioned increase of glucose-induced insulin secretion, high-dose antagonist treatment may neutralize not only the detrimental, but also beneficial effect of IL-1ß on glucose homeostasis. In fact, the bimodal role of IL-1ß is very similar to the role of ROS in pancreatic ß-cells. As mentioned above, ß-cells hardly express ROS-reducing enzymes with ROS itself having both a beneficial and detrimental role in ß-cell physiology. One may even speculate, that IL-1ß induced ROS may be a mechanism, by which IL-1ß acts on ß-cell function. Indeed, most pathologic features of IL-1ß are prevented by the addition of anti-oxidative treatment. Overall, while the pathological role of IL-1ß has been intensively studied, the physiologic role in pancreatic ß-cells has almost been forgotten and was only recently picked up by my host laboratory.

Besides making an impact on glucose-induced insulin secretion, IL-1ß may also play a role in survival and proliferation of pancreatic ß-cells. Indeed, low concentrations of IL-1ß have been shown to induce ß-cell proliferation in a FAS/FLIP (FLICE-like inhibitory protein) dependent manner, while higher concentrations led to increased apoptosis [114].

IL-6 and type 2 diabetes mellitus

IL-6 is a 26 kDa small cytokine, with both pro- and anti-inflammatory characteristics. It is mainly secreted by immune cells, but is also produced by adipocytes and myocytes. Therefore, it was classified as an adipo/cytokine and myokine, respectively. IL-6 binds to the membrane bound IL-6 receptor (IL-6R), further associating with the membrane glycoprotein (gp) 130, upon which signaling is initiated [115]. Through the activation of IL-6/IL-6R/gp130, downstream tyrosine janus kinases (JAK) are activated, recruit the transcription factor Stat 3, which dimerise and translocate to the nucleus inducing gene expression of various cytokines and chemokines [116].

IL-6 induced inflammatory processes are associated with various diseases, among them rheumatoid arthritis, giant-cell arteritis, systemic lupus erythematodes and type 2 diabetes. While the role and consequences certain cytokines have in the pathogenesis of type 2 diabetes are well understood (e.g. TNFα), others are discussed more controversially. This is especially true for IL-6. Studies showing a deleterious and insulin-resistance inducing role are challenged by others stating an insulin-sensitizing effect of IL-6 [117, 118]. In addition, as mentioned before, IL-6 plays an important role in the entero-endocrine loop, leading to improved glycemic control after exercise. A possible explanation for the dual role of IL-6 is the origin of IL-6. In contrast to muscle-derived IL-6 released upon exercise, inflammatory IL-6 production is increased as a reaction to an NF-κB activating signal, meaning that other inflammatory markers such as IL-1ß and TNFα are co-secreted, creating a inflammatory environment. In addition, peripheral levels of muscle-induced IL-6 during exercise are far lower than levels in adipose tissue during inflammation. Once again, while low level, exercise triggered myocyte-derived IL-6 seems to be beneficial in glucose homeostasis by potentiating glucose-induced insulin secretion, chronic, high-level, immune-cell or adipocyte-derived IL-6 causes insulin resistance and glycemic impairment. Interestingly, IL-1 antagonism has been shown to reduce systemic inflammation markers, such as IL-6 [107]. The regulation of muscle-derived IL-6 however, is not well understood.

Figure legends

Fig. 1. Glucose induced insulin secretion in pancreatic ß-cells.
Source: Diva D De León and Charles A Stanley, Mechanisms of Disease: advances in diagnosis and treatment of hyperinsulinism in neonates.
Nature Clinical Practice Endocrinology & Metabolism (2007) 3, 57-68.
doi:10.1038/ncpendmet0368

Fig. 2. Events leading up to islet β cell dysfunction in T2DM.
Source: Guo et. al, Inactivation of specific β cell transcription factors in type 2 diabetes.
J Clin Invest. 2013;123(8):3305-3316.
doi:10.1172/JCI65390.

Figures

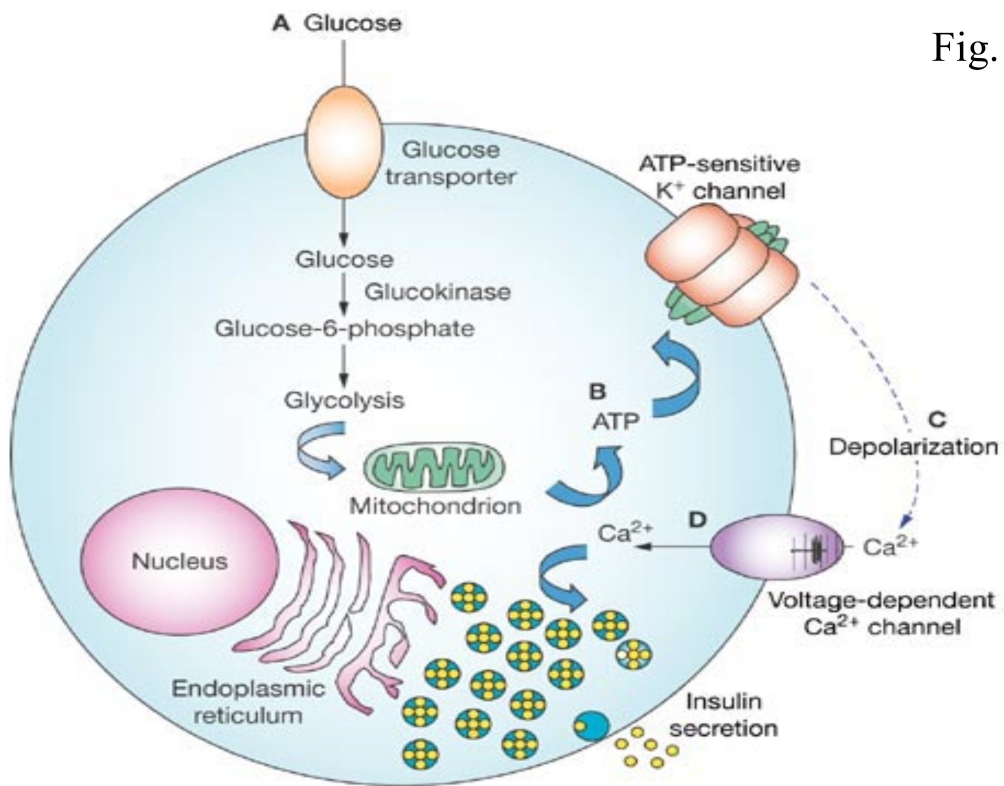

Fig. 1

Fig. 2

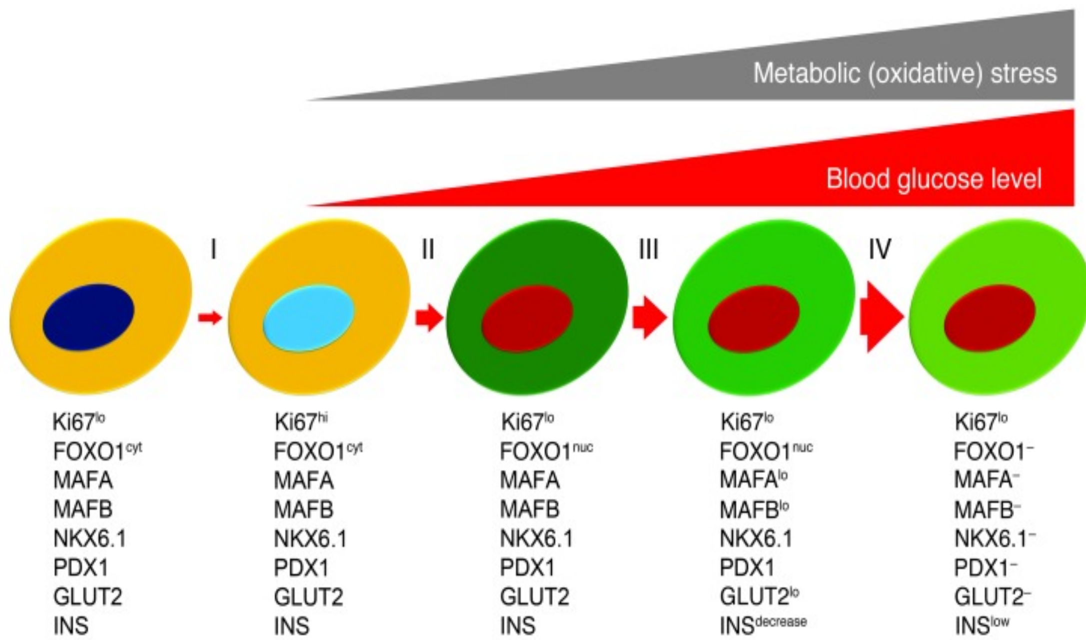

Aims of the Thesis

I. The role of IL-1ß in pancreatic ß-cell dedifferentiation?

II. Does combinatorial anti-inflammatory treatment, targeting both IL-1ß-induced ß-cell dysfunction and NF-κB/TNFα-induced insulin resistance in type 2 diabetic mouse models result in superior glycemic control compared to the corresponding monotherapy?

III. Is exercise-induced, muscle derived IL-6 secretion in humans regulated by IL-1?

Methods

The methods used in the human study (Manuscript III) are described within the corresponding section. All other methods are listed below.

Animal Experiments

Male C57Bl6/N were obtained from Charles River or from in house breeding using Charles River C57BL6/N mice. For the diet induced obesity (DIO) experiments, 4 or 8 week old C57BL6/N mice were fed a high fat diet (D12331; Research Diets, New Brunswick, NJ) for 6 – 17 weeks. For the DIO / Streptozotocin (STZ) experiments, 4 week old C57BL6/N mice were fed a high fat diet, and given a single i.p. injection of STZ (130mg/kg; Sigma Aldrich) at 8 weeks of age. Leptin-receptor deficient db/db mice were obtained from Charles River. The "hIAPP" mouse model corresponds to the F1 generation of male FVB/N-Tg(Ins2-IAPP) RHFSoel/J (008232; Jackson Lab) and female DBA (DBA/2J; 000671; Jackson Lab) mice and littermates were used as wild-type controls. All experiments using the hIAPP mouse, were performed in collaboration with Neurimmune. Experiments antagonizing IL-1ß were performed by i.p. injection of murine anti–IL-1β antibody (or saline) once weekly at a dose of 10mg/kg for the first two weeks, followed by 5mg/kg. The murine anti-IL-1ß antibody has the same specificity as canakinumab [119] and was kindly provided by Novartis (Basel, Switzerland). Sodium salicylate (S3007; Sigma-Aldrich) was incorporated into the high fat diet (D12331 +4g/kg sodium salicylate; Research Diets, New Brunswick, NJ) by the manufacturer. Saline or Etanercept (Enbrel®, Amgen) was administered subcutaneously, 3 times per week at a dose of 20mg/kg unless otherwise specified.

Mouse islet isolation

Animals were euthanized using CO_2. After clamping the bile duct at the proximity of the liver, the pancreas was perfused through the pancreatic duct via the sphincter of Oddi with a collagenase solution (collagenase IV [Worthington] in HBSS +CaCl2 +MgCl2 and 10 mM HEPES with 3.3 µg/ml DNase [Roche, Basel, Switzerland]),

removed and digested in the same solution for 28 min at 37°C. After incubation, the tissue was dissociated by shaking followed by the addition of quenching buffer (HBSS +CaCl2 +MgCl2 with 24 mM HEPES and 0.5% bovine serum albumin) in order to stop the digestion process. Next, centrifugation and sequential filtration through 500 µm and 70 µm cell strainers followed, before islets were handpicked for further processing. They were either lysed for mRNA extraction or cultured on extracellular matrix-coated single- or 24-well plates (Novamed, Israel) in RPMI-1640 (GIBCO) medium containing 11.1 mM glucose, 100 units/ml penicillin, 100 µg/ml streptomycin, 2 mM glutamax, 50 µg/ml gentamycin, 10 µg/ml fungison and 10% FCS (Invitrogen) for 48 hours before starting subsequent experiments. Mouse recombinant IL-1ß, IL-6, TNFα (all RnD) was used at different concentrations as noted within the experiment for 24 hours before further analysis. Palmitate, oleate and stearate were conjugated with low-endotoxin BSA (all from Sigma-Aldrich) at a ration of 6:1, following concentration measurement in the laboratory of the University Hospital of Zuerich, Switzerland. Conjugated free fatty acids or BSA-control were used at 0.25mM or 0.5mM for 24 hours before further analysis. IL-Ra (Anakinra, Kineret, Amgen) treatment was performed by addition of 1 µg/ml 30 minutes prior to other cytokine treatment. Sodium salicylate (SIGMA) was used at different concentrations as noted within the experiment.

Human pancreatic islets

Human islets were isolated in the islet transplantation centers of Lille and Geneva from pancreata of cadaver organ donors in accordance with the local Institutional Ethical Committee. They were obtained via the “islet for research distribution program” through the European Consortium for Islet Transplantation, under the supervision of the Juvenile Diabetes Research Foundation (31-2008-416). Islets were cultured in CMRL-1066 medium containing 5 mmol/l glucose, 100 units/ml penicillin, 100 µg/ml streptomycin, 2 mM glutamax and 10 % FCS (Invitrogen) on extracellular matrix-coated single- or 24-well plates (Novamed, Israel). Human recombinant IL-1ß (RnD) was used at 1ng/ml for 24 hours before further analysis. Palmitate and oleate were conjugated with low-endotoxin BSA (all from Sigma-Aldrich) at a ratio of 6:1, following concentration measurement in the laboratory of

the University Hospital of Zuerich, Switzerland. Conjugated free fatty acids or BSA-control were used at 0.25mM or 0.5mM for 24 hours before further analysis. IL-Ra (Anakinra, Kineret, Amgen) treatment was performed by addition of 1 µg/ml 30 minutes prior to other cytokine treatment.

Glucose tolerance tests

All mice were fasted in the morning for 6h. Thereafter 2 g glucose per kg body weight was injected intraperitoneally (ipGTT) or orally (oGTT) via gavage. Before injection (timepoint 0 min), 15 and 30 min after glucose administration, 25ul of blood was collected from the tail-vain into EDTA-containing eppendorf tubes on ice. At all timepoints (0, 15, 30, 60, 90, 120 min), the average blood glucose level of two measurements was determined using a glucose-meter (Freelite; Abbott Diabetes Care Inc.). Blood containing eppendorf tubes were subsequently centrifuged, supernatant transferred to a 96-well plate on dry-ice and stored at -20°C until further processing.

Insulin tolerance tests

All mice were fasted in the morning for 3h. Thereafter 1 Unit/ml of insulin (Actrapid; Novonordisk) per kg body weight was injected intraperitoneally. At all timepoints (0, 15, 30, 60, 90, 120 min), the average blood glucose level of two measurements was determined using a glucose-meter (Freelite; Abbott Diabetes Care Inc.).

Ex-vivo insulin signaling test

All mice were fasted in the morning for 6h. Thereafter 1 Unit/ml of insulin (Actrapid; Novonordisk) per kg body weight was injected intraperitoneally. At 8 minutes after injection, mice were euthanized using CO_2. Liver tissue was excised 11 minutes after injection, placed in an eppendorf tube and immediately snap-frozen in liquid nitrogen. Samples were stored at -80° until further testing.

Hormone measurements

Insulin concentrations were measured by electro-chemiluminescence, using mouse/rat insulin kits (Mesoscale Discovery). Mouse plasma samples were added undiluted. Samples from glucose-induced insulin secretion assays were diluted 1:101 (insulin content, chronic insulin release) or 1:11 (basal insulin release, stimulated insulin release).

Glucose-induced insulin secretion assay

For in vitro glucose-stimulated insulin secretion experiments, islets were seeded for 48 hours of culture in 24-well plates as described above and supernatant collected to determine chronic insulin release. Islets were then pre-incubated for 30 minutes in modified Krebs-Ringer bicarbonate buffer (KRB; 115 mM NaCl, 4.7 mM KCl, 2.6 mM CaCl2 2H2 O, 1.2 mM KH2 PO4 , 1.2 mM MgSO4 2H2O, 10 mM HEPES, 0.5 % bovine serum albumin, pH 7.4) containing 2.8 mM glucose. The KRB was then replaced by fresh KRB containing 2.8 mM glucose and collected after 1 hour to determine the basal insulin release. This was followed by 1 hour in KRB containing 16.7 mM glucose to determine the stimulated insulin release. Finally, islets were extracted with 0.18 N HCL in 70% ethanol overnight at 4°C for determination of insulin content. The stimulatory index was defined as the ratio of stimulated over basal insulin release per hour.

Oxygen consumption assay

Oxygen consumption rate was determined using the Seahorse extracellular flux analyzer XF24. Islets were plated 24 hours after isolation at a density of 70/well in XF24 islet capture microplates and treated for 1ng/ml IL-1ß (RnD) or 0.04 and 0.4 mg/ml sodium salicylate (SIGMA) for 24 hours, unless otherwise noted. Prior to the assay, cells were incubated in unbuffered RPMI for 3 hours. Then, oxygen consumption rate was measured for 2 minutes. Four basal measurements and 5 measurements each after injection of Glucose (26.8mM), oligomycin (1µM),

carbonilycyanide p-triflouromethoxyphenylhydrazone (FCCP; 2µM) and rotenone (1µM) were acquired (all from Sigma Aldrich).

Immunohistochemical staining

Human paraffin-embedded pancreatic tissue slides was received and performed with the support of the Network for Pancreatic Organ Donors with Diabetes (nPOD), a collaborative type 1 diabetes research project sponsored by JDRF. Organ Procurement Organizations (OPO) partnering with nPOD to provide research resources are listed at http://www.jdrfnpod.org/for-partners/npod-partners/. Tissue slides were simultaneously deparaffinized, rehydrated and stained with mouse anti-human CD45 (1:100, overnight at 4°C; DAKO, XO907) and anti-mouse-bio (1:200, 60min at room temperature, DAKO, M0701) and visualized with DAB (2 min, DAKO, K3467). Pictures of 30-35 islets per section were taken and CD45+ cells within islets counted. Intra-vessel CD45+ cells were not included. Staining, photo acquirement and cell counting was done in a blinded manner and unblinding occurred after counting all samples.

For mouse tissue sections, mouse formalin-fixed pancreata were embedded in paraffin, and cut into 4 µm thin sections. Tissue slides were deparaffinized, rehydrated and stained according to a standard H&E protocol.

RNA extraction and qPCR

RNA of isolated mouse and human islets was extracted with the NucleoSpin RNA II Kit (Machery Nagel, Germany). cDNA was prepared with random hexamers and Superscript II Reverse Transcriptase (Invitrogen). For quantitative PCR, the real time PCR system 7500 (Applied Biosystems) and the following TaqMan (Glut2: Mm00446230_g1, Hs01096908_m1; Gcg: Mm00801714_m1; Ins2: Mm00731595_g1; Pdx1: Mm00435565_m1, Hs00236830_m1; FoxO1: Mm00490671_m1, Hs01054576_m1; KC: Mm04207460_m1, Hs01100741_m1; CD45: Mm01293577_m1; Nkx6.1: Mm00454961_m1; IL-1ß: Mm00434228_m1; TNF: Mm00443258_m1; Oct-4: Mm03053917_g1; Nanog: Mm02019550_s1; IL-6:

Mm00446190_m1; iNOS: Mm00440502_m1; Gck: Mm00439129_m1, Hs01564555_m1; Glut-1: Mm00439129_m1, Hs00892681_m1; all from Applied Biosystems) or SybrGreen (MmGlut2: (F) TCAGAAGACAAGATCACCGGA, (R) GCTGGTGTGACTGTAAGTGGG; MmGck: (F) GCTGGTGTGACTGTAAGTG-GG, (R) GCAACATCTTTACACTGGCCT; MmFoxA2: (F) CCCTACGCCAACA-TGAACTCG, (R) CCCTACGCCAACATGAACTCG; MmFoxO1: (F) GTACG-CCGACCTCATCACCA, (R) TGCTGTCGCCCTTATCCTTG; MmPdx1: (F) CCCCAGTTTACAAGCTCGCT, (R) CTCGGTTCCATTCGGGAAAGG; MmIns2 (F) TGGCTTCTTCTACACACCCAAG, (R) ACAATGCCACGCTTCTGCC; MmActin: (F) GGCTGTATTCCCCTCCATCG, (R) CCAGTTGGTAACAATGCC-ATGT; MmNKX6.1: (F) TCAGGTCAAGGTCTGGTTCC, (R) CGATTTGTGC-TTTTTCAGCA; all from Microsynth) primers were used.

Western Blot

Human or mouse islets were washed on ice with PBS, and frozen tissue was thawed on ice before protein was extracted using a Tris-HCl lysis buffer (containing protease and phosphatase inhibitors) and subsequent centrifugation. Soluble protein concentration was measured with the BCA protein assay kit (Thermo Fisher Scientific) and kept at the desired concentration in a protein sample buffer (NuPage LDS Sample Buffer; Life Tech). After denaturation and addition of anti-reducing agent (Life Tech), 10-50ug of protein per lane was loaded, separated by electrophoresis (NuPage 4.12% Bis-Tris Gel; Life Tech) and wet-transferred onto nitrocellulose membranes. Successful transfer was verified using Ponceau staining. Membranes were blocked for 30 minutes on a shaker at room temperature, with TBS-0.1%Tween containing either 5% dry milk or 3%BSA, followed by overnight incubation with the following antibodies at 4°C: anti-FoxO1 (1:1000, CST #2880), anti-phospho FoxO1 (1:500, Ser-256, CST #9461), anti-pan-AKT (1:1000, CST #4691), anti-phospho AKT (1:1000, Ser 473, CST #9271), anti-ßactin (1:5000, Sigma). Membranes were then washed three times prior to incubation with the corresponding secondary antibodies (1:10000, all from santa-cruz) for 1 hour, at room temperature. After three washing steps, the membrane was visualized using ECL Blotting Substrate for HRP (Bio Rad).

HbA1c

HbA1c (%) was determined in EDTA blood at the Laboratory of the University Hospital of Basel (Tosoh G8 HPLC Analyzer, Somogen Diagnostics).

Statistical analysis

Statistical analysis was performed using GraphPad Prism 6.0 (Graphpad Software Inc., San Diego, CA). Data are presented as mean ± SEM and were analyzed using the two-tailed Mann-Whitney U tests. Differences were considered statistically significant when $P < 0.05$.

I. The Role of IL-1ß in Pancreatic ß-Cell Dedifferentiation

(Manuscript in preparation)

Abstract

Type 2 diabetes is an inflammatory disease caused by dysfunctional ß-cells and reduced ß-cell mass. ß-cell dedifferentiation has recently been proposed as a possible mechanism, implicating that treatment leading to redifferentiation would restore intrinsic glucose homeostasis. Yet the cause of dedifferentiation remains unclear. Here we show that CD45+ immune cells infiltrate human type 2 diabetic pancreatic islets and may release cytokines. Among the cytokines involved in type 2 diabetes associated islet-inflammation, pro-inflammatory IL-1ß most prominently drives ß-cell dedifferentiation in both human and mouse pancreatic islets. Interestingly, ß-cell identity maintaining transcription factor FoxO1 is downregulated upon IL-1ß exposure. Furthermore, IL-1ß causes impairment of glucose-induced and maximal respiratory capacity. To test the relevance of IL-1ß induced dedifferentiation in vivo, 3 animal models of type 2 diabetes were investigated for the presence of ß-cell dedifferentiation and the impact of long term IL-1ß antagonism. All 3 models showed signs of islet-inflammation and ß-cell dedifferentiation, emphasizing their importance in type 2 diabetes. IL-1ß antagonism ameliorated hyperglycemia in DIO/STZ mice and improved glucose-induced insulin secretion in isolated islets of DIO/STZ and db/db mice. Surprisingly, IL-1ß antagonism failed to restore reduced expression of key ß-cell identity markers. Thus, while IL-1ß triggers dedifferentiation and dysfunction in vitro, glycemic improvement through IL-1ß antagonism is not due to ß-cell redifferentiation in vivo.

Introduction

Type 2 diabetes mellitus (T2DM) is a metabolic disorder, characterized by the presence of both insulin resistance and ß-cell dysfunction. By now, the disease has reached an epidemic dimension, affecting more than 350 million people worldwide [120]. Under physiologic conditions glucose values are tightly regulated and initially

occurring insulin resistance is encountered with a compensatory increase in ß-cell insulin production. Overt disease however, only occurs when ß-cell failure emerges [66].

Over the past few years, many pathogenic mechanisms such as glucotoxicity, lipotoxicity, ER-stress and islet associated ß-amyloid have been proposed to trigger ß-cell dysfunction [99, 100, 105, 121]. Unlike insulin resistance, ß-cell dysfunction in T2DM has only recently been linked with inflammation [96]. Interestingly, all pathogenic mechanisms mentioned above, have been shown to elicit an inflammatory response in the context of T2DM, with the activation of innate immunity and subsequent interleukin-1beta (IL-1ß) driven pathways most prominently involved. By now, a causal and deleterious relationship between T2DM and IL-1ß has been established. Accordingly, IL-1ß antagonism in type 2 diabetic humans as well as rodent models is able to reduce the disease burden and improve glucose homeostasis [96, 122].

ß-cell mass is reduced in human type 2 diabetic patients [58-60], contributing to ß-cell dysfunction and overt T2DM. The loss of ß-cell mass reduction was proposed to be mainly due to increased apoptosis and insufficient proliferation [58]. Only recently, Talchai and colleagues proposed a new mechanism termed ß-cell dedifferentiation, with FoxO1 as the master regulator maintaining ß-cell identity [69].

ß-cell dedifferentiation is a potentially reversible loss of identity, characterized by reduced expression of key ß-cell genes, such as Ins2, Glut2, Pdx1 and Nkx6.1, eventually leading to dysfunctional and reduced insulin secretion. Furthermore, dedifferentiated ß-cells can revert into a progenitor-like condition characterized by the expression of important ß-cell development genes such as Oct4 and Nanog. Rather than occurring acutely, the process of dedifferentiation is a continuum of alterations within the ß-cells, explaining both ß-cell dysfunction and ß-cell loss. In contrast to apoptosis, dedifferentiation is a potentially reversible mechanism, implying that by means of redifferentation, glucose homeostasis can be restored [72].

To date the mechanisms causing ß-cell dedifferentiation are not well understood. Both glucotoxicity and oxidative stress have been shown to induce ß-cell dedifferentiation in vitro [69, 73]. Given the importance of IL-1ß driven inflammation in T2DM, we hypothesize, that IL-1ß induced ß-cell stress causes dedifferentiation. Indeed, several

studies have shown, that cytokine stress causes dysfunctional ß-cells characterized by reduced expression of key ß-cell genes and impaired glucose-induced insulin secretion [91, 92]. However, most of these studies were conducted in the context of type 1 diabetes and thus used multiple cytokine mixtures. IL-1ß driven dedifferentiation and redifferentation mediated by IL-1ß antagonism in type 2 diabetes models in vivo have not been assessed.

In this study, we aim to elucidate the role of IL-1ß in ß-cell dedifferentiation both in vitro and in vivo. We report, that IL-1ß is more prominently involved in type 2 diabetes associated islet-inflammation than other cytokines, causes ß-cell dedifferentiation in vitro and is partially responsible for free fatty acid induced ß-cell identity loss. As a consequence, IL-1ß causes impairment of glucose-induced and maximal respiratory capacity. Further, all investigated type 2 diabetes rodent models show signs of ß-cell dedifferentiation, along with elevated levels of inflammation emphasizing the importance of dedifferentiation in type 2 diabetes. Surprisingly, IL-1ß antagonism failed to restore reduced expression of key ß-cell identity markers, in spite of its beneficial effect on glucose homeostasis in vivo and improved glucose-induced insulin secretion in isolated islets.

Results

Type 2 diabetic, human pancreatic islets contain more CD45+ immune cells than non-diabetic subjects

In order to characterize the presence of immune cell infiltration in human type 2 diabetic patients, paraffin embedded pancreatic tissue of 17 type 2 diabetic and 16 control subject was assessed. There were significantly more CD45+ immune cells around (5.68 ± 0.52, 2.72 ± 0.28 cells, respectively; p = < 0.0001; Fig. 1a) and within (4.10 ± 0.70, 1.44 ± 0.24 cells, respectively; p = 0.0003; Fig. 1b) pancreatic islets of type 2 diabetic patients compared to control. Both cohorts were similar in age (T2D: 44.51 ±3.67, ND: 43.52 ± 3.90 years; p = 0.8799; Fig. 1c), while type 2 diabetic subjects had a higher BMI (T2D: 33.08 ± 1.67, ND: 27.44 ± 1.02 kg/m2; p = 0.02; Fig. 1d). HbA1c levels were higher (T2D: 7.683 ± 0.4199, ND: 5.6 ± 0.12 %; p=0.0043; Fig. 1e) and C-peptide levels numerically lower (T2D: 3.89 ± 1.54, ND:

7.34 ± 1.90 ng/ml; p = 0.0988; Fig. 1f) in type 2 diabetic patients compared to control. Mean diabetes duration was 9.75 ± 3.12 years.

In vitro cytokine induced dedifferentiation is most prominently triggered by IL-1ß in mouse and human islets

To determine the quantitative effect of single cytokine exposure, pancreatic islets were treated with IL-1ß, IL-6 or TNFα for 24 hours. Surprisingly, 1 ng/ml IL-1ß induced the most potent suppression on genes important for proper ß-cell function (Fig. 2a) compared to IL-6 and TNFα. Next, we treated mouse islets with various concentrations of IL-1ß, which dose-dependently caused downregulation of important ß-cell genes Ins2, Glut2, Glut2 and Nkx6.1 (Fig. 2b). This was accompanied by the upregulation of ß-cell progenitor markers, such as Oct4 and Nanog and inflammatory markers KC, iNOS and IL-6. To test the relevance of these findings in human tissue, human pancreatic islets were treated with IL-1ß. Indeed, 24-hour treatment of human pancreatic islets caused a decrease in gene expression levels of ß-cell identity markers, such as Glut2 and Pdx1 (Fig. 2c). Interestingly, in contrast to rodent islets, Gck was not downregulated in human islets while Glut1 appeared to be upregulated. Overall, these data suggest IL-1ß induced ß-cell dedifferentiation in mouse and human pancreatic islets.

FoxO1 is downregulated in vitro in response to IL-1ß in mouse and human islets

The transcription factor FoxO1 was recently proposed to be a central regulator of ß-cell identity, with reduced expression of FoxO1 in pancreatic ß-cells leading to loss of ß-cell identity. In order to test whether IL-1ß causes the downregulation of FoxO1, mouse and human islets were treated with 1ng/ml IL-1ß for 24 hours. Truly, upon IL-1ß treatment FoxO1 was reduced on both gene expression level (Fig. 4a) and protein level (Fig. 4b; of note n=1 and needs confirmation) in mouse pancreatic islets. Exposure of human islets revealed a similar picture, with both a reduction on gene expression level (Fig. 4d) and protein level (Fig. 4e). In summary, FoxO1 is downregulated in both human and mice pancreatic islets upon IL-1ß exposure.

In vitro free fatty acid induced dedifferentiation is partially dependent on IL-1ß

Free fatty acids have been shown to lead to a decrease of ß-cell markers in pancreatic islets. To test whether this effect is dependent on IL-1ß we treated mouse islets with 0.25mM stearate, the main free fatty acid in mice, in the presence or absence of 1µg/ml IL-1 receptor antagonist (IL-1Ra). Stearate induced downregulation of important ß-cell genes, such as Glut2, Nkx6.1 and Pdx1, and was partially prevented by IL-Ra treatment (Fig. 4). Furthermore, also the reduction of the transcription FoxO1 upon stearate exposure was prevented by IL-1Ra treatment. These results point to a role of IL-1ß in dedifferentiation induced by FFA in murine pancreatic ß-cells.

IL-1ß reduces glucose-induced and maximal oxygen consumption rate in mouse pancreatic islets in vitro

When treating mouse islets with 1ng/ml of IL-1ß, we noticed a reduction in gene expression levels of glucokinase and uncoupling protein (UCP) 2, two important molecules in glucose oxidation. In order to assess the maximal and glucose-induced mitochondrial respiratory capacity, oxygen consumption rates (OCR) of pancreatic islets after exposure to IL-1ß or saline for 24 hours were measured (Fig. 5a, b). Interestingly, IL-1ß not only reduced the mitochondrial response to glucose (Fig. 5c), but also blunted the overall capacity of mitochondrial respiration within pancreatic islets (5e). The response to the ATP-synthase inhibitor oligomycin (Fig. 5d) and complex-I inhibitor rotenone (Fig. 5f) was similar in both groups.

In contrast, OCR response in human islets (Fig. g, h) was not detectable in response to glucose. No difference in response to 16.7mM glucose (Fig. 5i), an ATP-synthase inhibitor (Fig. 5j), a complex-I inhibitor (Fig. 5k) and overall capacity of mitochondrial respiration (Fig. 5l) was evident between IL-1ß or saline treated islets.

Overall, these data show that IL-1ß induces reduced mitochondrial respiration capacity in pancreatic mouse islets.

In vivo IL-1ß antagonism ameliorates diabetic phenotype without affecting ß-cell dedifferentiation

In order to evaluate whether IL-1ß driven dedifferentiation plays a role in vivo, the presence of dedifferentiation and subsequent effect of IL-1ß antagonism in diet-induced / streptozotocin (DIO-STZ), db/db, and hIAPP-mice, 3 mouse-models of type 2 diabetes, was analyzed.

4-week-old C57BL6/N mice were fed a high fat diet (HFD) and received a single injection of streptozotocin (STZ; 130mg/kg) or sodium-citrate at 8 weeks of age. STZ injection in DIO mice caused mild fasting hyperglycemia (Fig. 6a) but profound glucose intolerance (Fig. 6b), in combination with decreased insulin levels (Fig. 6c) and secretory capacity (Fig. 6d). IL-1ß antagonism improved glucose tolerance (Fig. b) during the first 30 minutes, without reaching overall AUC statistical significance (p=0.0545). No effect on insulin secretion capacity was noticeable (Fig. 6d). Next, gene transcription levels of isolated islets were analyzed. CD45 was slightly increased in STZ/DIO mice (Fig. 6e) and ß-cell identity markers were downregulated (Fig. 6f) as in human disease. Surprisingly, IL-1ß antagonism did not improve gene expression levels of ß-cell identity and inflammatory markers (Fig. 6f). To further characterize ß-cell function, glucose-induced insulin secretion of isolated islets was measured. As expected, STZ caused a reduction in the stimulatory capacity, partially prevented by IL-1ß antagonism (Fig. 6g).

In leptin-receptor deficient db/db mice, random (Fig. 7a) and fasting (Fig. 7b) glucose levels as well as body weight (Fig. 7c) were highly elevated already at 6 weeks of age. Furthermore, blood IL-1ß levels were elevated compared to db/+ mice (not measurable; Fig. 7d). Ex vivo gene expression analysis of isolated islets, revealed reduced ß-cell identity marker (Fig. 7e) and elevated IL-1Ra (Fig. 7f) levels. From age 6 to 16 weeks, db/db mice became increasingly obese (Fig. 7h) and diabetic (Fig. 7g). Treatment with an anti-IL-1ß antibody starting at 6 weeks of age resulted in a significant decrease in fasting blood glucose levels (Fig. 7g), however, this improvement was not reproducible in a second cohort (Fig. 7i) and did not reach significance when pooled ($P = 0.0731$; Fig. 7j), although having numerically lower blood glucose levels than non-antibody treated. Gene expression analysis of isolated

islets after 3 weeks of treatment showed no difference in ß-cell identity markers Glut2 and FoxO1 between treatment groups (Fig. 7k). Interestingly, IL-1ß expression in pancreatic islets did no differ between treatment groups, while IL-1α was significantly upregulated in the antibody treated group only (Fig. 7l). Unexpectedly, glucose-induced insulin secretion of isolated islets treated with anti-IL-1ß was significantly improved compared to non-treated db/db islets (Fig. 7m).

As a third model, a transgenic type 2 diabetes mouse model with ß-cell specific overexpression of human islet amyloid polypeptide (hIAPP) was generated and further investigated. hIAPP and WT mice were treated with anti-IL-1ß starting at 4 weeks of age. hIAPP mice were significantly more glucose intolerant due to lower insulin secretion capacity than control mice at both 6 (Fig. 8a) and 8 weeks (Fig. 8b) of age. However, antibody-treatment did not affect glucose tolerance or insulin secretion (Fig. 8a,b). Examining gene expression levels at 8 weeks of age, all ß-cell identity markers were downregulated in the Tg mouse (Fig. 8c), with a pronounced elevation of CD45 and IL-1ß expression (Fig. 8d) within pancreatic islets. IL-1ß antagonism was not able to revert the downregulation of ß-cell identity markers in the Tg mouse (Fig. 8c). Surprisingly, gene expression levels of several ß-cell identity markers (Glut2, FoxO1, Nkx6.1) were even lower in anti-IL-1ß treated compared to untreated hIAPP mice. On the other hand, IL-1ß antagonism reduced IL-1ß expression significantly and tended to elevate ß-cell identity marker expression in WT mice, but no statistical significance was reached (Fig. 8c,d).

Discussion

Type 2 diabetes mellitus imposes a growing burden on society in terms of morbidity, healthcare costs and overall quality of life. Continuous effort is put into understanding the mechanisms involved in disease manifestation and possible treatment strategies. Rather than permanent loss of function due to apoptosis, dedifferentiating ß-cells offer a potential therapeutic approach, since redifferentiation could restore intrinsic insulin production and glycemic control [72, 73]. The mechanisms involved in ß-cell identity loss however, are not well understood. Given the importance of IL-1ß driven inflammation in the pathogenesis of type 2 diabetes mellitus [96], we hypothesized

that IL-1ß may drive ß-cell dedifferentiation and IL-1ß antagonism may prevent or even reverse this process.

We were able to show that CD45+ immune cells accumulate within and around pancreatic islets of type 2 diabetic, human patients. This emphasizes the importance of immune cell infiltration in type 2 diabetes and histologically confirms recent data acquired by flow cytometer analysis [123]. Pancreatic immune cell infiltration is believed to be the consequence of inflammation-driven chemotaxis, further potentiating local inflammation. To determine the effect of inflammation within pancreatic islets, the influence of essential cytokines involved in type 2 diabetic islet inflammation (IL-1ß, IL-6 and TNFα) were compared. While all cytokines were able to provoke partial downregulation of key ß-cell genes, IL-1ß was most potent. Upon further examination, the effect of IL-1ß was dose-dependent, causing not only downregulation of important ß-cells genes such as Ins2, Glut2 and Pdx1, but also increased expression of markers usually expressed in immature and developing ß-cells (Oct4, Nanog). In addition, we provide the first demonstration that exposure of human pancreatic islets to IL-1ß also causes beta cell dedifferentiation. In parallel, IL-1ß dose-dependently induced inflammatory factors and oxidative stress markers.

The transcription factor FoxO1 was proposed to be a master regulator of ß-cell identity. Strikingly, both FoxO1 gene expression and protein levels were reduced after 24 hour incubation of human and mouse pancreatic islets with IL-1ß. To further test the importance of IL-1ß induced dedifferentiation, pancreatic islets were exposed to FFAs, with or without IL-1Ra. Indeed, the FFA effect was partially prevented by IL-1 inhibition, further supporting the importance of the IL-1 system in various pathogenic mechanism causing ß-cell dedifferentiation.

Observing that several genes downregulated by IL-1ß are crucial for glucose-uptake (Glut2) and metabolism (Gck, Ucp2) we wondered whether this caused alterations in oxidative phosphorylation. Both glucose-induced and maximal respiratory capacity was heavily compromised in IL-1ß treated mouse islets. Surprisingly, these observations were not apparent in human islets, maybe due to preserved glucokinase and upregulated Glut1 expression seen after 24 hours of IL-1ß in human islets, potentially compensating for the loss of Glut2.

To test the relevance of IL-1ß induced dedifferentiation in vivo, 3 animal models of type 2 diabetes were extensively investigated for the presence of ß-cell dedifferentiation and the impact of long term IL-1ß antagonism. Using the combination of diet-induced obesity and streptozotocin, a model resembling human disease was established, showing mild fasting hyperglycemia, pathological glucose tolerance, low-grade inflammation and reduced expression levels of ß-cell genes (Ins2, Glut2, Pdx1 and Nkx6.1). Truly so, 2 weeks of anti-IL-1ß treatment improved glucose tolerance. Furthermore, while in vivo insulin secretion appeared unchanged, isolated islets from anti-IL-1ß treated mice were able to mount a stronger insulin response compared to islets from untreated mice. Despite glycemic improvement, anti-IL-1ß treatment had no impact on gene expression levels of all ß-cell identity markers.

Next, leptin-receptor deficient db/db mice were analyzed. We were able to confirm previous data, showing reduced ß-cell identity markers in db/db as early as 6 weeks of age [124]. The systemically elevated IL-1ß levels and indications for local, pancreatic IL-1 action implied that this model might be suitable to study the effects of IL-1ß on islet dedifferentiation. At the age of 6 weeks when glycemia already deteriorates, IL-1ß antagonism was initiated. Even though mean fasting blood glucose levels were improved in 1 of 2 cohorts, IL-1ß antagonism did not affect expression levels of ß-cell identity genes. Also in this model, isolated pancreatic islets of anti-IL-1ß treated mice responded with a significantly improved insulin response compared to untreated mice.

Finally, a novel genetic model of diabetes expressing hIAPP specifically in ß-cells of the more diabetes prone DBA mouse was used. As observed in the past, the effect of hIAPP overexpression on glycemia and inflammation is strongly dependent on the background, gender and caloric state [106]. Similar to previous studies, our hIAPP mouse shows highly elevated levels of immune cell marker CD45 and IL-1ß mRNA expression. Furthermore, we provide for the first time, a detailed gene expression analysis of ß-cell identity markers in this mouse model. Indeed, in parallel to rapid deterioration of glucose homeostasis, key ß-cell identity markers are downregulated, clearly showing, that dedifferentiation occurs in this mouse model, which most closely resembles human type 2 diabetes. Possibly due to the extreme diabetic phenotype and its rapid deterioration, IL-1ß antagonism failed to improve both glucose homeostasis and ß-cell identity loss.

In summary, we demonstrate that IL-1ß drives pancreatic islet dedifferentiation in vitro in both human and mouse islets. Furthermore, in all 3 tested animal models of type 2 diabetes, low-grade inflammation and signs of dedifferentiation were present, emphasizing their importance in type 2 diabetes mellitus. To our surprise, antagonizing IL-1ß did not affect the expression levels of key ß-cell genes in a dedifferentiated state. Even so, in cases where treatment related glycemic improvement was present.

We can only speculate why this discrepancy between in vitro and in vivo findings exists. One explanation might be the redundancy of inflammatory pathway signaling. IL-1ß is known to induce the NF-kB pathway, the final signaling cascade of many if not most inflammatory signaling pathways of the innate immune system, triggering many pro-inflammatory cytokines. We observed, that not only IL-1ß is able to provoke downregulation of ß-cell identity genes and that IL-1ß antagonism of FFA-treated islets only partially inhibits dedifferentiation. Hence, the redundancy of inflammatory pathways such as Toll like receptor activation [27], IL-6 signaling [9] or TNF-alpha exposure [123], all of which have been shown to occur in pancreatic islets of type 2 diabetic patients, might maintain the inflammatory environment causing ß-cell dedifferentiation, even in the absence of IL-1ß. Thus, while we provide evidence for the further understanding of ß-cell dedifferentiation, a suitable and effective target preventing dedifferentiation or even promoting redifferentiation in vivo remains to be identified. Furthermore, our study reveals that the beneficial role of IL-1ß antagonism in the treatment of type 2 diabetes is not due to ß-cell redifferentiation.

Figure legends

Fig. 1. Type 2 diabetic, human pancreatic islets contain more CD45+ immune cells than non-diabetic subjects

(a) Peri-islet and (b) intra-islet CD45+ immune cell quantification in human pancreatic tissue sections, as well as (c) age, (d) BMI, (e) HbA1c and (f) C-peptide levels of type 2 diabetic (T2D) and non-diabetic (ND) control subjects.
(a-d) n=17, 16 for T2D and ND subjects, respectively. (a-b) n=30-35 islets/section. (e) n=6 each, according to availability. (f) n=16, 14 for T2D and ND subjects, respectively, according to availability. *P < 0.05, **P < 0.01, ***P < 0.001, ****P < 0.0001. Statistical significance (P) was determined using the two-tailed Mann-Whitney U test. All error bars denote s.e.m.

Fig. 2. In vitro cytokine induced dedifferentiation is most prominently triggered by IL-1ß in mouse and human islets
(a) mRNA expression levels in mouse islets after 24 hours of cytokine treatment. (b) mRNA expression levels in mouse islets at various concentrations of 24 hours IL-1ß treatment. (c) mRNA expression levels in human islets after 24 hours IL-1ß treatment.
(a) n=3/group, 1 experiment. (b) n=6/group, 2 experiments. (c) n=10, 3 experiments. *P < 0.05, **P < 0.01, ***P < 0.001, ****P < 0.0001 of treatment group vs. untreated control. Statistical significance (P) was determined using the two-tailed Mann-Whitney U test. All error bars denote s.e.m.

Fig. 3. FoxO1 is downregulated in vitro in response to IL-1ß in mouse and human islets

(a) mRNA expression levels, (b) protein quantification and a representative Western blot of FoxO1 in mouse islets after 24 hours treatment with IL-1ß or saline. (c) mRNA expression levels, (d) protein quantification and a representative Western blot of FoxO1 in human islets after 24 hours treatment with IL-1ß or saline.
(a) n=7-8, 2 experiments; (b) n=1, 1 experiment; (c) n=9, 3 experiments; (d) n=6-7, 3 experiments. *P < 0.05, **P < 0.01, ***P < 0.001, ****P < 0.0001. Statistical significance (P) was determined using the two-tailed Mann-Whitney U test. All error bars denote s.e.m.

Fig. 4. In vitro free fatty acid induced dedifferentiation is partially dependent on IL-1ß

mRNA expression levels in mouse islets after 24 hours treatment with stearate ± IL-1 receptor antagonist (IL-1Ra).
n=14-16 each, 3 experiments. */# P < 0.05, **/##P < 0.01, ***/### P < 0.001, ****/####P < 0.0001 of (*) stearate vs. BSA and (#) stearate/IL-1Ra vs. stearate. Statistical significance (P) was determined using the two-tailed Mann-Whitney U test. All error bars denote s.e.m.

Fig. 5. IL-1ß reduces glucose-induced and maximal oxygen consumption rate in mouse pancreatic islets in vitro

(a) Absolute and (b) baseline-corrected oxygen consumption (OCR) rates of mouse islets, treated for 24 hours with IL-1ß or saline. Mean fold increase of OCR in mouse pancreatic islets upon (c) glucose, (d) oligomycin, (e) FCCP and (f) rotenone compared to baseline, calculated from the data shown in (b).
(g) Absolute and (h) baseline-corrected OCR of human islets, treated for 24 hours with IL-1ß or saline. Mean fold increase of OCR in pancreatic islets upon (i) glucose, (j) oligomycin, (k) FCCP and (l) rotenone compared to baseline, calculated from the data shown in (h).
(a-f) n = 21 wells IL-1ß, 19 wells saline, 3 experiments, 70 islets / well. (g-l) n = 23 wells each, 3 experiments, 70 islets / well. *P < 0.05, **P < 0.01, ***P < 0.001, ****P < 0.0001. Statistical significance (P) was determined using the two-tailed Mann-Whitney U test. All error bars denote s.e.m.

Fig. 6. Antagonizing IL-1ß in vivo, improves glycemia but does not rescue ß-cell dedifferentiation in DIO/STZ mice

(a-g) 4-week-old mice were fed a high fat diet (HFD) followed by a single injection of streptozotocin (STZ) at 8 weeks of age simultaneously beginning treatment with anti-IL-1ß. Fasting (a) blood glucose and (c) insulin levels as well as (b) plasma glucose and (d) insulin levels with corresponding area under the curve following an intraperitoneal glucose injection after 2 weeks of treatment. (e,f) mRNA expression levels in mouse islets 3 weeks after treatment initiation. (g) Fold insulin secretion of ex-vivo glucose-induced insulin secretion in isolated islets after 3 weeks of treatment initiation.

(a-d) n=18-19/group, (e-f) n=20-27/group, (g) n=15/group, 3 experiments. *P < 0.05, **P < 0.01, ***P < 0.001, ****P < 0.0001. Statistical significance (P) was determined using the two-tailed Mann-Whitney U test. All error bars denote s.e.m.

Fig. 7. Antagonizing IL-1ß in vivo, improves islet secretory capacity but does not rescue ß-cell dedifferentiation in db/db mice

(a) Random and (b) fasting blood glucose levels, as well as (c) body weight and (d) serum-IL-1ß levels at 6 weeks of age. (e,f) mRNA expression levels of isolated islets at 6 weeks of age. (g-m) db/+ and db/db mice receiving anti-IL-1ß treatment at 6 weeks of age. (g) Fasting blood glucose levels and (h) weight growth curves of the first of two cohorts. (i) Fasting blood glucose levels of the second cohort. (j) Pooled fasting blood glucose levels of both cohorts. (k,l) ex vivo mRNA expression levels and (m) fold insulin secretion of glucose-induced insulin secretion of isolated islets after 2 weeks of treatment.

(a-c) n=25 and 44 for db+ and db/db, resp., 2 experiments. (d) n=5 each. (e,f) n=7-8/group, 1 experiment, normalized to ß-actin. (g-i) n=7-8 per db/db ± treatment group and n=5 for db/+, 1 experiment. (j) n= 16-18, 2 experiments. (k,l) n=8-9 per db/db ± treatment group, n=4 for db/+, 1 experiment, normalized to ß-actin. (m) n=4-5/group, 1 experiment. *P < 0.05, **P < 0.01, ***P < 0.001, ****P < 0.0001. Statistical significance (P) was determined using the two-tailed Mann-Whitney U test. All error bars denote s.e.m.

Fig. 8. Antagonizing IL-1ß in vivo, does not rescue ß-cell dedifferentiation in hIAPP mice

(a-d) hIAPP-Tg and WT mice, receiving anti-IL-1ß treatment at 4 weeks of age. (a,b) Plasma glucose, insulin levels and corresponding area under the curve following an oral glucose bolus after (a) 2 weeks and (b) 4 weeks of treatment. (c,d) ex vivo mRNA expression levels after 4 weeks of treatment.

(a,b) n=6 per WT cohort, 9-10 per Tg cohort, 2 experiments. (c,d) n=9-14/group, 2 experiments. *P < 0.05, **P < 0.01, ***P < 0.001, ****P < 0.0001. Statistical significance (P) was determined using the two-tailed Mann-Whitney U test. All error bars denote s.e.m.

Figures

Fig. 1

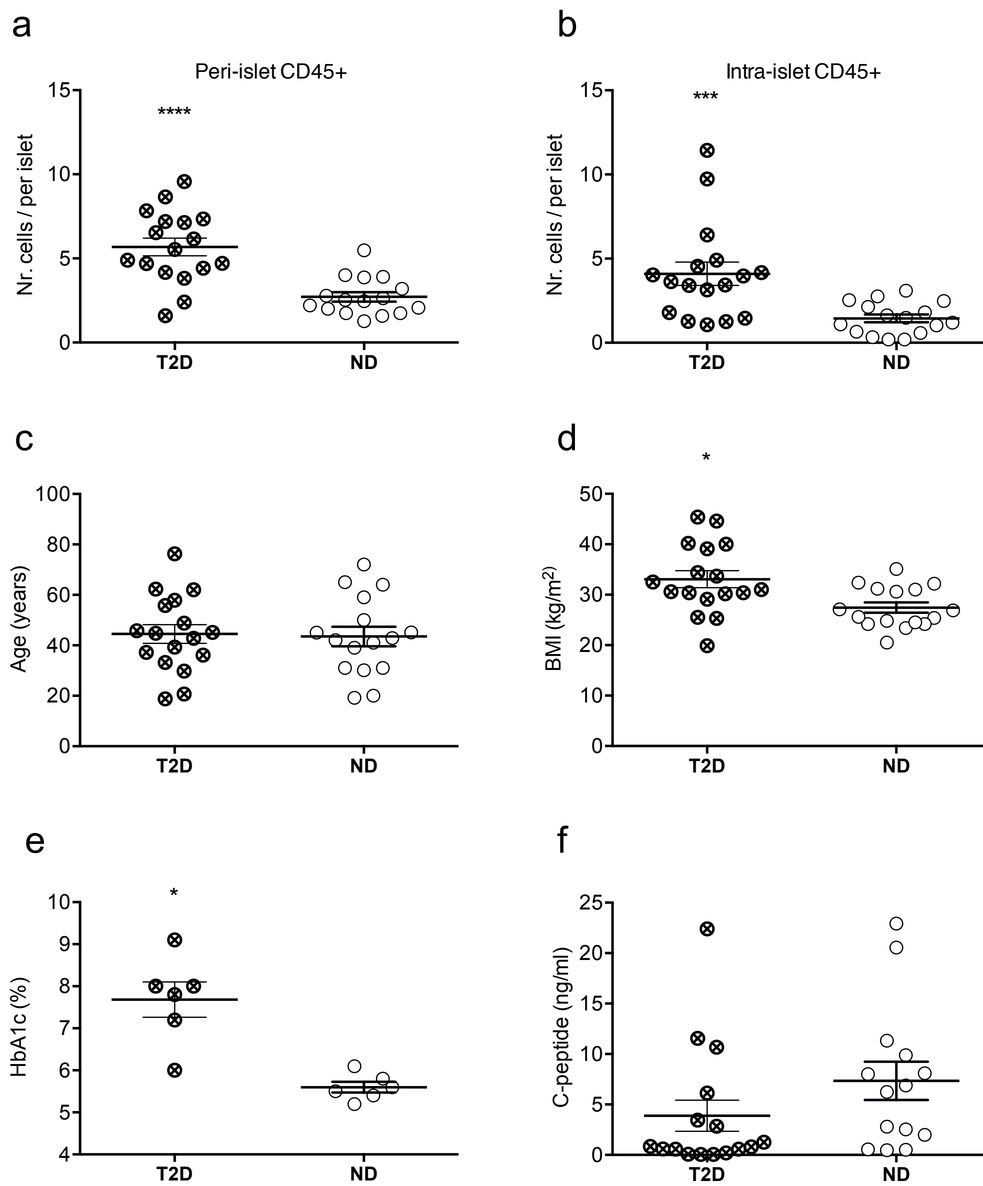

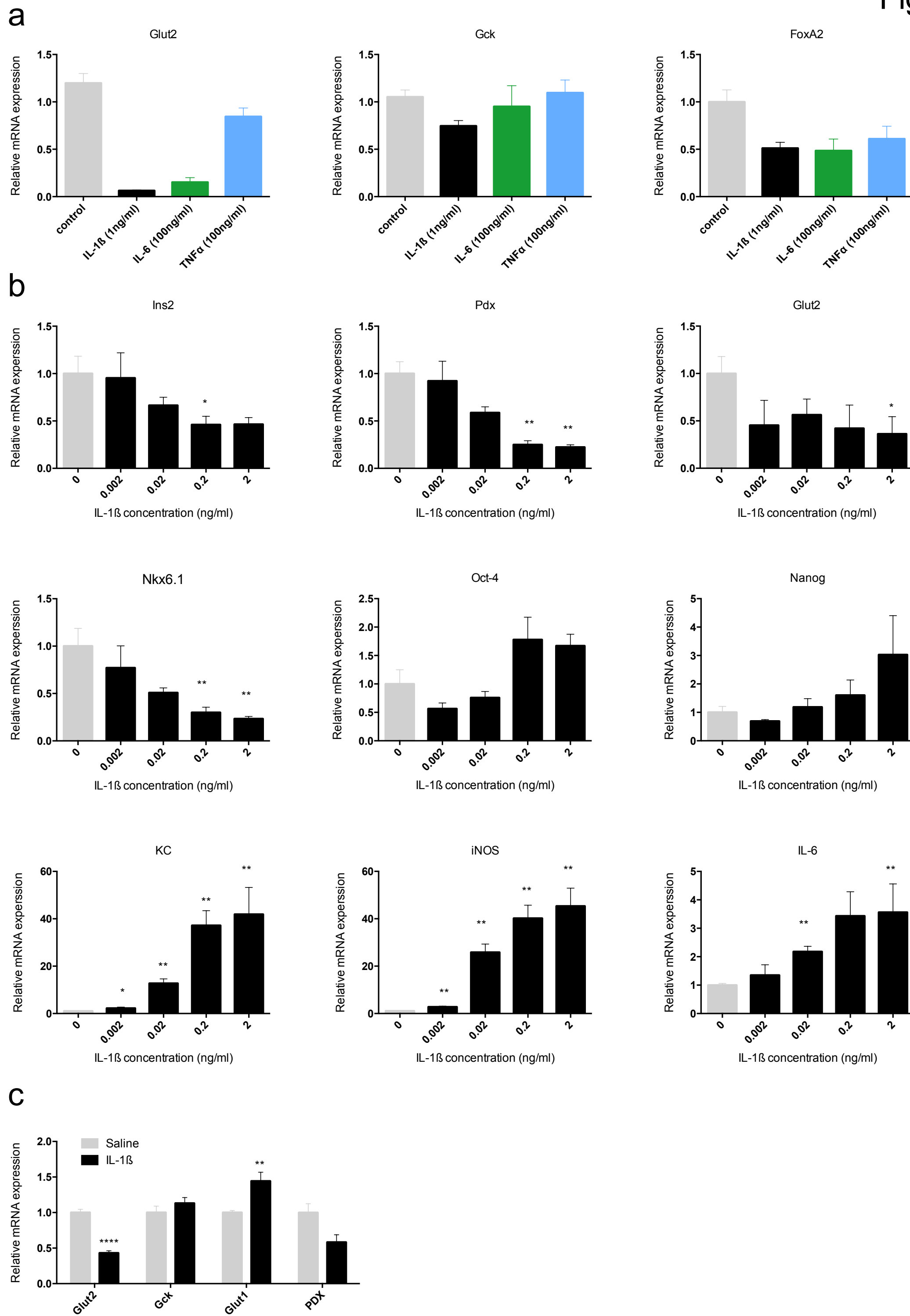
Fig. 2
a
Glut2
Gck
FoxA2
Relative mRNA expression
control
IL-1ß (1ng/ml)
IL-6 (100ng/ml)
TNFα (100ng/ml)
b
Ins2
Pdx
Glut2
Nkx6.1
Oct-4
Nanog
KC
iNOS
IL-6
IL-1ß concentration (ng/ml)
c
Saline
IL-1ß
Glut2
Gck
Glut1
PDX

Fig. 3

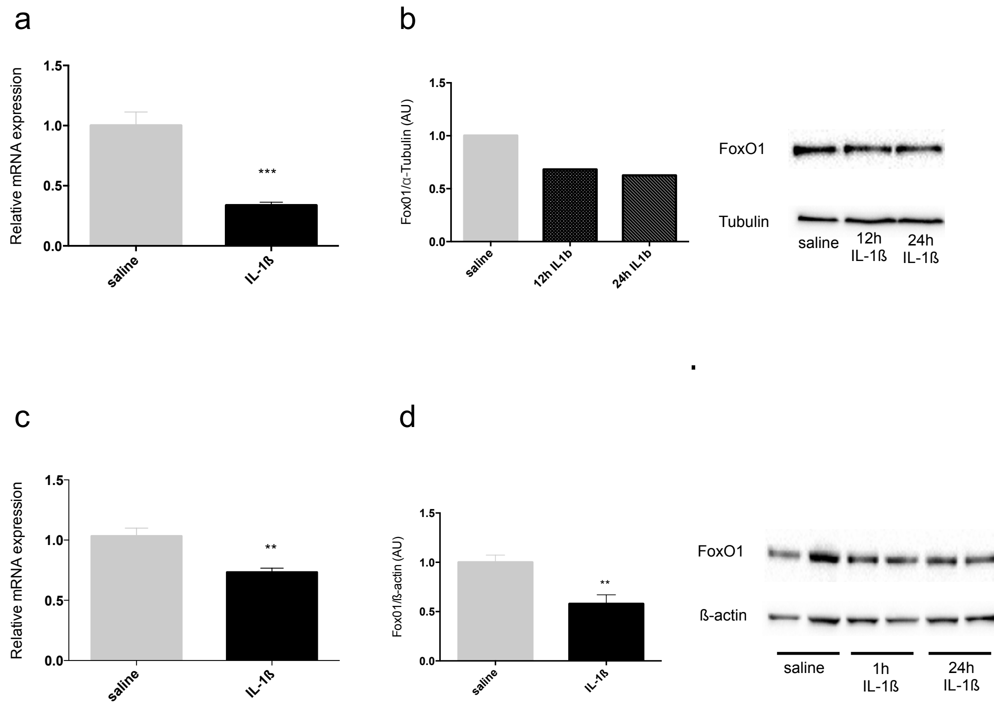

Fig. 4

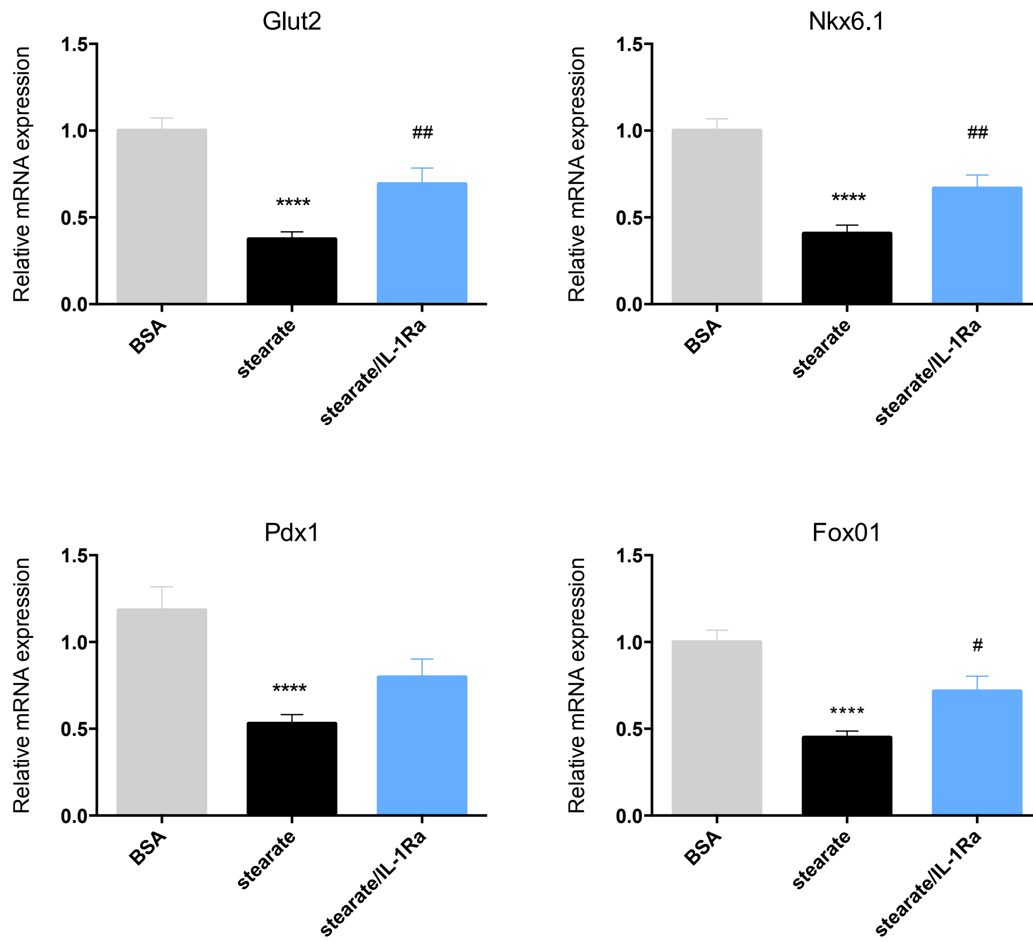

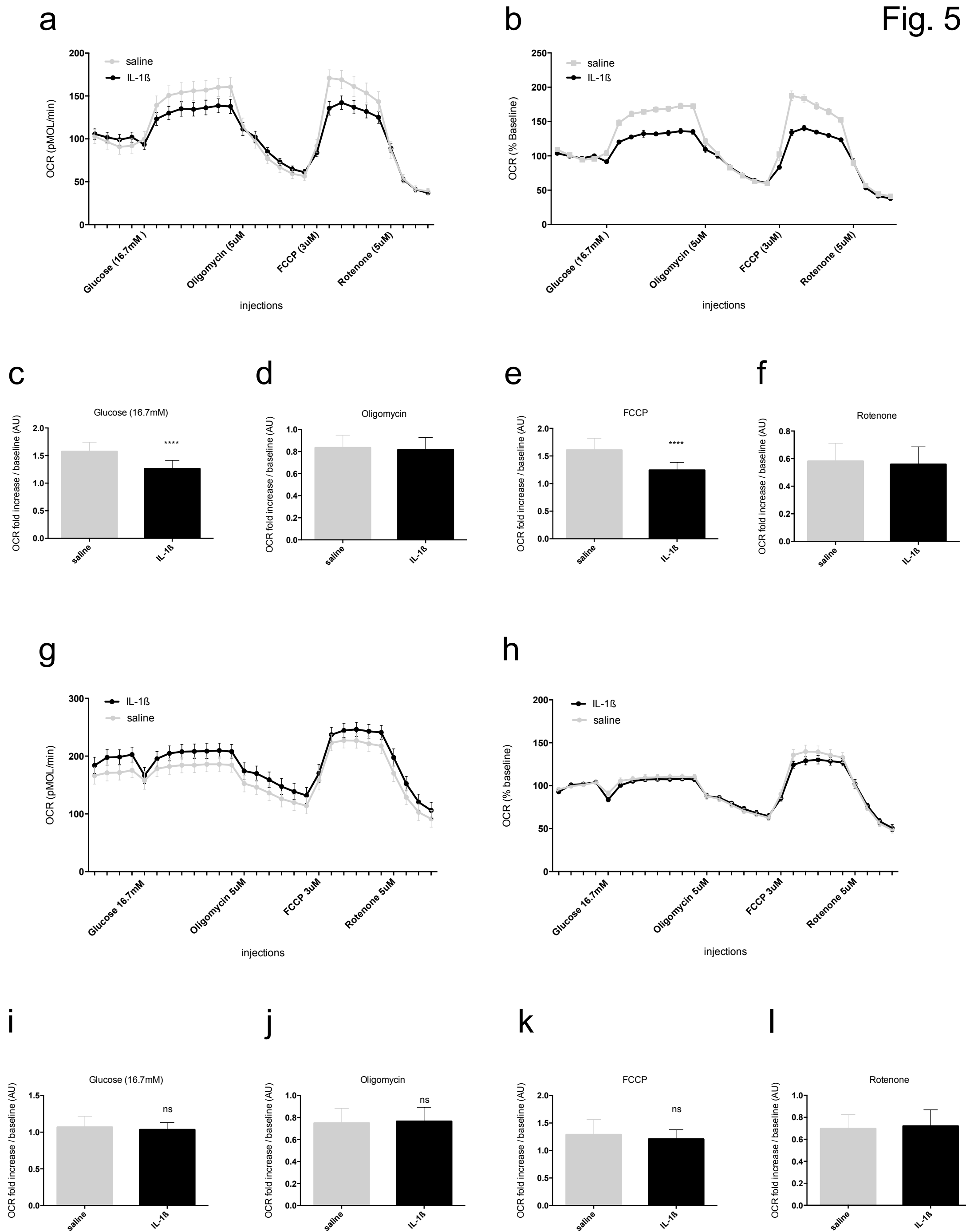
Fig. 5
a
b
c
d
e
f
g
h
i
j
k
l
saline
IL-1ß
OCR (pMOL/min)
OCR (% Baseline)
OCR (% baseline)
injections
Glucose (16.7mM)
Oligomycin (5uM
FCCP (3uM)
Rotenone (5uM)
Glucose 16.7mM
Oligomycin 5uM
FCCP 3uM
Rotenone 5uM
Glucose (16.7mM)
Oligomycin
FCCP
Rotenone
OCR fold increase / baseline (AU)
****
ns

Fig. 6

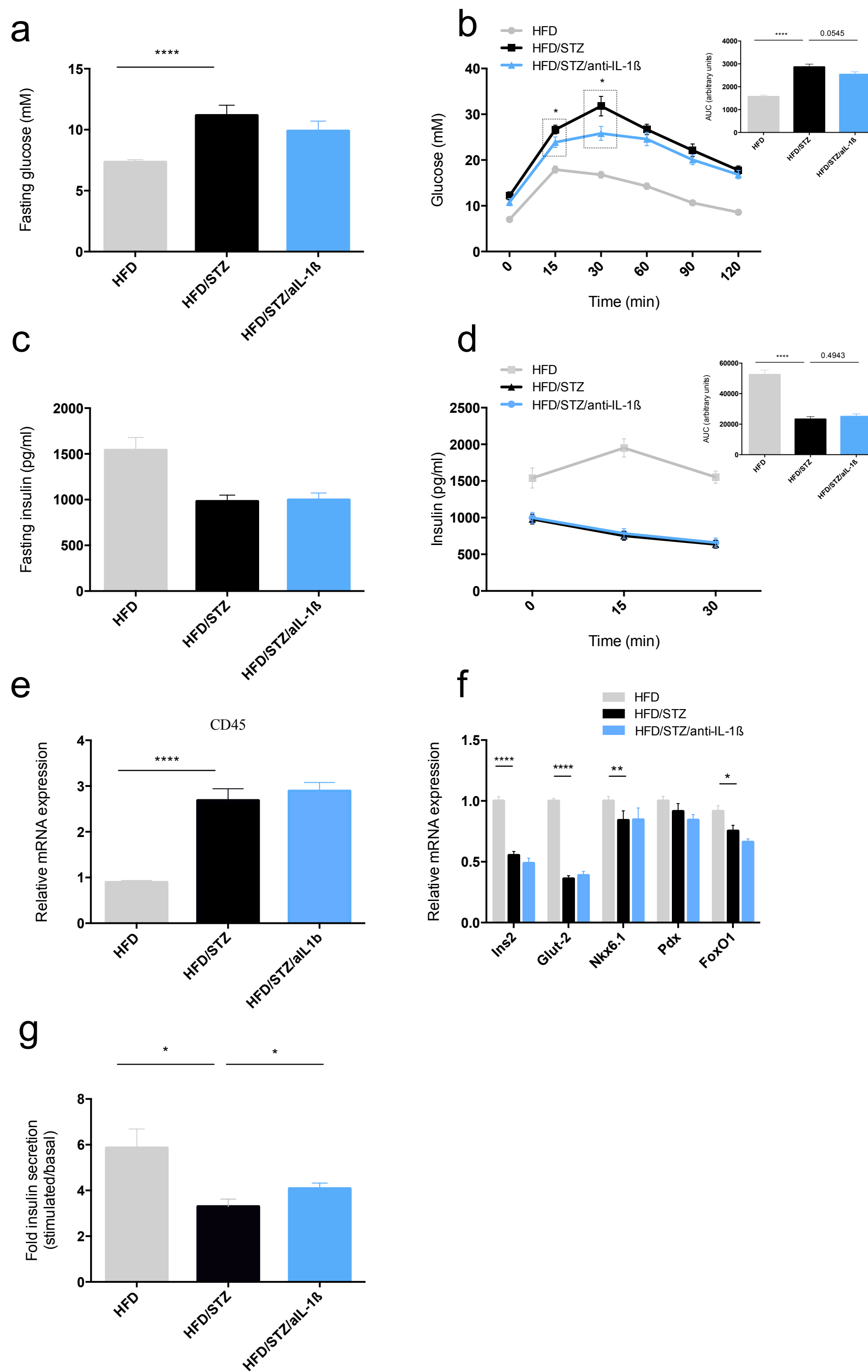

Fig. 7

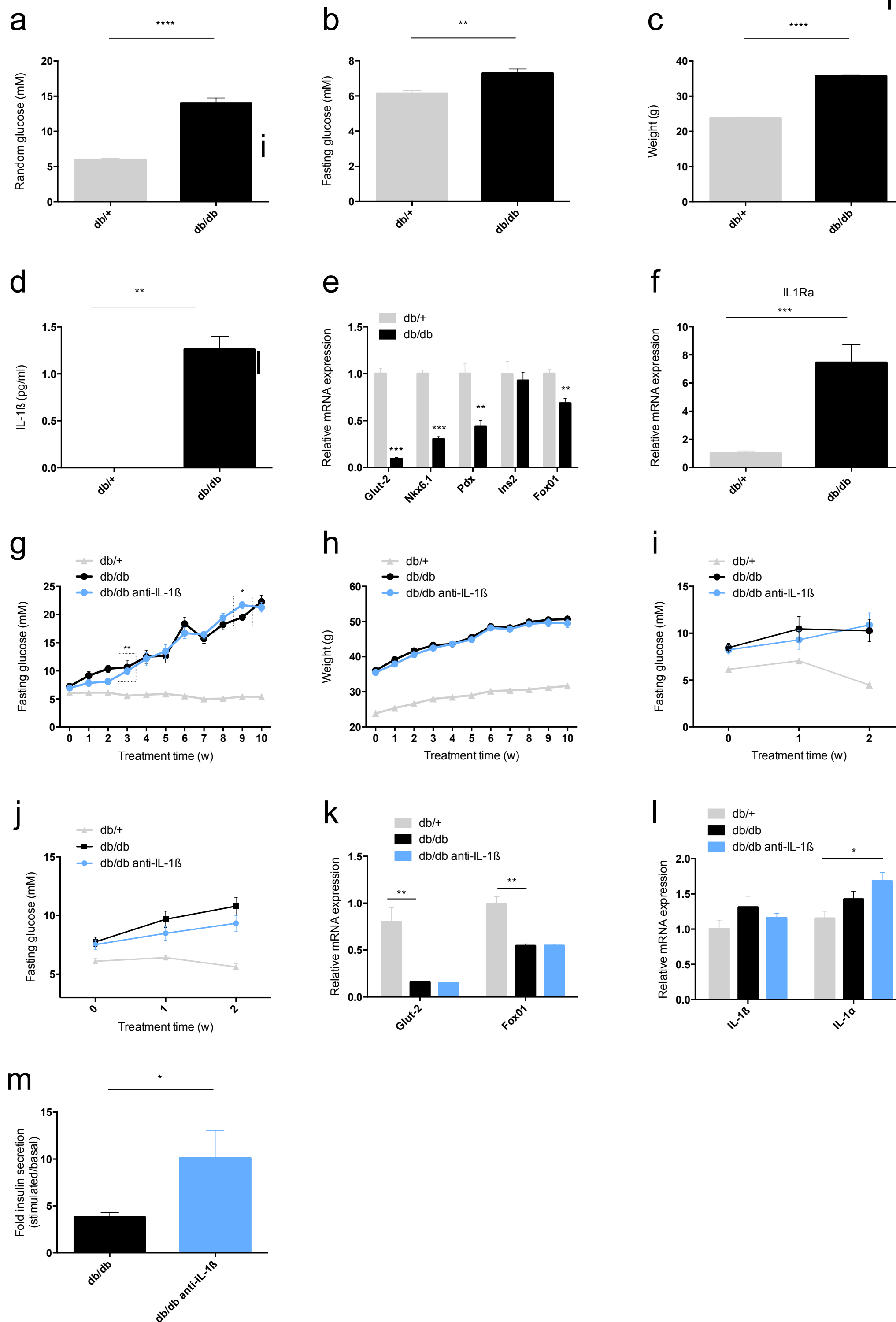

Fig. 8

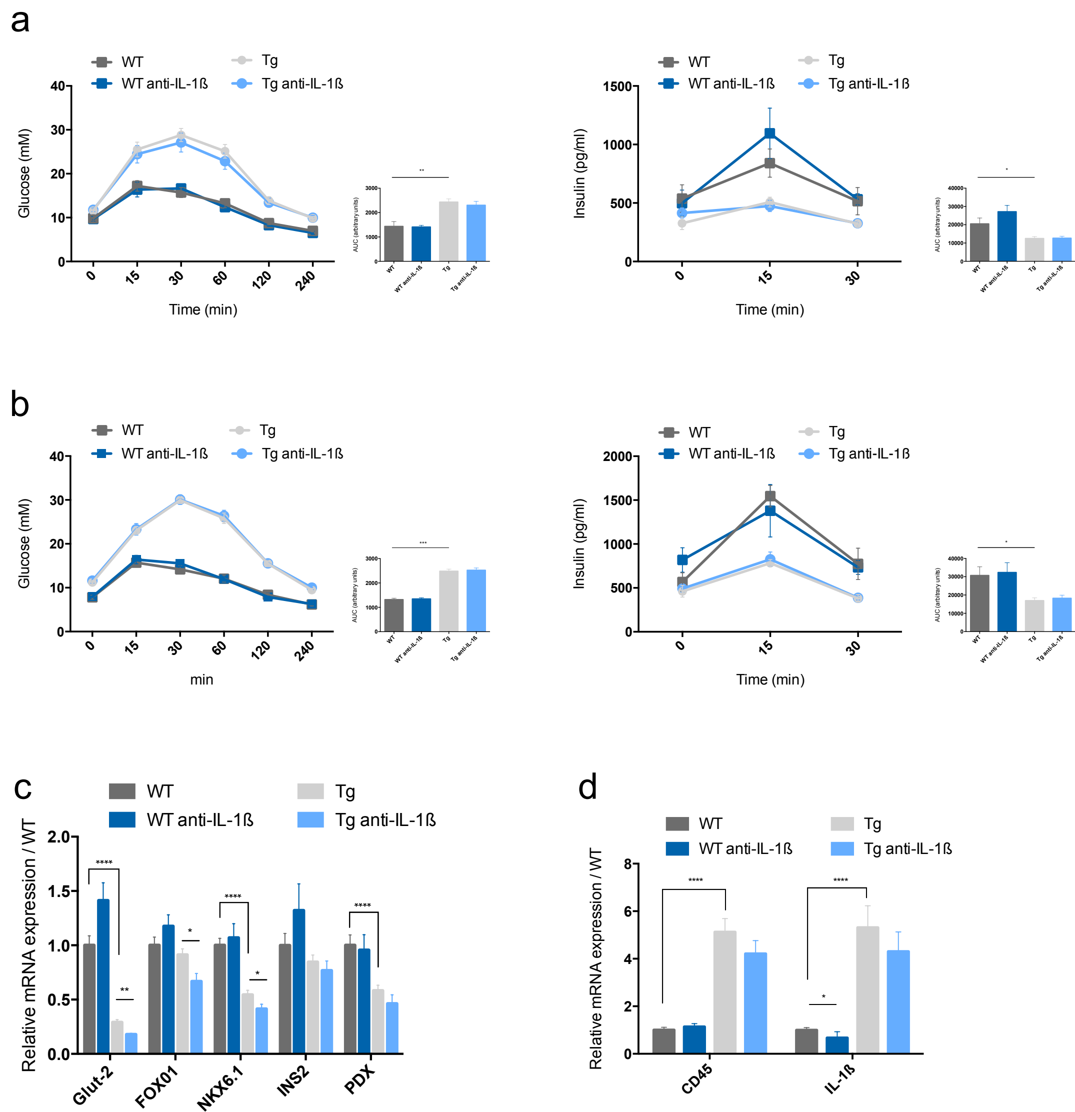

II. Combinatorial Anti-Inflammatory Treatment Strategies for Type 2 Diabetes Mellitus

(Unpublished)

Salicylate & IL-1ß antagonism

Diet induced obesity / streptozotocin model

4-week-old C57BL6/N mice were fed a high fat diet (HFD) and received a single injection of STZ (130mg/kg) or sodium-citrate at 8 weeks of age. At the same time, treatment regimens were started. Anti-IL-1ß (aIL-1ß) antibody was injected once weekly and sodium salicylate was incorporated within the food at a concentration of 4g/kg. For convenience reasons, the term HFD/STZ will be omitted when mentioning aIL-1ß and/or salicylate treated mice, as all these mice have been fed a HFD and injected with STZ. HFD/STZ mice will be referred to as untreated, STZ-injected mice.

Sodium salicylate reached similar levels in both salicylate (0.23mM ± 0.04) and salicylate/aIL-1ß (0.26mM ± 0.15) treated groups (Fig. 1a) and was undetectable in non-salicylate groups.

STZ injection caused a transient weight-gain arrest compared to non-STZ (HFD) treated mice (Fig. 1b). Anti-IL-1ß treated mice showed similar weight development as untreated STZ-injected mice. In contrast, salicylate and salicylate/aIL-1ß treated mice lost weight within 1 week of STZ injection and maintained a lower body weight throughout the experiment. Both salicylate-induced change in food bitterness and subsequent reduced food intake, as well as recently documented activation of brown adipose tissue through salicylates [44] could account for the observed weight loss. However, since weight gain under salicylate treatment in other, non-STZ cohorts was not reduced compared to non-salicylate treated mice (Fig. 2a, 3a) and no apparent adipocyte morphology difference of interscapular brown-adipose tissue (iBAT) was present (Fig. 1c), reduced food-uptake and activation of brown-adipose tissue seem unlikely. Thus, the reasons for initial weight loss in salicylate and salicylate/aIL-1ß treated mice remain unclear and reduced food intake due to a potential bitter taste of salicylate cannot be excluded.

Weekly measurement of random (morning) glucose levels showed progressive worsening of untreated, STZ injected compared to non-STZ control mice (Fig. 1d). No clear difference was seen in the aIL-1ß group while salicylate treated mice had nearly normal glucose levels after 2 weeks of STZ injection. Surprisingly, glucose levels in the aIL-1ß/salicylate group were similar to the aIL-1ß treated group rather than the salicylate group.

Similarly, fasting blood glucose levels were elevated in untreated, STZ-injected mice compared to non-STZ mice (Fig. 1e). Salicylate and salicylate/aIL-1ß had significantly reduced fasting blood glucose levels, while aIL-1ß treated mice had a slight decrease in fasting blood glucose levels, which did not reach statistical significance.

In addition, long-term glucose homeostasis after 2 weeks of treatment was assessed as quantified by the percentage of glycosylated Hemoglobin-A1 levels (HbA1c; Fig. 1f). As expected, HbA1c levels were higher in untreated, STZ-injected compared to non-STZ injected mice. Salicylate treatment most profoundly improved long-term glucose levels, while a numerical decrease in HbA1c levels was also present in aIL-1ß and salicylate/aIL-1ß treatment groups, however not quite reaching statistical significance ($p=0.6619$ and 0.0684 respectively).

2 weeks after STZ and treatment, an intraperitoneal glucose tolerance test was performed (Fig. 1g). Strong glucose intolerance and reduced insulin levels were present in untreated, STZ-injected mice compared to HFD control mice, alongside reduced insulin levels. Mean glucose levels after glucose injection were lower in all treatment groups and significantly lower in salicylate and salicylate/aIL-1ß treated mice. Furthermore, fasting insulin levels were lower in the salicylate/aIL-1ß treated mice, and did not change in all treatment groups in response to glucose injection.

RNA expression levels of islets isolated after 2 weeks of treatment were analyzed (Fig. 1h). Some ß-cell markers were downregulated (Ins2, Glut2) in untreated, STZ-injected compared to HFD mice, while other ß-cell markers remained unchanged (Pdx1, Nkx6.1, FoxO1). In addition, inflammatory (KC, CD45) and α-cell markers (Gcg) were increased. Surprisingly, all treatment groups had no beneficial effect on expression levels of ß-cell, α-cell or inflammatory gene markers.

Glucose-induced insulin secretion of ex-vivo isolated islets was next measured (Fig. 1i). Untreated, STZ-injected mice had significantly lower insulin levels within islets (content), with lower basal and stimulated insulin response compared to HFD mice, however not reaching statistical significance (P=0.0685 and 0.0593, respectively). Only salicylate treated islets had an improved stimulatory index, probably due to enhanced insulin stimulated insulin response and higher insulin content.

Diet induced obesity model

7-week-old C57BL6/N mice were fed a HFD and treated with aIL-1ß and/or salicylate. Anti-IL-1ß antibody was injected once weekly and sodium salicylate was incorporated within the food at a concentration of 4g/kg. For convenience reasons, the term HFD will be omitted when mentioning aIL-1ß and/or salicylate treated mice, as all these mice have been fed a HFD.

Weight gain under HFD was similar in all groups (Fig. 2a). 2, 6, 11 and 15 weeks after treatment initiation, glucose tolerance and associated insulin secretion were assessed following an intraperitoneal glucose injection (Fig. 2b). Over time, glucose tolerance increasingly deteriorated in HFD mice, along with rising levels of insulin secretion indicating progressive insulin resistance. Surprisingly, only salicylate treated mice showed partial treatment response with higher insulin levels 11 weeks after treatment and a trend towards improved glucose levels 15 weeks after treatment, not reaching statistical significance ($AUC_{HFD\ vs.\ salicylate}$ P=0.1296).

Insulin resistance was evaluated at 3,9 and 16 weeks after treatment initiation by measuring blood glucose levels following an intraperitoneal injection of insulin (Fig. 2c). Over time, no obvious differences between treatment groups were present. Interestingly, both salicylate and salicylate/aIL-1ß treated mice had a trend towards lower blood glucose values after 3 and not 6 hours (Fig. 2d). On the other hand, HbA1c levels after 17 weeks of treatment were significantly lower in both salicylate and salicylate/aIL-1ß mice (Fig. 2e). While numerically, HbA1c levels were lower in the salicylate/aIL-1ß (4.1%) compared to salicylate treated mice (4.2%), this did not reach statistical significance ($HbA1c_{salicylate\ vs.\ salicylate/aIL\text{-}1ß}$ P= 0.2889)

Given the fact that C57BL6/N are resistant to islet-cell failure [125] and were able to compensate for insulin resistance with even more insulin, possibly obscuring a

potential beneficial treatment effect, overt diabetes was induced through a single dose of STZ (130mg/kg) after 17 weeks of HFD ± treatment. Indeed, 1 week after STZ injection, all mice were similarly hyperglycemic after 6 hours of fasting and responded with a similar rise in glucose levels after intraperitoneal glucose injection (Fig. 2f). Strikingly, salicylate and/or aIL-1ß treated mice sustained higher levels of insulin after STZ injection compared to STZ injected HFD mice (P=0.0541, 0.1638 and 0.0093 for aIL1-ß, salicylate and salicylate/aIL-1ß, respectively; Fig. 2f).

In type 2 diabetic patients, average time from disease onset to diagnosis is 4-10 years [126, 127]. In order to mimic human disease more closely, C57BL6/N mice were fed a HFD at 8 weeks of age and only 11 weeks later treated with salicylate or salicylate/aIL-1ß, at 19 weeks of age, after randomization according to body weight and intraperitoneal glucose tolerance testing.

HFD caused more rapid weight gain (Fig. 3a), glycemic deterioration and hyperinsulinemia (Fig. 3b) compared to chow-diet (CD) fed animal. Both salicylate and salicylate/aIL-1ß treated mice gained slightly more weight than HFD control mice (Fig. 3a). Hypothesizing, that salicylate and aIL-1ß both ameliorate insulin resistance, weight gain as a consequence would be expected. However, insulin tolerance testing did not reveal an obvious difference between both treatment groups, 3 (Fig.3c) and 6 (Fig. 3e) weeks after treatment initiation. Surprisingly, there was also no difference between HFD and CD mice, questioning the sensitivity of the test. 2 weeks after treatment initiation, an intraperitoneal glucose tolerance test was performed showing slightly improved glucose tolerance in salicylate and salicylate/aIL-1ß mice, alongside lower insulin levels (Fig. 3b). In order to assess maximal insulin secretion capacity in vivo, an oral glucose tolerance test 8 weeks after treatment initiation was performed, revealing that salicylate and salicylate/aIL-1ß treated mice were able to secrete more insulin, not leading to an improvement in glucose control however (Fig. 3d). Long-term glucose homeostasis was impaired in HFD vs. CD mice and subtly improved in both treatment groups (HbA1c; Fig. 3f).

TNFα inhibition & IL-1ß antagonism

Diet induced obesity / streptozotocin model

4-week-old C57BL6/N mice were fed a HFD and received a single injection of STZ (130mg/kg) or sodium citrate at 8 weeks of age. At the same time, treatment regimens were started. Anti-IL-1ß antibody was injected once weekly and anti-TNFα (aTNFα) decoy receptor (Etanercept) was injected 3x/week. For convenience reasons, the term HFD/STZ will be omitted when mentioning, since a-IL-1ß and or aTNFα treated mice were all fed a HFD and injected with STZ. HFD/STZ mice will be referred to as untreated, STZ-injected mice.

STZ injection caused a transient weight-gain arrest compared to non-STZ injected, HFD mice, while weight gain was similar in the anti-inflammatory treated and untreated, STZ-injected mice (Fig. 4a).

Weekly measurement of random (morning) glucose levels showed progressive worsening of all STZ-injected mice compared to non-STZ, HFD control mice (Fig. 4b). With no difference in the aIL-1ß group, both aTNFα and aTNFα/aIL-1ß treated mice showed a numerical decrease in both random (Fig. 4a) and 6h fasting (Fig. 4d) glucose levels 2 weeks after treatment compared to untreated, STZ-injected mice. This however did not reach statistical significance.

2 weeks after STZ treatment, an intraperitoneal glucose tolerance test was performed (Fig. 4e). Mild glucose intolerance between HFD and CD fed mice was present, together with highly elevated insulin levels clearly indicating insulin resistance. On the other hand strong glucose intolerance was evident in untreated STZ-injected mice compared to non-STZ, HFD mice, alongside reduced insulin levels indicating ß-cell failure. Glucose levels were significantly lower in aTNFα and aTNFα/aIL-1ß treated mice 15min and 15/30min after glucose injection, respectively. In contrast insulin secretion upon glucose challenge was similar in all STZ injected cohorts.

In order to assess the degree of insulin resistance, an insulin tolerance test was performed in which a-TNFα and aTNFα/aIL-1ß had overall lower glucose levels than untreated, STZ-injected mice (Fig. 4f). However, since fasting glucose levels differed strongly between aTNFα, aTNFα/aIL-1ß and untreated, STZ-injected mice, the insulin tolerance test must be interpreted with caution. In a further attempt to quantify

insulin resistance, the phospho-AKT to AKT ratio in liver lysate was determined 11 minutes after exogenous insulin injection (Fig. 4g). Interestingly, only aTNFα treated mice had significantly improved insulin signaling compared to untreated, STZ-injected mice. On the other hand, aIL-1ß had only a minor effect and the combination of aTNFα and aIL-1ß even abolished the improvement of the aTNFα treatment.

RNA expression levels of islets isolated after 2 weeks of treatment were analyzed (Fig. 4h). Some ß-cell markers were downregulated (Ins2, Glut2) in untreated, STZ-injected compared to non-STZ injected, HFD mice, while other ß-cell markers remained unchanged (Nkx6.1, Pdx1, FoxO1). In addition, the inflammatory marker KC was increased. Anti-IL-1ß treatment partially rescued Ins2 expression levels compared to untreated, STZ-injected mice but surprisingly failed to inhibit upregulation of KC, a supposedly IL-1ß driven cytokine. Anti-TNFα treatment rescued Glut2 and Ins2 expression compared to untreated, STZ-injected mice and numerically decreased upregulation of KC, the latter however not reaching statistical significance. The combination of both aIL-1ß and aTNFα resulted in a significant rescue of Ins2 expression and also partially inhibited the upregulation of KC. Interestingly, gene expression levels of Nkx6.1 were significantly lower in the combination group compared to untreated, STZ-injected mice.

Finally, glucose-induced insulin secretion of ex-vivo isolated islets was measured (Fig. 4i). Untreated STZ-injected mouse islets had significantly lower insulin levels within islets (content) and released less insulin into the supernatant along with lower basal and stimulated insulin response resulting in an impaired stimulation index compared to HFD mouse islets. Anti-IL-1ß had no impact and aTNFα showed only minor effects on glucose-induced insulin secretion. In contrast, the combination of both resulted in a significantly improved stimulated insulin release and subsequent stimulation index with more insulin levels within islets compared to untreated STZ-injected mouse islets.

Since TNFα-antagonism showed the most prominent effect in vivo, we hypothesized that aTNFα-mediated glycemic improvement could be due to improvement of insulin resistance, limitation of STZ-induced pancreatic islet damage or both. In order to differentiate between the two, 4-week-old C57BL6/N mice were fed a HFD and received a single injection of STZ (130mg/kg) or sodium citrate at 8 weeks of age. Only 2 weeks later, STZ-injected mice (randomized according to weight and plasma

glucose levels) were treated with aTNFα decoy receptor (Etanercept) 3x/week. Similar to previous experiments, STZ caused weight-gain cessation (Fig. 5a) and severe random (Fig. 5b) and fasting (Fig. 5c) hyperglycemia compared to non STZ-injected, HFD mice. Weight gain was similar in aTNFα treated mice compared to untreated STZ-injected mice (Fig. 5a), with no apparent difference in both random (Fig. 5b) and fasting (Fig. 5c) glucose levels. Plasma glucose levels following an intraperitoneal glucose injection tended to be slightly lower 30 min after injection in aTNFα treated mice, however not reaching significance at this timepoint nor overall (Fig. 5d).

Diet induced obesity model

C57BL6/N mice were fed a HFD at 8 weeks of age and only 11 weeks later treated with aTNFα and/or aIL-1ß at 19 weeks of age, after randomization according to body weight and intraperitoneal glucose tolerance testing.

The aIL-1ß antibody was injected i.p. once weekly. The TNFα antagonist (Etanercept) was injected s.c., twice weekly at a dose of 1mg/kg, based upon dosage in human studies and published literature in mice [128, 129]. For convenience reasons, the term HFD will be omitted when mentioning aIL-1ß and/or aTNFα treated mice, as these mice have been fed a HFD.

HFD mice were heavier (Fig. 6a), with impaired glucose tolerance upon intraperitoneal glucose challenge (Fig. 6b) compared to CD after 11 weeks of HFD. Both aIL-1ß and/or aTNFα had no effect on body weight compared to HFD mice (Fig. 6a). 2 weeks after treatment initiation, an intraperitoneal glucose tolerance test was performed. However, no beneficial effect was apparent in both aIL-1ß and/or aTNFα treated mice (Fig. 6b). Similarly, insulin sensitivity was unchanged in both aIL-1ß and/or aTNFα treated mice, evaluated by measuring the change in glucose levels following an intraperitoneal insulin injection after 3 weeks of treatment initiation (Fig. 6c). Since an improvement in insulin resistance was to be expected from aTNFα treatment, we speculated that the dose of the TNFα antagonist was too low and adjusted the dose to 5mg/kg. Still, both glucose tolerance (Fig. 6d) and insulin resistance (Fig. 6e) testing remained similar in aIL-1ß and/or aTNFα treated mice, 3 and 4 weeks after aTNFα dose adjustment, respectively. In accordance, long-

term glucose homeostasis was unchanged in treatment groups, as levels of Hba1c were similar in aIL-1ß and/or aTNFα compared to HFD mice (Fig. 6f).

Gene expression levels of ß-cell identity markers Glut2 and Nkx6.1 were significantly lower in HFD compared to CD mice (Fig. 6g). On the other hand, IL-1ß expression was slightly higher and TNFα slightly lower in HFD mice, not reaching statistical significance. While aTNFα/aIL-1ß treatment partially rescued the decline of Nkx6.1, no effect was seen on Glut2, IL-1ß and TNFα expression. In contrast, aIL-1ß potently reduced IL-1ß expression but had no effect on the other genes. Surprisingly, aTNFα reduced IL-1ß expression but also significantly decreased Glut2 expression.

Discussion

Type 2 diabetes mellitus (T2DM) is a metabolic disorder, characterized by the presence of both insulin resistance and ß-cell dysfunction. By now, the disease has reached and epidemic dimension, affecting more than 350 million people worldwide [120]. The current and state of the art treatment of T2DM involves agents directly lowering blood glucose by either stimulating ß-cell insulin secretion (sulfonylurea, glinides), increasing insulin sensitivity (metformin, PPARγ agonists) or increasing glucose excretion (SGLT2 agonists). While these agents are targeting the consequence of T2DM, no FDA-approved drug is trying to target the causative nature of the disease.

Interestingly, inflammation has been shown to cause both ß-cell dysfunction and insulin resistance. In support, IL-1ß antagonism [96] as well as NF-κB [29] more than TNFα inhibition [26] has been shown to improve ß-cell-function and insulin resistance, respectively. As both pancreatic ß-cell failure and insulin resistance are crucial pathogenic elements, we speculated that combinatorial anti-inflammatory treatment, targeting both IL-1ß-induced ß-cell dysfunction and NF-κB- or TNFα-induced insulin resistance would result in superior glycemic control compared to the corresponding monotherapy. Furthermore, in contrast to current symptom-oriented treatment strategies, targeting inflammation has the potential to prevent further disease progression and ameliorate associated, partially inflammation-driven

complications such as retinopathy [130], nephropathy [131] and peripheral neuropathy [132].

In order to test our hypothesis, we tested the effect of anti-IL-1ß and/or anti-TNFα or salicylate induced NF-κB inhibition in 2 different mouse models of type 2 diabetes: the DIO mouse with pronounced insulin resistance and the DIO/STZ mouse with both insulin resistance and ß-cell failure.

In both models, aIL-1ß had minimal to no effect in vivo on glycemic indices (ipGTT, ITT, HbA1c). Ex-vivo, aIL-1ß did not prevent the decrease of ß-cell identity markers (Glut2, Pdx1, Nkx6.1, FoxO1, Ins2) and increase of downstream inflammatory marker (KC) on an mRNA levels, nor was the negative impact of HFD±STZ on glucose-induced insulin secretion averted. Our findings are quite surprising, as they are in contrast to previous studies in mice, showing a beneficial role of IL-1Ra in a similar setting but in a different mouse strain (C57BL6/J) [122], known to have reduced insulin secretion due to a naturally occurring mutation in nicotinamide nucleotide transhydrogenase (NNT). NNT is an anti-oxidant defense enzyme encoding gene, without which ROS levels are elevated. On the other hand, and more in line with our data, Osborn and colleagues observed no effect on fasting glucose levels and glucose/insulin tolerance testing after long-term treatment with the same aIL-1ß antibody we used in our DIO mice [133]. In contrast, HbA1c levels were significantly (P=0.049) reduced in antibody treated mice, an observation we were not able to confirm. In addition, information whether C57BL6/J or -/N mice were used, was not given. While some controversy remains about the effect of anti-IL-1ß in type 2 diabetic mouse models, antagonizing IL-1ß in obese and type 2 diabetic humans has been done with various agents (IL-1Ra, different mAb) and nearly always had a beneficial, yet modest effect on glucose homeostasis, emphasizing the importance of IL-1ß in human type 2 diabetic disease.

The ancient drug salicylate, has the potential to be a major treatment option in T2DM. It's effects go way beyond cyclooxygenase 2 inhibition and include NF-κB inhibition [29], AMPK activation [45], brown-adipose tissue activation [44] and cortisol production inhibition [43]. Salsalate, due to its safety advantages (less gastrointestinal toxicity, no thrombocyte aggregation inhibition) has been used as a salicylate prodrug rather than sodium salicylate or salicylic acid (aspirin). Accordingly, salsalate has been used in various human studies, with an astonishing beneficial effect on glucose

homeostasis, but had to be taken 3 times per day. In our experiments, salicylate treated DIO/STZ mice, salicylate significantly improved fasting and random glucose levels as well as glucose tolerance testing and HbA1c levels as early as 2 weeks after treatment initiation. Interestingly, ex-vivo assessed glucose-induced stimulatory insulin secretion index was higher in salicylate treated mice compared to untreated mice. However, no change was seen on an mRNA level of both ß-cell identity and inflammatory markers and due to unknown reasons, salicylate treated mice, were leaner than untreated mice, a potential confounding factor of the above mentioned glycemic improvement. Long-term salicylate treatment in HFD fed mice showed a clear trend towards lower glucose levels during the glucose tolerance test. Along with this observation, HbA1c levels in salicylate treated mice were lower compared to untreated mice after 17 weeks of HFD and salicylate treatment. Surprisingly, insulin levels tended to be higher in salicylate treated groups. Assuming that salicylate improves insulin resistance, the opposite would be expected and might hint towards a direct effect of salicylate on ß-cells. When exposing isolated pancreatic islets to chronic salicylate, at concentrations similar to our in vivo model, we observed a dose-dependent decrease in stimulated glucose-induced insulin secretion (Fig. 7a), again the opposite of what was to be expected. Furthermore, there was a dose-dependent effect on oxygen-consumption rates in islets, similarly published for other AMPK activators (Fig. 7b). Surprisingly, only low-dose chronic (24h) and short-term (30min) treatment elevated oxygen consumption rate (Fig. 7c), suggesting that it might be best to prescribe salsalate prior to food ingestion in order to benefit from both long (NF-κB inhibition) and short-term (elevated oxygen consumption) effects.

Without a doubt, TNFα plays a major role in insulin resistance in both humans and mice. Astonishingly, clear results from proper, prospective and randomized, controlled human studies as to whether TNFα antagonism directly improves insulin sensitivity, are still lacking. Furthermore, scarce literature exists showing that chronic pharmacological inhibition (rather than genetic modulation) of TNFα improves glucose homeostasis in rodents. Here we show for the first time, that in HFD/STZ mice TNFα antagonism improves glycemia after only 2 weeks of treatment. Interestingly, TNFα antagonism did so, not only by improving insulin resistance, but also via a ß-cell improving effect, with reversal of reduced ß-cell identity and inflammatory markers. Indeed, evidence exists that TNFα is elevated in human

pancreatic islets of type 2 diabetic patients [123] and may therefore explain the ß-cell effect of TNFα antagonism in our mice. However whether the ß-cell effect observed derived indirectly via improved insulin resistance or directly on ß-cells, remains to be investigated. There are though, limitations to our study. The dosage used in the DIO/STZ mouse model (20mg/kg, 3x/week) was higher than what is used in human patients (0.7mg/kg, 2x/week), even though the TNFα antagonist used (Etanercept) carries the human TNF-receptor 2 and is therefore more potent in humans. Secondly TNFα antagonism was initiated at the same time as STZ was injected. As STZ causes ß-cell specific damage, probably also inducing TNFα, antagonism of the latter would protect ß-cell damage in a potentially artificial way. This is strengthened by the fact that TNFα inhibition 2 weeks after STZ injection only caused minor improvement in glucose homeostasis. In the DIO mouse model, we therefore used a more "physiologic" dose (1mg/kg, 2x/week). However, no beneficial effect on glucose homeostasis was seen, even after raising the dose to 5mg/kg. On the other hand, TNFα-antagonism, decreased pancreatic islet-associated IL-1ß expression significantly.

The effect combining IL-1ß antagonism with salicylate or aTNFα treatment was not clear-cut. Combining aIL-1ß and salicylate in DIO/STZ mice led to the lowest fasting insulin levels compared to all other treatment groups and is probably due to the insulin sensitizing effect of both aIL-1ß and salicylate. On the other hand, the combination abolished the beneficial effect of salicylate treatment on glycemic parameters and improvement of glucose-induced insulin secretion in isolated islets. The same phenomenon was apparent in aIL-1ß/salicylate treated DIO mice, where the combination was inferior to the mono-therapy with salicylate. When combing aIL-1ß and a-TNFα in DIO/STZ mice glucose-induced insulin secretion was significantly improved, unlike aIL-1ß or aTNFα treatment. Surprisingly though, amelioration of insulin resistance by TNFα-antagonism was annulled by the combination with aIL-1ß. Probably due to the sum of positive and negative effects, similar glycemic control in aTNFα and aTNFα/aIL-1ß treated mice was reached. In summary, while we provide evidence for the beneficial role of both salicylate and aTNFα in T2DM, antagonism of IL-1ß showed only minimal effects. Hence, our data do not argue for a meaningful additive effect of IL-1ß inhibition and TNFα antagonism or NF- κB suppressing salicylate.

How do these findings correlate with the current knowledge of anti-inflammatory treatment, impacting further clinical treatment approaches?

Clearly, combining aIL-1ß with aTNFα or salicylate did not show the expected effect. Especially the effect of aIL-1ß in both mouse models was marginal, even though vigorously tested. In addition, particularly the influence of aIL-1ß and salicylate were minimal when comparing to the large body of evidence gathered in human type 2 diabetes and therefore of great importance. One potential explanation can be found in the fundamental differences between mouse and man. Naturally, preclinical data acquired in rodents can provide crucial data, leading to clinically significant achievements. On the other hand, especially inflammatory responses to various pathogens seem to differ largely between mice and humans [134]. Rightly so, while clinical research must be influenced by the results obtained in preclinical rodent studies, it must not solely depend on it.

Having said that, it remains interesting, as to why the combination of aIL-1ß and salicylate/aTNFα does not result in the expected beneficial effect, as objective study of literature would suggest. The term inflammation, comes from the Latin word *flamma*, fire and was described by the roman Aulus Cornelius Celsus with the 4 cardinal symptoms "*rubor et tumor cum calore et dolore*". As did to Rome, many roads lead to inflammation and throughout time, we have learned to understand many mechanism involved in the (patho)physiology of inflammation. By now, there is no human disease, in which inflammatory pathways do not contribute. Inflammation is usually thought to be harmful. As a consequence, many anti-inflammatory agents, especially monoclonal antibodies are generated and tested in various diseases. Yet it is naïve to believe, that such a fundamental process in our body exists only to do harm. Increasing evidence suggest, that inflammation is necessary for physiologic processes to function. One such visible example is wound healing, a process that would not function without inflammation [135]. Similarly, a certain degree of inflammation might be needed in maintaining glucose homeostasis. This is especially true for IL-6, a (pro-)inflammatory cytokine heavily involved in the entero-endocrine axis, augmenting insulin secretion upon physical activity [9]. But there is also evidence suggesting a beneficial role for IL-1ß, TNFα and NF- κB.

With the highest levels of IL-1R1 expressed on pancreatic ß-cells [100] and documented potentiation of insulin secretion upon short-term, low-dose IL-1ß

exposure [112, 113], it is easy to believe that IL-1ß may also play a beneficial, physiological part in glucose homeostasis. Similarly, TNFα can mediate glucose uptake in immune cells [136] under inflammatory conditions. A potentially important compensating factor during times of elevated glucose levels such as T2DM. Finally, NF-κB has been shown to be important in glucose-induced insulin secretion in ß-cells [137]. It is conceivable that chronic and high-grade inflammation is detrimental for many diseases, including T2DM. Yet, targeting different inflammatory pathway simultaneously and therefore completely preventing inflammation might not be the right way to go. Without a doubt, further research is desperately needed in order to elucidate the correct targets of anti-inflammatory treatment therapy. One day, we will hopefully know how much antagonism is "just right" for treatment of type 2 diabetes mellitus.

Figure legends

Fig. 1. Analysis of the diet-induced obese (DIO) / streptozotocin (STZ) mouse model following treatment with anti-IL-1ß and/or salicylate

4-week-old mice were fed a high fat diet (HFD) followed by a single injection of STZ at 8 weeks of age simultaneously beginning treatment with anti-IL-1ß and/or salicylate. Control mice were not injected with STZ (HFD). (a) Serum salicylate levels and (b) weight development in HFD-control and differentially treated DIO/STZ mice. (c) Representative 20x hematoxylin-eosin brightfield image of interscapular brown adipose tissue from STZ control mice ± salicylate treatment. (d) Random glucose levels over time and at 2 weeks after treatment as well as (e) fasting glucose levels after 2 weeks of treatment. (f) HbA1c levels in 10-week-old mice. (g) Plasma glucose, insulin levels and corresponding area under the curve following intraperitoneal glucose injection after 6 hours of fasting in 10-week-old HFD-control and differentially treated DIO/STZ mice 2 weeks after STZ injection. (h,i) In isolated islet (h) mRNA expression levels and (i) glucose-induced insulin secretion were assessed.

(a) n=12-15/group, 2 experiments. (b,d,e) n=14-16/group, 2 experiments. (c) n= 1/group. (f,g) n=12-15/group, 2 experiments. (h) n=13-22/group, 2 experiments. (i) n= 10/group, 2 experiments. *P < 0.05, **P < 0.01, ***P < 0.001, ****P < 0.0001. Statistical significance (P) was determined using the two-tailed Mann-Whitney U test. All error bars denote s.e.m. Abbreviations: Lower limit of detection (LLOD), high fat diet (HFD), streptozotocin (STZ), anti-IL-1ß (aIL-1ß), sodium salicylate (salicylate).

Fig. 2. Analysis of the diet-induced obese (DIO) mouse model following long-term treatment with anti-IL-1ß and/or salicylate

7 week-old mice were fed a high fat diet (HFD) and treated with anti-IL-1ß and/or salicylate at 7 weeks of age. (a) Weight growth curves over time for the different treatment groups compared to HFD control. (b) Plasma glucose, insulin levels and corresponding area under the curve following an intraperitoneal glucose injection at the indicated age. (c) Plasma glucose and corresponding area under the curve following intraperitoneal insulin injections, at the indicated age. (d) 3h and 6h fasting blood glucose 16 weeks after HFD ± treatment. (e) HbA1c levels after 17 weeks of HFD ± treatment. (f) Glucose, insulin and corresponding area under the curve

following an intraperitoneal glucose injection 1 week after streptozotocin injection in mice fed a HFD and treated with anti-IL-1ß and/or salicylate for 18 weeks.

(a-c,e-f) n=10/group, (d) 6-9/group, 1 experiment. *P < 0.05, **P < 0.01, ***P < 0.001, ****P < 0.0001. Statistical significance (P) was determined using the two-tailed Mann-Whitney U test. All error bars denote s.e.m. Abbreviations: High fat diet (HFD), streptozotocin (STZ), anti-IL-1ß (aIL-1ß), sodium salicylate (salicylate).

Fig. 3. Analysis of the diet-induced obese (DIO) mouse model following long-term treatment with anti-IL-1ß and/or salicylate

8 week-old mice were fed a high fat diet (HFD) for 10 weeks, randomized and subsequently treated with salicylate or salicylate/anti-IL-1ß at 19 weeks of age. A small cohort of chow-diet (CD) fed mice was analyzed in parallel. (a) Weight growth curves over time for the different treatment groups compared to HFD control. (b,d) Plasma glucose, insulin levels and corresponding area under the curve following (b) an intraperitoneal glucose injection 2 weeks after treatment initiation and (d) oral glucose gavage 8 weeks after treatment initiation. (c,e) Plasma glucose levels following an intraperitoneal insulin injections (c) 3 and (e) 6 weeks after treatment initiation. (f) HbA1c levels 9 weeks after treatment initiation.

(a-f) n=4,5,5 and 2 for HFD, salicylate, salicylate/aIL-1ß and CD, respectively. No statistical analysis was performed due to low number of animals in only 1 experiment. All error bars denote s.e.m. Abbreviations: Chow diet (CD), high fat diet (HFD), anti-IL-1ß (aIL-1ß), sodium salicylate (salicylate).

Fig. 4. Analysis of the diet-induced obese (DIO) / streptozotocin (STZ) mouse model following treatment with anti-IL-1ß and/or anti-TNFα

4 week-old mice were fed a high fat diet (HFD) followed by a single injection of STZ at 8 weeks of age simultaneously beginning treatment with anti-IL-1ß and/or aTNFα. Control mice either received no HFD (CD) or were not injected with STZ (HFD). (a) Weight growth curves and (b) random blood glucose levels over time. (c) Random and (d) 6h-fasting plasma glucose levels 2 weeks after STZ and treatment begin. (e) Glucose, insulin levels and corresponding area under the curve following an intraperitoneal glucose injection 2 weeks after STZ and treatment begin. (f) Glucose levels following an intraperitoneal insulin injection 2 weeks after STZ and treatment begin.

(g) Western Blot quantification of pAKT/AKT ratio in liver lysate, 11 minutes after exogenous insulin injection. (h) mRNA expression levels and (i) ex-vivo glucose-induced insulin secretion in isolated islets.

(a-e) n=10-11/group, 2 experiments. (g) 4/group, 2 experiments. (h) 7-11/group, 2 experiments. (h) 10/group, 2 experiments. *P < 0.05, **P < 0.01, ***P < 0.001, ****P < 0.0001. Statistical significance (P) was determined using the two-tailed Mann-Whitney U test. All error bars denote s.e.m. Abbreviations: Chow-diet (CD), high fat diet (HFD), streptozotocin (STZ), anti-IL-1ß (aIL-1ß), anti-TNFα (aTNFα).

Fig. 5. Analysis of the diet-induced obese (DIO) / streptozotocin (STZ) mouse model following therapeutic treatment with anti-TNFα

4 week-old mice were fed a high fat diet (HFD) followed by a single injection of STZ at 8 weeks of age. 2 weeks later, treatment with aTNFα was initiated. Control mice were not injected with STZ (HFD). (a) Weight growth curves and (b) random and (c) fasting blood glucose levels after treatment initiation over time. (d) Glucose levels and corresponding area under the curve following an intraperitoneal glucose injection 2 weeks after treatment initiation.

(a-d) n=4,6,6 for HFD, HFD/STZ and HFD/STZ/aTNFα, respectively. 1 experiment.

*P < 0.05, **P < 0.01, ***P < 0.001, ****P < 0.0001. Statistical significance (P) was determined using the two-tailed Mann-Whitney U test. All error bars denote s.e.m. Abbreviations: High fat diet (HFD), streptozotocin (STZ), anti-TNFα (aTNFα).

Fig. 6. Analysis of the diet-induced obese (DIO) mouse model following long-term treatment with anti-IL-1ß and/or anti-TNFα

8 week-old mice were fed a high fat diet (HFD) for 10 weeks, randomized and subsequently treated with anti-IL-1ß and/or anti-TNFα at 19 weeks of age. Anti-TNFα was initially given at 1mg/g and raised to 5mg/g 3 weeks after treatment initiation. A small cohort of chow-diet (CD) fed mice was analyzed in parallel. (a) Weight growth curves over time. (b,d) Plasma glucose, insulin levels and corresponding area under the curve following an intraperitoneal glucose injection (b) 2 and (d) 6 weeks after treatment initiation. (c,e) Plasma glucose levels following an intraperitoneal insulin injections (c) 3 and (e) 7 weeks after treatment initiation. (f) HbA1c levels 8 weeks after treatment initiation. (g) mRNA expression levels in isolated islets 8 weeks after treatment initiation.

(a-f) n=4 for CD and 6 for all other groups, 1 experiment. (g) n=6/group, 1 experiment. *P < 0.05, **P < 0.01, ***P < 0.001, ****P < 0.0001. Statistical significance (P) was determined using the two-tailed Mann-Whitney U test. All error bars denote s.e.m. Abbreviations: Chow diet (CD), high fat diet (HFD), anti-IL-1ß (aIL-1ß), anti-TNFα (aTNFα).

Figure 7. Effect of Salicylate on mouse islets in vitro

(a) Glucose-induced insulin secretion in pancreatic mouse islets. (b,c) Oxygen consumption rate after (b) 24h chronic, or (c) 30min acute treatment pancreatic mouse islets, challenged with glucose, oligomycin, FCCP and rotenone.

(a) n=8/group, 2 experiments. (b,c) n=5/group, 1 experiment. *P < 0.05, **P < 0.01, ***P < 0.001, ****P < 0.0001. Statistical significance (P) was determined using the two-tailed Mann-Whitney U test. All error bars denote s.e.m. Abbreviations: Oxygen consumption rate (OCR).

Figures

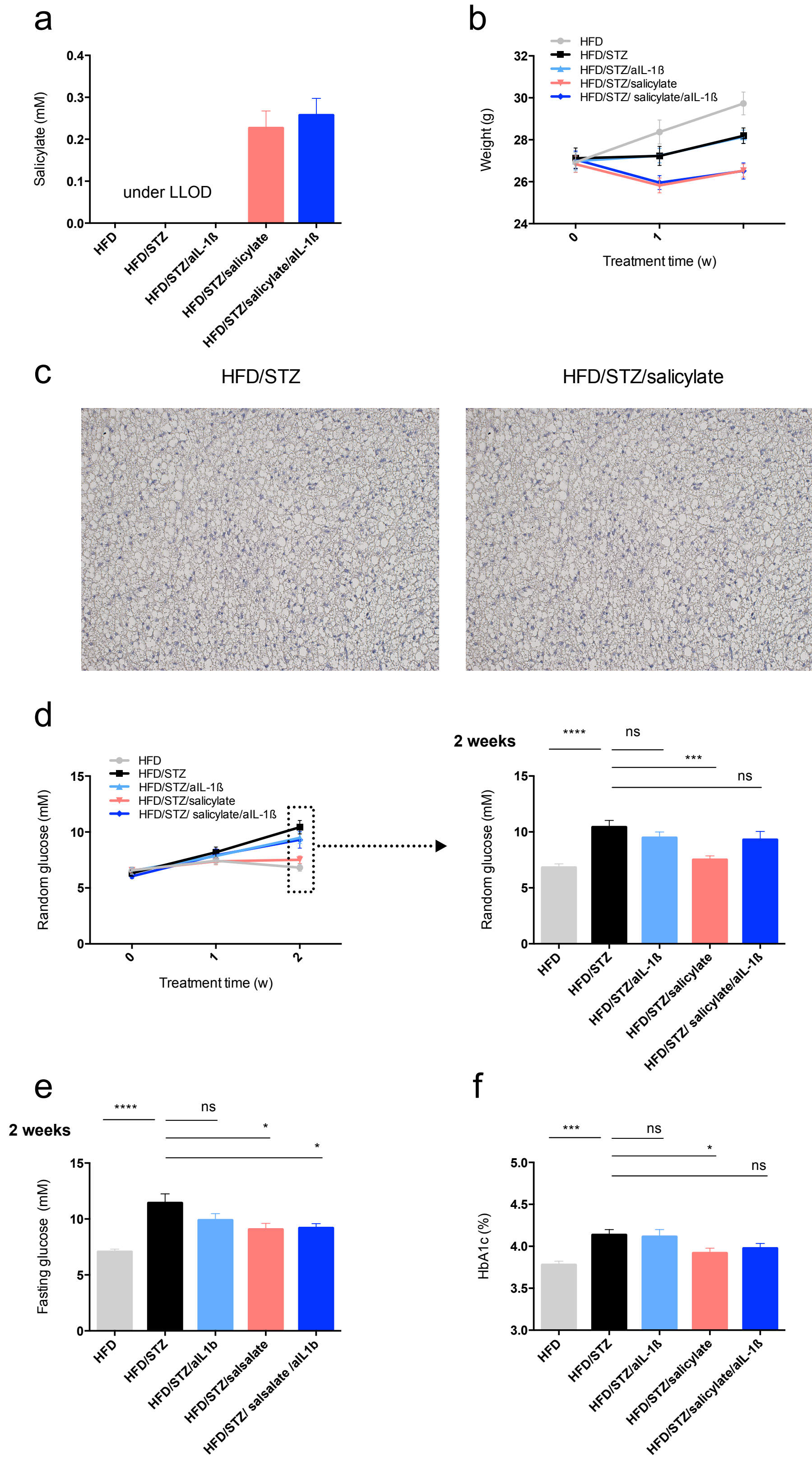

Fig. 1. cont.

g

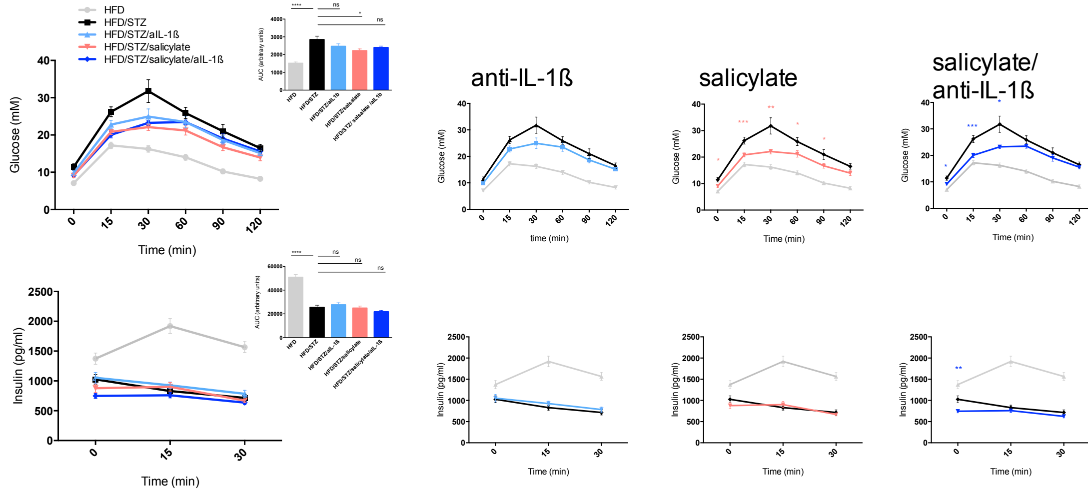

h

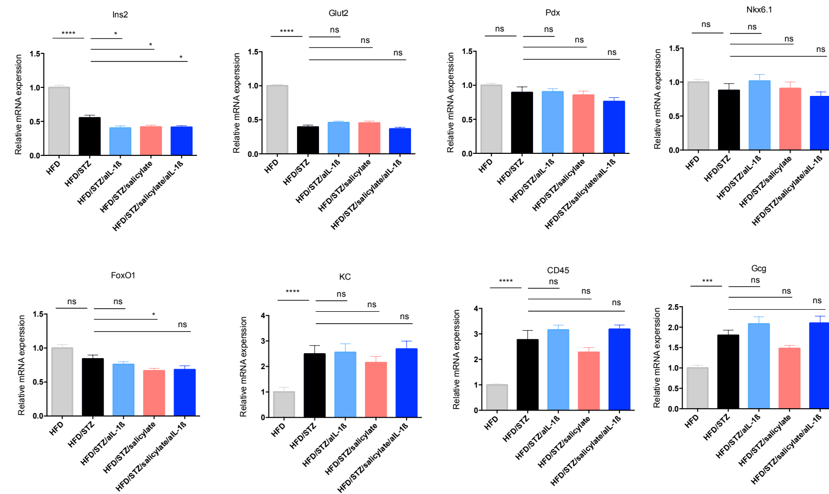

i

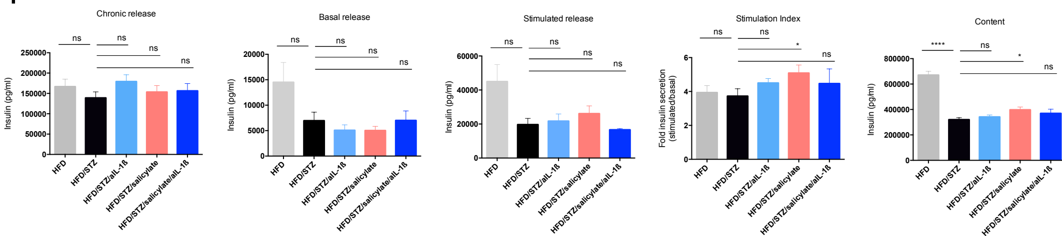

a

Fig. 2

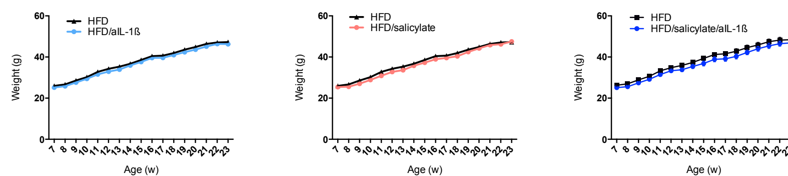

b

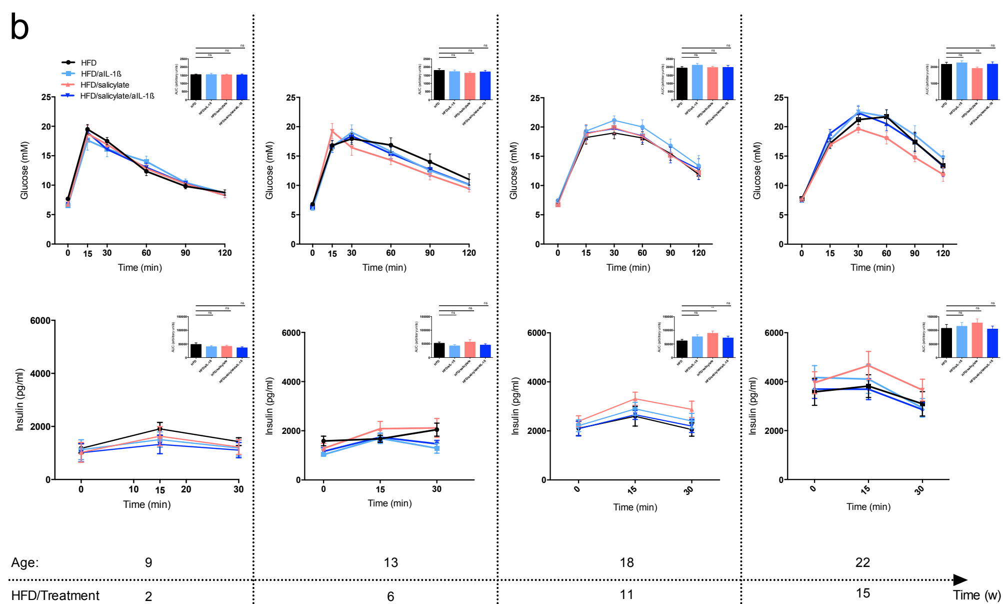

c

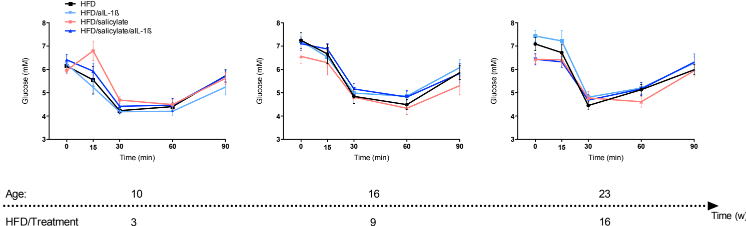

d

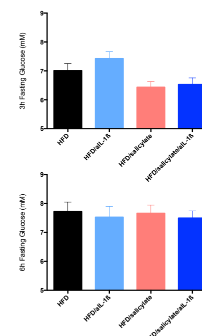

e

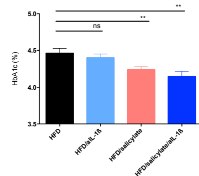

f

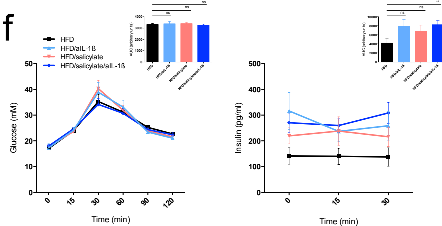

a

Fig. 3

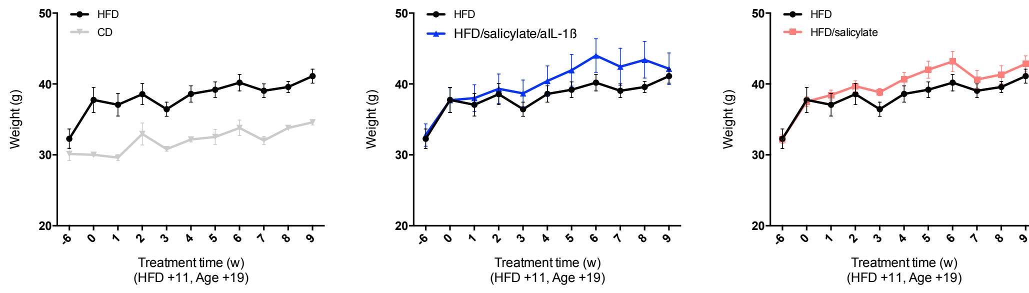

b

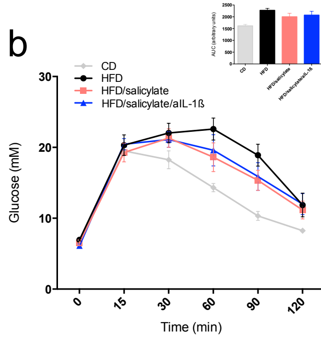

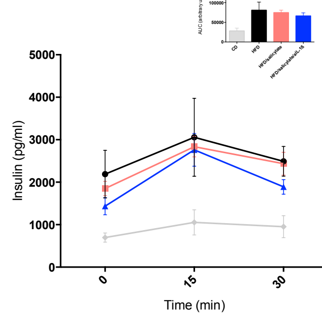

c

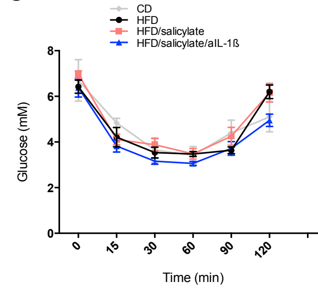

d

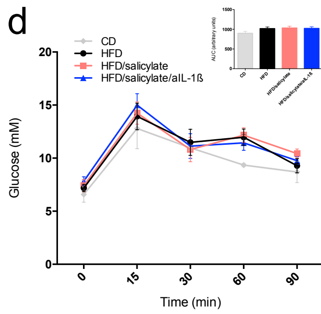

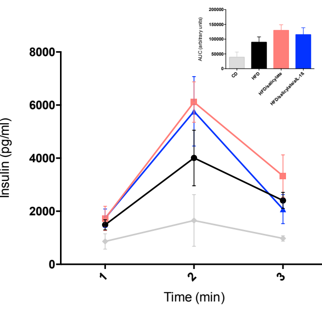

e

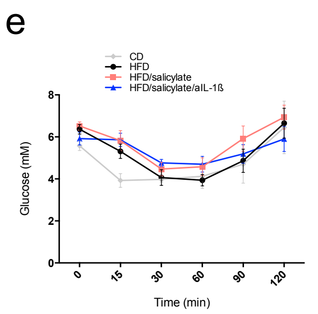

f

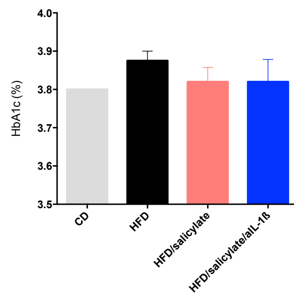

Fig. 4

a

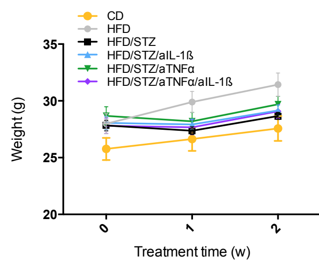

b

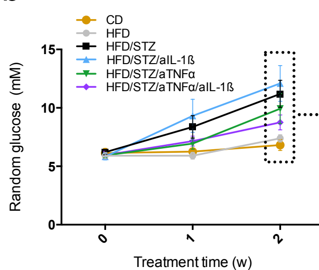

c

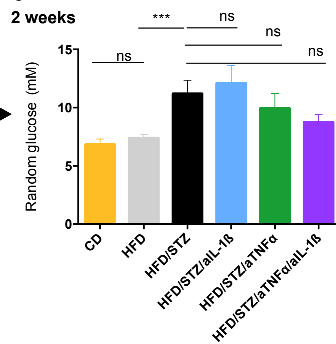

d

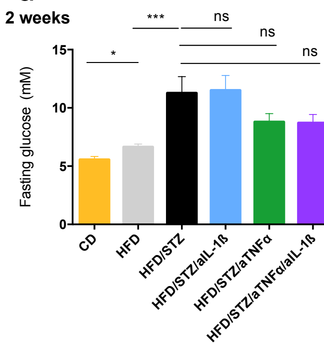

e

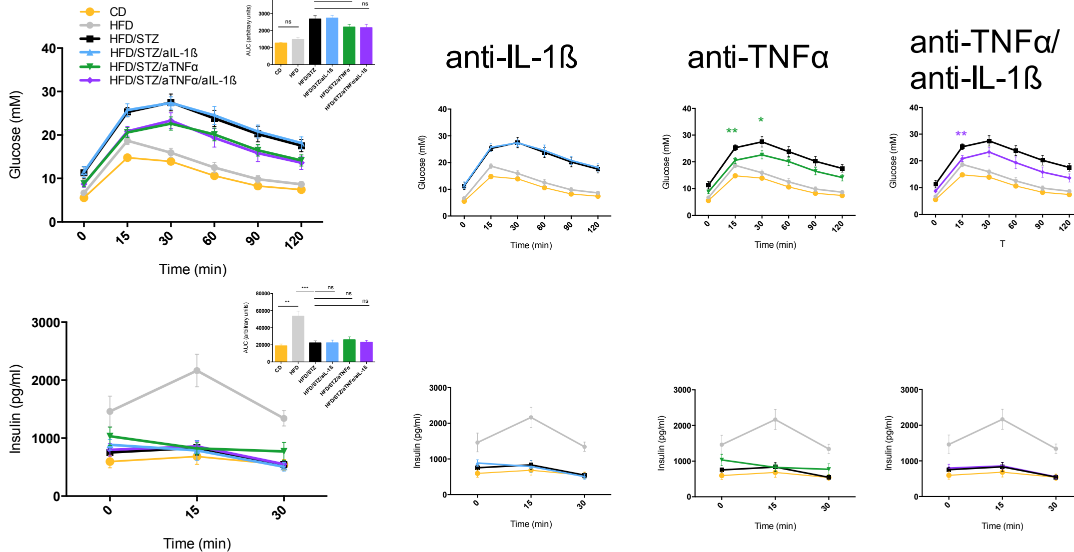

Fig. 4. cont.

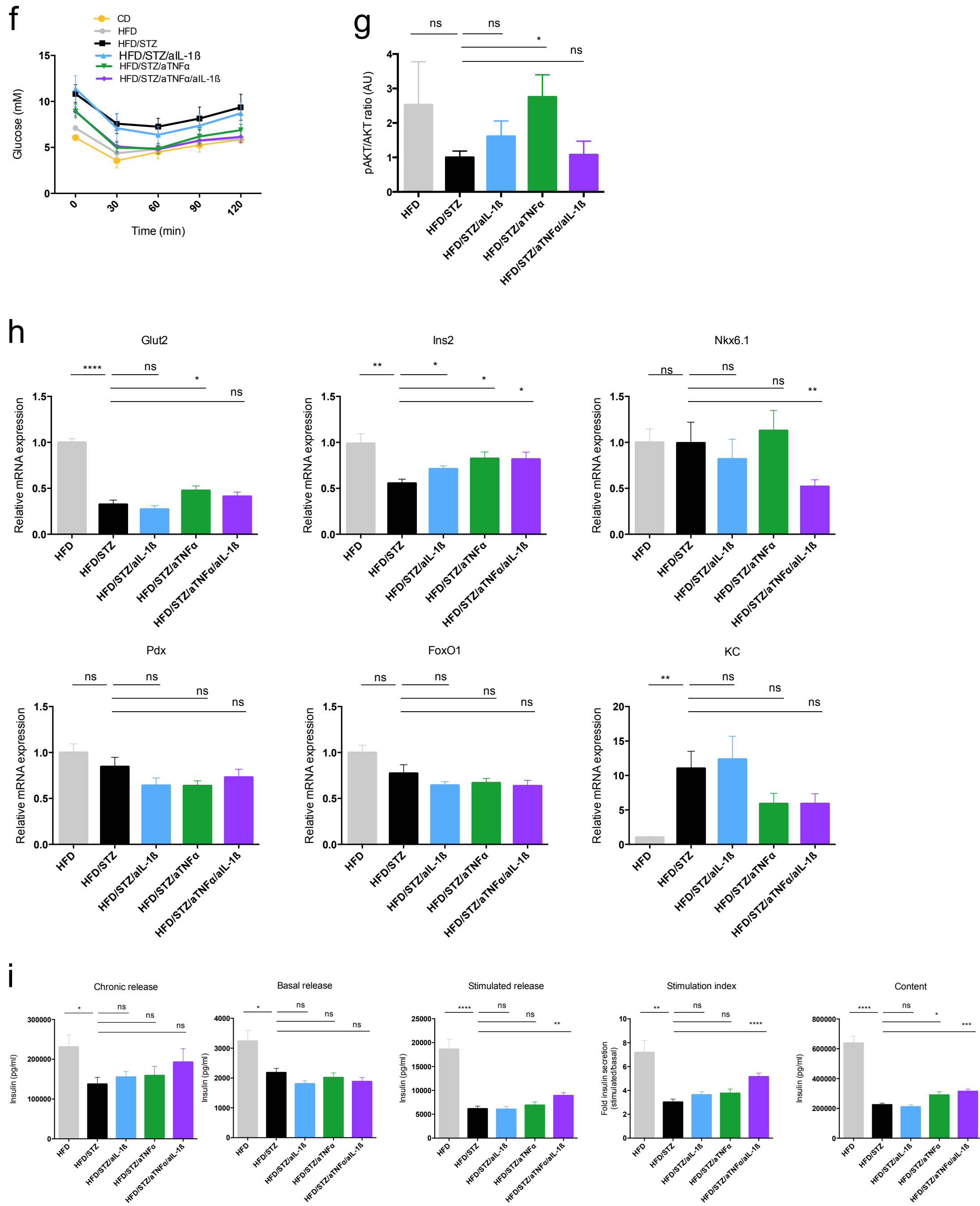

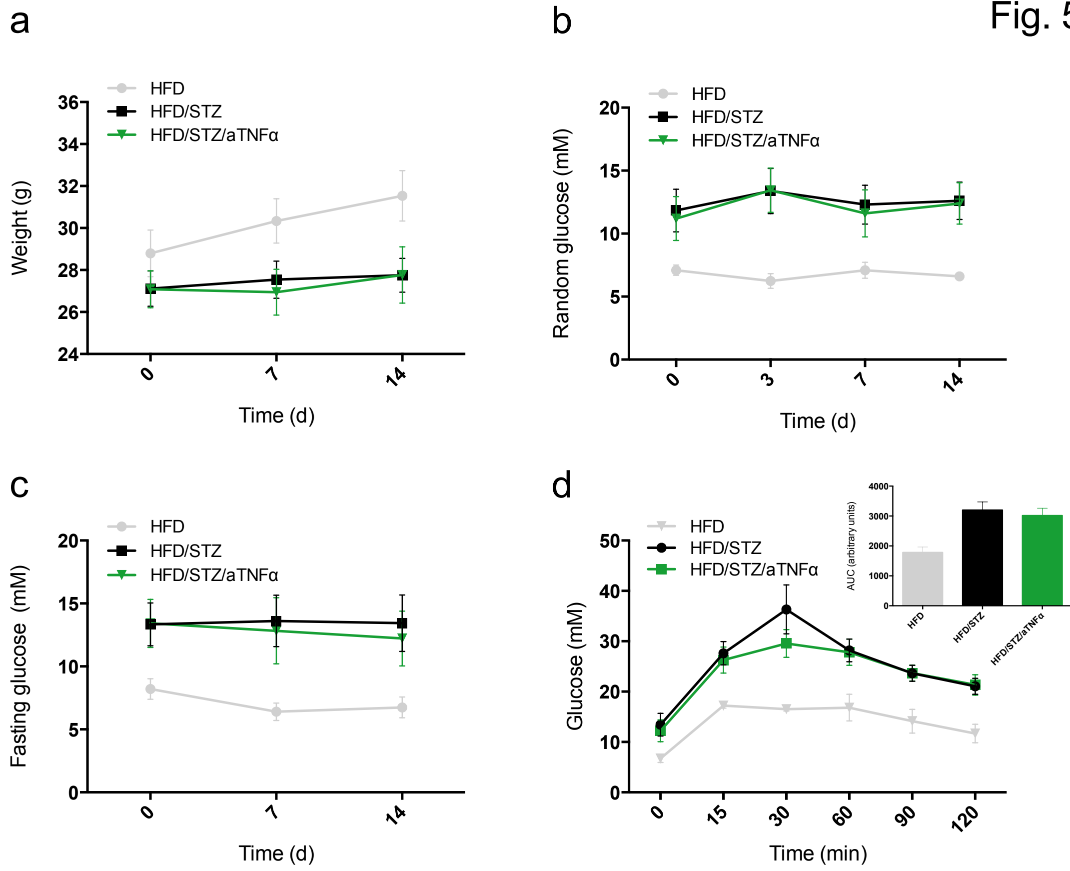
Fig. 5
a
HFD
HFD/STZ
HFD/STZ/aTNFα
Weight (g)
36
34
32
30
28
26
24
0
7
14
Time (d)
b
HFD
HFD/STZ
HFD/STZ/aTNFα
Random glucose (mM)
20
15
10
5
0
0
3
7
14
Time (d)
c
HFD
HFD/STZ
HFD/STZ/aTNFα
Fasting glucose (mM)
20
15
10
5
0
0
7
14
Time (d)
d
HFD
HFD/STZ
HFD/STZ/aTNFα
Glucose (mM)
50
40
30
20
10
0
0
15
30
60
90
120
Time (min)
AUC (arbitrary units)
4000
3000
2000
1000
0
HFD
HFD/STZ
HFD/STZ/aTNFα

Fig. 6.

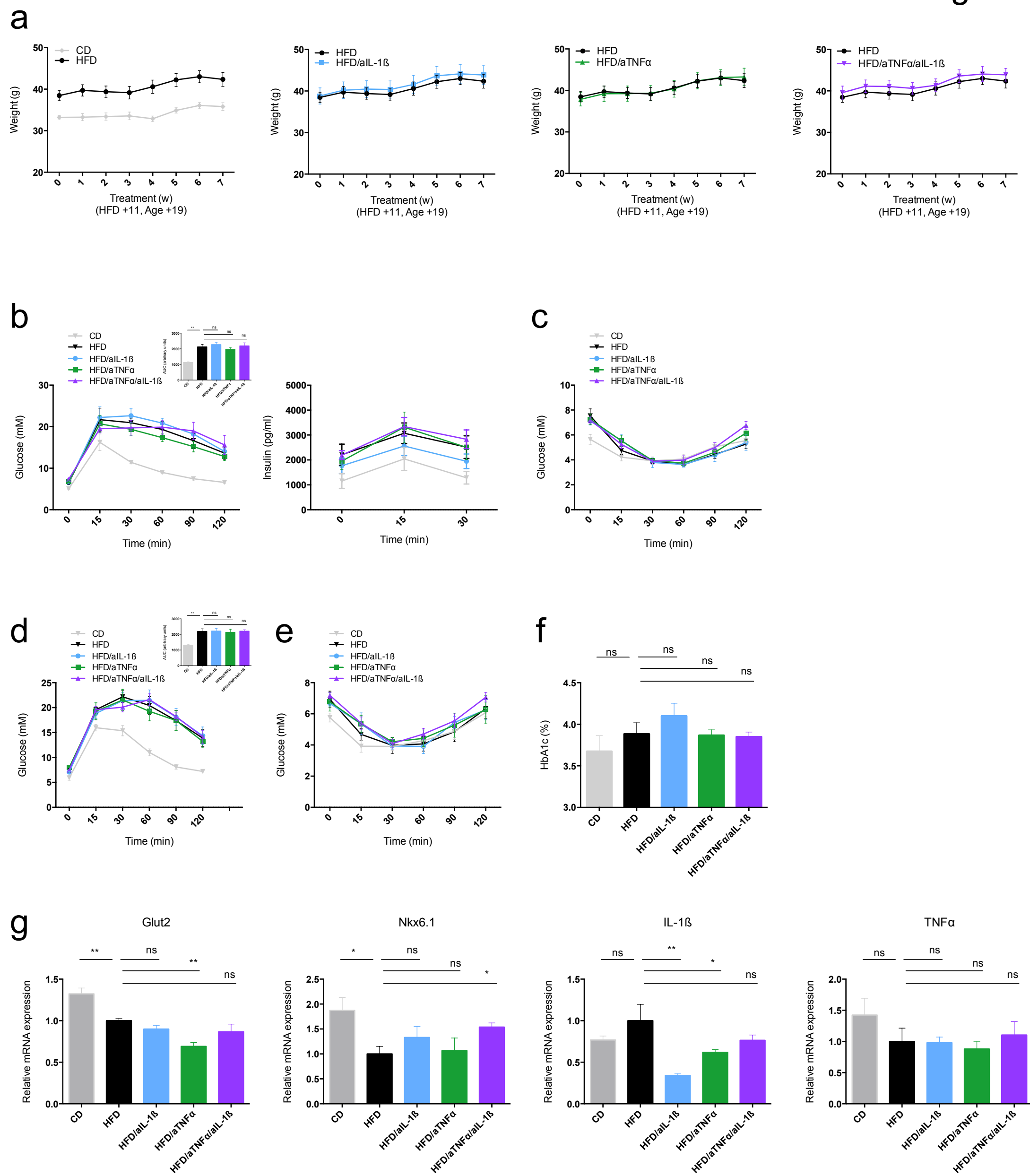

Fig. 7

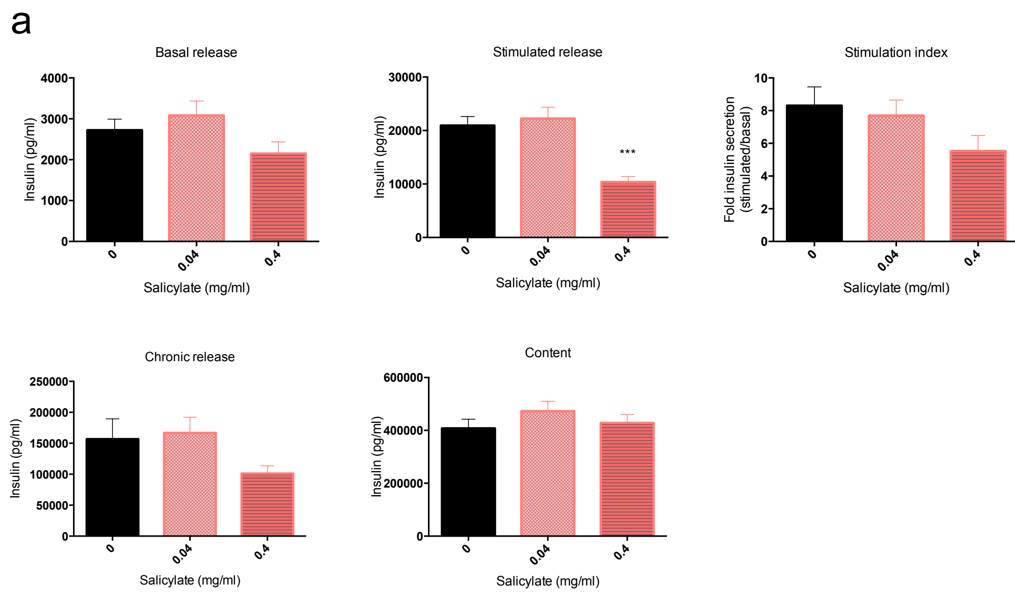

b

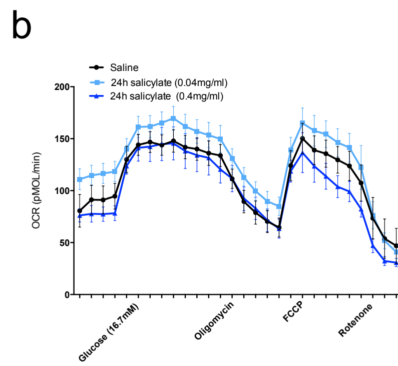

c

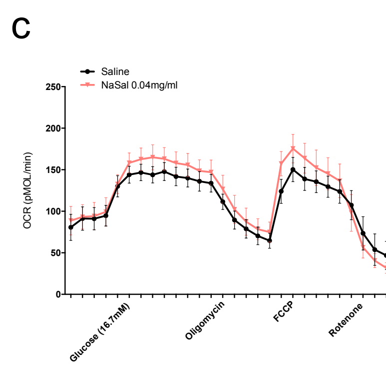

III. Muscle-derived IL-6 is not regulated by IL-1 during exercise

(published, doi: 10.1371/journal.pone.0139662)

A double blind, placebo-controlled, randomized crossover study.

Thierry M. Nordmann[1¶]*, Eleonora Seelig[1¶], Katharina Timper[1¶], Mareike Cordes[2], Michael Coslovsky[3], Henner Hanssen[2], Arno Schmidt-Trucksäss[2], Marc Y. Donath[1]

[1]Clinic of Endocrinology, Diabetes and Metabolism University Hospital Basel, and Department Biomedicine. University of Basel, 4031 Basel, Switzerland

[2]Division of Sports and Exercise Medicine, Department of Sport, Exercise and Health, Medical Faculty, University of Basel, Basel, Switzerland

[3]Clinical Trial Unit, University Hospital Basel, 4031 Basel, Switzerland

* Corresponding author

E-mail: t.nordmann@unibas.ch

¶ These authors contributed equally to this work, in alphabetical order.

Abstract

Exercise increases muscle derived Interleukin-6 (IL-6) leading to insulin secretion via glucagon-like peptide-1. IL-1 antagonism improves glycemia and decreases systemic inflammation including IL-6 in patients with type 2 diabetes. However, it is not known whether physiological, exercise-induced muscle-derived IL-6 is also regulated by the IL-1 system. Therefore we conducted a double blind, crossover study in 17 healthy male subjects randomized to receive either the IL-1 receptor antagonist IL-1Ra (anakinra) or placebo prior to an acute treadmill exercise. Muscle activity led to a 2-3 fold increase in serum IL-6 concentrations but anakinra had no effect on this exercise-induced IL-6. Furthermore, the IL-1 responsive inflammatory markers CRP, cortisol and MCP-1 remained largely unaffected by exercise and anakinra. We conclude that the beneficial effect of muscle-induced IL-6 is not meaningfully affected by IL-1 antagonism.

Keywords: IL-6, IL-1, cortisol, muscle, exercise

Introduction

Exercise improves glycaemia in patients with type 2 diabetes. This is due to multiple factors including increased calorie consumption and insulin independent glucose uptake in muscle. Furthermore, the active muscle produces several molecules that may have endocrine functions and contribute to the beneficial effect of exercise on metabolism [138, 139]. Indeed, in response to muscle contraction, IL-6 is released into the circulation in abundance [139]. Under physiological conditions, IL-6 appears to increase insulin sensitivity [118]. Furthermore, we have recently shown that IL-6 enhances glucagon-like peptide-1-mediated insulin secretion [9]. However, possibly due to the prevailing inflammation, in obese individuals IL-6 may have negative effects and precipitate insulin resistance [117].

Numerous observations and clinical studies have shown that inflammation has a substantial role in the pathogenesis of type 2 diabetes. In particular, pathological activation of IL-1 contributes to impaired insulin secretion and action [140]. Accordingly, IL-1 antagonism improves glycaemia and β-cell secretory function in patients with type 2 diabetes [96, 110]. Furthermore, IL-1 blockade reduces systemic inflammation including IL-6 [96, 110].

Little is known about the regulation of muscle-derived IL-6 during exercise. Although it seems to be independent of the nuclear factor 'kappa-light-chain-enhancer' of activated B-cells (NFκB)-pathway [141], it is not known whether IL-1 regulates muscle derived IL-6 during contraction. Therefore, the aim of this study was to investigate whether exercise-induced IL-6 is dependent on the IL-1 system. Furthermore, because IL-1β is linked to fatigue in patients with type 2 diabetes [142] and stimulates the hypothalamic-pituitary-adrenal axis [143], fatigue and cortisol levels were also studied.

Materials and Methods

Study design

The clinical study was designed as a double-blind, randomized, placebo-controlled, crossover, single-center study. Patient recruitment and all follow up visits were performed from November 2011 to May 2013 at the University Hospital Basel, Switzerland in accordance with the ICH-GCP guidelines and the Declaration of Helsinki, and approved by the Ethics Committee of Basel (Ref. 294/10) and Swissmedic (Ref. Nr. 2011DR1084). The study was registered on clinicaltrials.gov (NCT01771445). Because this study is a mechanistic study and not a treatment study, we realized only with a 3-month delay that it had to be registered. The authors confirm that all ongoing and related trials for this drug/intervention are registered. Written informed consent was obtained from all participants before study inclusion. The sample size was based on clinical and practical considerations.

Study participants

Subjects were eligible for the study if they were male, apparently healthy, non-smoking, aged between 20 and 50 years with a body mass index between 18 and 26 kg/m^2. Further inclusion criteria were regular exercise including a minimum of two runs weekly with a total duration of more than 2 hours.

Subjects were excluded if they showed clinical signs of infection, impaired fasting plasma glucose of more than 5.5 mmol/L, hematologic, renal, hepatic, cardiac, pulmonary or inflammatory disease, history of carcinoma or tuberculosis, increased alcohol consumption, known allergy to anakinra and current treatment with any drug. Subjects were not eligible for the study if they had used any investigational drug within 30 days prior to enrollment or within 5 half-lives of the investigational drug, whichever was longer.

Treatment Assignment and Blinding

Once screening was completed and subject eligibility was confirmed, a subject was assigned a subject number randomly assigned to receive study medication. The

Clinical Trial Unit of the University Hospital Basel, Switzerland, was responsible for treatment blinding and preparation of trial drugs throughout the study.

Study procedure

The study consisted of one screening visit followed by 2 study visits separated by 7 days, and a follow up visit.

At the screening visit, a physical and laboratory examination, and an ECG were performed. Body composition was assessed using the Body Impedance Analyzer (Bodyimpedance Analyzer Model BIA 101, Akern Srl Florence Italy). A treadmill ergometer test was performed determining individual heart rate-oxygen consumption (VO_2) relationships, and VO_2max on which the exercise load for the acute exercise bout was based. Once eligible, patients were allocated according to a randomization list created by a biostatistician unrelated to the study. Patients as well as study personnel were blinded to the medication allocation.

For the 2 study visits, subjects were requested to fast 6-10 hours prior to the visit and were then asked to fill in an Activity Induced Fatigue Scale [144] followed by the Symbol Digit Modalities Test, a cognitive screening-test to evaluate information processing speed and working memory [145] and the Beck-Depression-Inventory Fast Screen to evaluate the impact of fatigue on cognitive, motoric, and emotional behavior [145]. Afterwards an intravenous catheter for blood drawings was placed in the forearm. 60 minutes before the start of the exercise bout and right after the first blood sample was taken, subjects received a single subcutaneous injection of 100mg anakinra (Kineret®) or placebo in a double-blind, crossover manner. At time 0, the subject started to run with a 5 minutes warm up period at 2 to 4 km/h at an incline of 0.5%. The treadmill speed was then increased to 75% of VO_{2max} based on heart rate measurements for 60 minutes followed by a "cool down" at walking speed for 5 minutes. 60 minutes after exercise the intravenous catheter was removed. In total, blood was drawn at 12 time points: 60 minutes before exercising (-60min.), every ten minutes starting immediately prior to the exercise until immediately after (0, 10, 20, 30, 40, 50, 60min.) and four times within the hour following the exercise (+10aE, 20aE, 30aE, 60aE). 1-2 hours after the end of the exercise bout, the study participants were asked again to fill in the fatigue, processing and emotional tests. The same

procedures were performed one week after the first visit followed by a safety visit after an additional week.

Study endpoints

Primary outcome measure was change in exercise-stimulated IL-6 plasma levels after administration of placebo and anakinra.

Secondary outcome measures were change in plasma levels of glucose, cortisol, inflammatory markers (high-sensitive (hs)-CRP, IL-8, monocyte chemotactic protein 1 (MCP-1)), and creatine kinase, as well as fatigue, information processing speed and working memory, and depression/ cognitive, motoric and emotional features.

Sample collection and analytic procedure

Blood was collected into prechilled tubes that were immediately centrifuged at 4°C and aliquoted. All samples were immediately frozen and stored at -80°C until measurement. IL-6, IL-8, IL-1Ra, keratinocyte-derived chemokine (KC) and MCP-1 were measured using an electrochemiluminescence immunoassay according to the manufacturer's instructions (Mesoscale Discovery [MSD], Gaithersburg, MD, USA). MSD plates were analyzed on a Sector™ MSD 2400 instrument and data were analyzed using DISCOVERY WORKBENCH 4.0 software. Measurements of hs-CRP, cortisol, and glucose were performed by automated biochemical analyses in the University Hospital Central Laboratories.

MIN6B1 cell cultures

MIN6B1 cells were kindly provided by Dr. Philippe Halban (University of Geneva, Geneva, Switzerland) with permission from Dr. Junichi Miyazaki, University of Osaka. 3.5×10^4 cells per well were seeded in 96-well plates and cultured in DMEM supplemented with 15% fetal bovine serum (FBS), 100 U/mL penicillin, 100 µg/mL streptomycin for 48 hours. Cells were subsequently incubated with 20v/v % of patient serum obtained at time point -60 and 40 min. after anakinra injection or after placebo from one study participant, in combination with 0.02 ng/ml recombinant mouse IL-1β

(rmIL-1β; R&D Systems, Abingdon, UK) for 24 hours. Supernatant was harvested and KC levels were analyzed as outlined above.

Statistical analysis

Descriptive measurements are reported as median and interquartile range.

For the pre-exercise time, the absolute change in biomarker measurement was calculated by detracting the values at injection time (-60 min.) from those at exercise begin (0 min.) in each period and modeling them.

To analyze the repeated measurements during exercise, linear mixed-effects models (LMM) were utilized. Endpoints were log-transformed in models where heteroscedasticity was detected. All models included study period as a fixed effect, to account for the crossover design. The interaction of study period and treatment was tested in all models; however, since it never was significant for biomarker models (all $p > 0.33$), it was removed from all biomarker models. Treatment arm and time were included as fixed effects in the models. To test for linear and quadratic trends in time, time and time-squared were entered as continuous variables centered on mean exercise time (30 min.). The interactions between both time terms and the treatment-arm were first included in models, and when not significant, removed to make interpretation of main effects easier. To account for non-independence of measurements from the same subject, subject ID was included as a random effect in all models. In addition, models with >2 time points of measurements included an auto-regressive correlation structure of order 1 (AR1) to account for the correlation between observations measured close to each other. Least square means (predicted marginal values) and confidence intervals were calculated at specific time points for post-hoc tests. Marginal p-values are reported.

Fatigue and depression-indices measurements were analyzed similarly as described above, except that, since having only two measurements per endpoint, an ANCOVA approach was used. The post-exercise measurement was modeled with the pre-exercise measurement as a covariate and including study period, treatment and their interaction as fixed effects. As above, subject ID was included as a random effect in the models.

Analysis was performed using R - 3.2.0 (R Core Team, 2015). Mixed effects models were fit using the R-package nlme (Pinheiro & Bates, 2000). LS means were calculated using the lsmeans package (Lenth & Hervé, 2015).

Results

Participant flow

Out of 19 subjects enrolled in the study 17 completed the study and were analyzed (Fig. 1). Two subjects dropped out after the first exercise bout, one due to the difficulties due to blood sampling during the exercise and one due to a musculoskeletal injury after the visit.

Baseline characteristics

Median age was 25 [23, 32] years and median body mass index was 23 [21, 25] kg/m^2 (Table 1). The individuals studied reflected a typical population of apparently healthy Swiss people of the same age and body mass index.

IL-6

Plasma levels of IL-6 increased 2-3 fold from beginning to the end of exercise (Fig. 2; placebo: 0.78 [0.55, 1.14] pg/ml to 2.32 [1.75, 3.11] pg/ml; anakinra: 0.63 [0.56, 0.95] pg/ml to 1.91 [1.54, 2.48] pg/ml) following a quadratic trend ($p < 0.001$). There was no difference in the increase of IL-6 levels over time between treatment groups (quadratic interaction: $p = 0.189$; linear Interaction: $p = 0.595$) and no overall difference in absolute IL-6 levels between placebo and anakinra treatment ($p = 0.172$). Estimated values per time point and model summary are provided in Table A and Table B in S1 File, respectively.

IL-8, hs-CRP, MCP-1

Plasma levels of IL-8 slightly increased from beginning to the end of exercise (Fig. 3; placebo: 6.70 [5.96, 7.38] pg/ml to 8.71 [6.31, 11.13] pg/ml; anakinra (7.54 [5.91, 9.09] pg/ml to 8.43 [7.35, 9.30] pg/ml) following a linear trend ($p = <0.001$). There was no difference in the increase of IL-8 levels over time between treatment groups (linear interaction $p = 0.998$; quadratic interaction $p= 0.502$) and no overall difference in absolute IL-8 levels between placebo and anakinra treatment ($p = 0.743$). Estimated

values per time point and model summary and are provided in Table C and Table D in S1 File, respectively.

Hs-CRP did not change over time during exercise in both treatment groups (Fig. 4; placebo: 0.55 [0.24, 0.85] mg/l to 0.41 [0.23, 0.85] mg/l; anakinra: 0.52 [0.20, 1.12] mg/l to 0.53 [0.22, 1.22] mg/l). Summary of the model is given in Table E in S1 File.

MCP-1, measured at 60 min. before and at 40 min. during exercise, decreased during exercise (Fig. 5; placebo: 264.68 [224.63, 303.99] pg/ml to 238.75 [201.90, 278.36] pg/ml; anakinra 244.61 [201.84, 335.73] pg/ml to 252.62 [223.63, 327.62] pg/ml). There was no difference in the decrease of MCP-1 levels between treatment groups ($p = 0.52$) and no overall difference in absolute levels between placebo and anakinra (-60 min.: $p = 0.970$; 40 min.: $p = 0.500$).

Glucose

There was a significant decrease in glucose levels from injection time to exercise begin (Fig. 6; placebo: 4.60 [4.40, 4.80] mmol/l to 4.30 [4.10, 4.60] mmol/l; anakinra: 4.70 [4.60, 4.80] mmol/l to 4.60 [4.40, 4.70] mmol/l; $p=0.038$). The change in glucose values over time did not differ among the treatments ($p = 0.466$). Interestingly, glucose levels in the anakinra treated group were overall slightly higher compared to the placebo treated group ($p=0.06$).

During exercise, glucose levels increased slightly (Fig. 6; placebo: 4.30 [4.10, 4.60] mmol/l to 4.45 [4.07, 4.75] mmol/l; anakinra: 4.60 [4.40, 4.70] mmol/l to 4.75 [4.18, 4.93] mmol/l), following a quadratic trend ($p < 0.001$). There was no difference in the increase of glucose levels over time between treatment groups (quadratic interaction $p = 0.792$; linear interaction $p = 0.758$) and, in contrast to the pre-exercise values, no difference in absolute values at any of the measured time points between placebo and anakinra (all $p > 0.11$). Model summary is provided in Table F in S1 File.

Cortisol

There was a significant decrease in cortisol levels from injection time to exercise begin (Fig. 7; placebo: 400 [320, 527] nmol/l to 350 [287, 441] nmol/l; anakinra 417 [349, 516] nmol/l to 328 [274, 428] nmol/l; $p = 0.019$). While the change from

injection time until the begin of exercise was more pronounced in the anakinra treated subjects (placebo: -19 [-107.5, 22.5] nmol/l; anakinra: -87 [-110.5, -37.5] nmol/l) there was no significant decrease of cortisol levels over time ($p = 0.436$) and no overall difference in absolute cortisol levels between placebo and anakinra treatment ($p = 0.902$).

During exercise, cortisol levels did not change over time (Fig. 7; placebo: 350.00 [287.00, 441.00] nmol/l to 354.50 [228.00, 450.50] nmol/l; anakinra: 328.00 [274.00, 428.00] nmol/l to 391.50 [222.75, 496.00] nmol/l) and did not differ between treatments overall ($p = 0.912$), or at any of the time points measured (all $p > 0.32$). Model summary is provided in Table G in S1 File.

Creatine kinase

Creatine kinase levels, measured 60 minutes before (-60 min.), at the end of exercise (60 min.) and 60 min. after exercise (60 min. aE), increased during exercise (Fig. 8; placebo: 109.0 [79.0, 142.0] U/l to 130.5 [109.5, 189.25] U/l; anakinra 113.0 [81.0, 176.0] U/l to 143.0 [111.25, 227.25 U/l; $p = <0.001$). There was no difference in the increase over time between the treatment groups ($p = 0.912$) and no difference in absolute levels between placebo and anakinra treatment ($p = 0.637$). Model summary is provided in Table H in S1 File.

Fatigue, processing and emotional tests

There was no difference in fatigue measurements between placebo and anakinra treatment (placebo: 25.5 [21.5, 30.05] points to 23 [21.0, 31.5] points; anakinra: 24.0 [21.0, 32.0] points to 25.5 [22.5, 31.5] points). Further, statistical analysis revealed a significant interaction of the treatment sequence ($p=0.05$). Model summary is provided in Table I in S1 File.

There was no difference in the depression indices (placebo: 0 [0, 2] to 0 [0, 1.2] points; anakinra: 0 [0, 1.5] to 0 [0, 2]) before and after exercise and no difference between placebo and anakinra treatment. Interestingly, measurements were lower in the second study visit of each subject, independently of the treatment received. Model summary is provided in Table J in S1 File.

There were also no changes in processing and emotional tests (not shown)

Biological activity of injected Anakinra

Serum levels of IL-1Ra increased following injections of anakinra, along the randomization protocol (Table 2). To investigate whether the batch of injected anakinra led to biologically active inhibition of IL-1, serum of a subject was tested *in vitro* on the pancreatic β-cell line MIN6. As a read out, we used IL-1β induced KC, the rodent homologous of IL-8. IL-1β strongly induced KC secretion in the presence of placebo-serum but not in the presence of anakinra-serum (Fig. 9).

Discussion

The aim of this study was to explore the regulation of muscle-derived IL-6 during exercise and particularly, whether it is regulated via the IL-1 system. Consistent with previous findings [139], plasma IL-6 levels increased significantly during exercise. There was no difference in IL-6 levels after administration of the IL-1 receptor antagonist anakinra and placebo. Furthermore, the IL-1 responsive inflammatory markers IL-8, hsCRP and MCP-1 remained largely unaffected by exercise and anakinra. Therefore, our data support the concept that the release of IL-6 during exercise is a physiological response of the muscle and that it is not regulated by the pro-inflammatory IL-1 system. This finding is crucial in the context of evolving therapies with IL-1 antagonists in patients with type 2 diabetes. IL-1 is a strong inducer of autoinflammatoy processes leading to β-cell death and subsequently diabetes mellitus. It has been shown that IL-1 up regulates IL-6 in vitro [139]. In accordance, IL-1 antagonism decreases levels of IL-6 in chronic inflammatory disease [146]. But compared to IL-1, the role of IL-6 in the pathogenesis of diabetes is controversial. Studies indicating that IL-6 is associated with insulin resistance [117] are challenged by several findings showing that IL-6 actually has insulin-sensitizing effects [118] and that blocking of IL-6 may induce insulin resistance [147]. Moreover, IL-6 mediates insulin secretion during exercise by increasing secretion of glucagon-like peptide 1 [9]. Due to this beneficial effect of IL-6 on glucose metabolism during exercise, we note that there was no evidence of detrimental impact of the IL-1 receptor antagonist on exercise-induced increase of IL-6. Thus, we hypothesize that treatment strategies with IL-1 antagonists will not abolish the beneficial effect of exercise induced IL-6 on glucose metabolism.

The exercise load in our study, compared to other studies [148] is relatively mild, accounting for the only mildly elevated IL-6 levels we observed and limiting our study. Nevertheless, it was our aim to study the effect of muscle-derived IL-6 levels during a physiological setting, avoiding high-intensity activity with subsequent muscle damage. Indeed, the treadmill exercise at our target intensity level of 75% VO2max induced a significant increase in IL-6 levels without affecting pro-inflammatory parameters (hs-CRP, MCP-1, IL-8), which we found to be the optimal setting to study the effect of physiological, muscle-derived IL-6.

IL-1β has been shown to stimulate the release of adrenocorticotropic hormone [143]. While cortisol levels remained stable during exercise, we observed a decrease right after injection of either IL-1Ra or placebo and before physical activity had started. While both groups had a decrease in median cortisol levels, the reduction was more pronounced after treatment with IL-1Ra. It could be that IL-1Ra slightly decreases serum cortisol levels. It will take further investigation to specifically test this hypothesis.

Current literature suggests that IL-1ß is detrimental in the setting of type 2 diabetes and antagonizing it leads to an improvement in glucose homeostasis. In contrast, very low concentrations of IL-1ß promotes insulin secretion [114] possibly explaining that glucose levels were higher during the hour prior to exercise in IL-1Ra compared to placebo treated subjects.

In conclusion, antagonizing IL-1 does not seem to undermine the potential beneficial effect of exercise induced acute IL-6. This finding is important in the context of evolving therapies with IL-1 antagonists in patients with type 2 diabetes. Furthermore, we hypothesize that interleukin-1 receptor antagonist may have a favorable effect in some conditions linked to cortisol overproduction.

Acknowledgements

We thank Kaethi Dembinski, Susanne Ruesch, Susanna Nussbaumer for their excellent technical assistance, Dr. Marianne Böni-Schnetzler for advice, and Dr. Anja Rossmeissl for physical examination of study subjects.

Figure legends

Fig. 1. Study flowchart and CONSORT diagram.

Fig. 2. Plasma IL-6 levels.

Plasma IL-6 levels before (-60 min.), during (0 to 60 min.) and after (+10aE to +60aE min.) exercise. Data represent the median and interquartile range, n = 17 subjects. aE = after exercise.

Fig. 3. Plasma IL-8 levels.

Plasma IL-8 levels before (-60 min.), during (0 to 60 min.) and after (+10aE to +60aE min.) exercise. Data represent the median and interquartile range, n = 17subjects. aE = after exercise.

Fig. 4. Plasma hs-CRP levels.

Plasma hs-CRP levels before (-60 min.), during (0 to 60 min.) and after (+10aE to +60aE min.) exercise. Data represent the median and interquartile range, n = 17 subjects. aE = after exercise.

Fig. 5. Plasma MCP-1 levels.

Plasma MCP-1 levels before (-60 min.) and during (40 min.) exercise. Data represent the median and interquartile range, n = 17 subjects. aE = after exercise.

Fig. 6. Plasma glucose levels.

Plasma glucose levels before (-60 min.), during (0 to 60 min.) and after (+10aE to +60aE min.) exercise. Data represent the median and interquartile range, n = 17 subjects. aE = after exercise.

Fig. 7. Plasma cortisol levels.

Plasma cortisol levels before (-60 min.), during (0 to 60 min.) and after (+20aE, and+60aE min.) exercise (b). Data represent the median and interquartile range, n = 17 subjects. aE = after exercise.

Fig. 8. Plasma creatine kinase levels.

Plasma creatine kinase levels before (-60 min.), during (60 min.) and after (+60aE min.) exercise. Data represent the median and interquartile range, n = 17 subjects. aE = after exercise.

Fig. 9. KC inhibition by anakinra-serum.

Increase in KC concentration in supernatants of MIN6 cells exposed to IL-1β compared to solvent alone in the presence of serum from participant 6 before (-60 min.) and after (40 min.) placebo or anakinra administration. Data represent the median and interquartile range, n =3wells/condition. KC = keratinocyte-derived chemokine.

Figures

Fig. 1

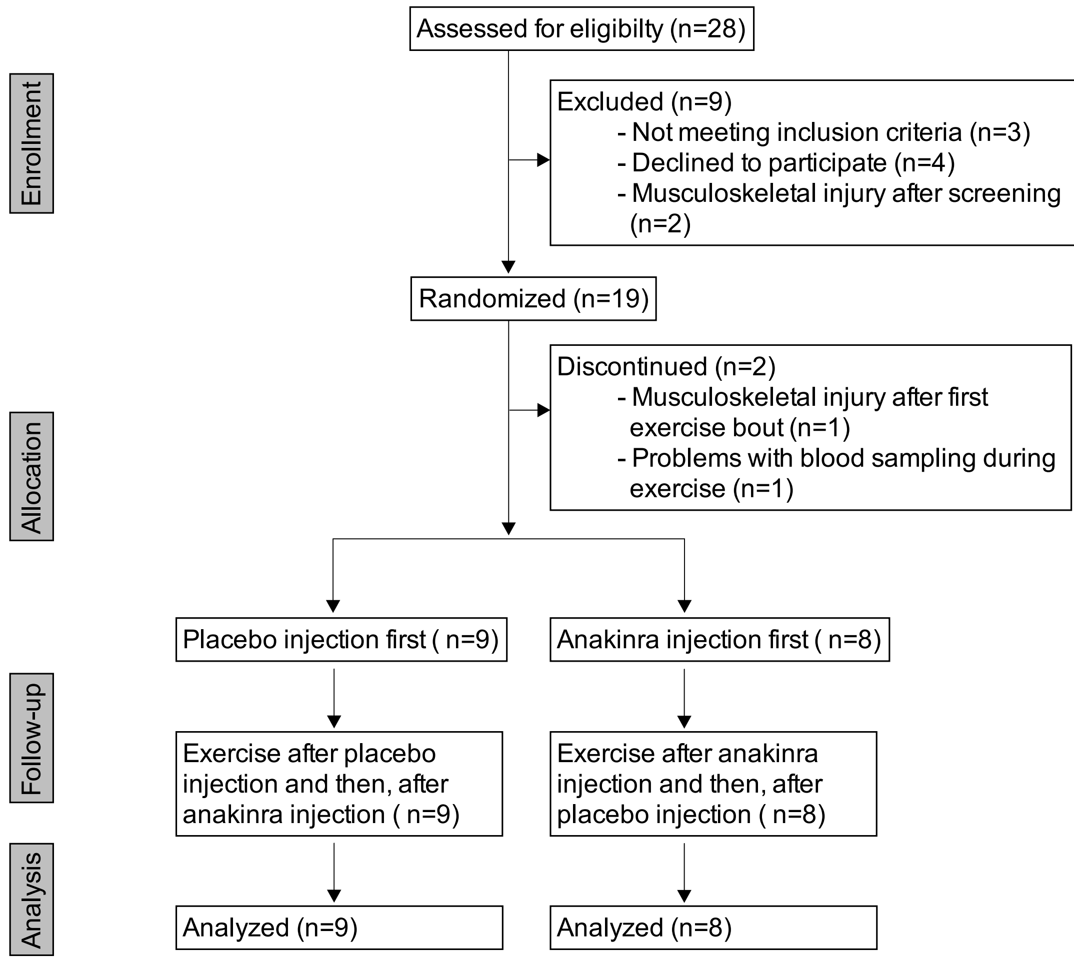

Fig. 2

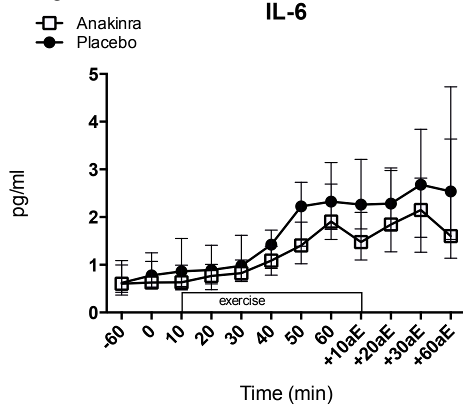

Fig. 3

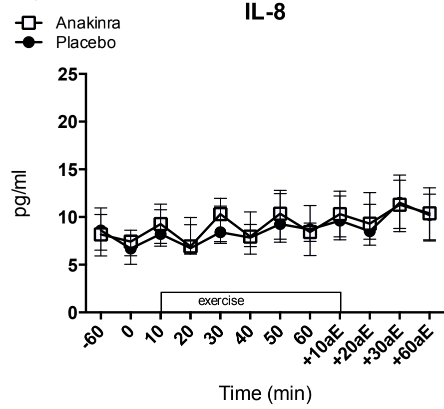

Fig. 4

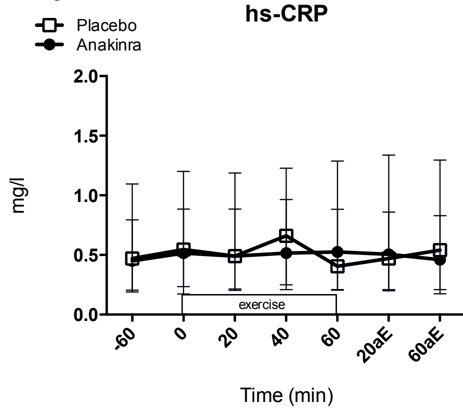

Fig. 5

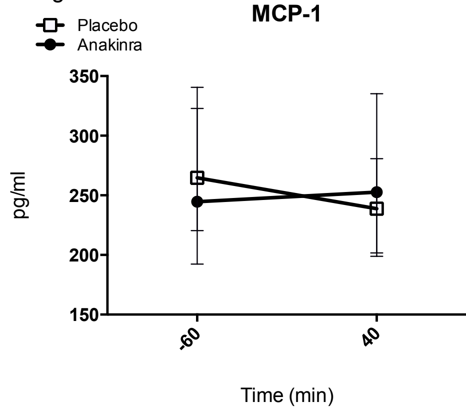

Fig. 6

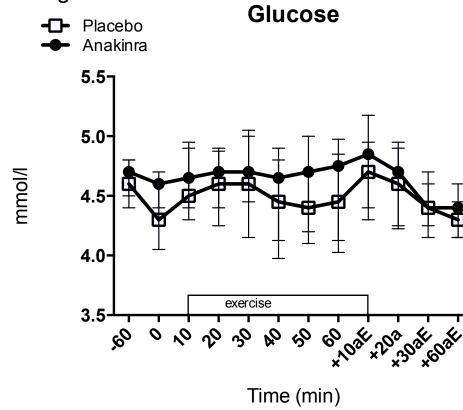

Fig. 7

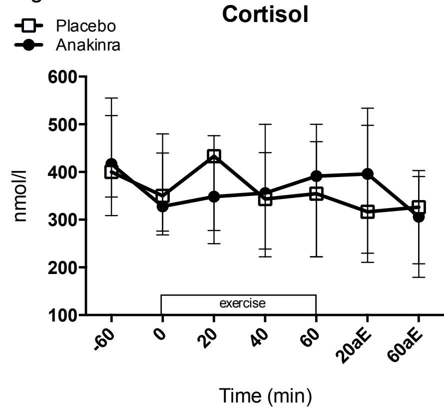

Fig. 8

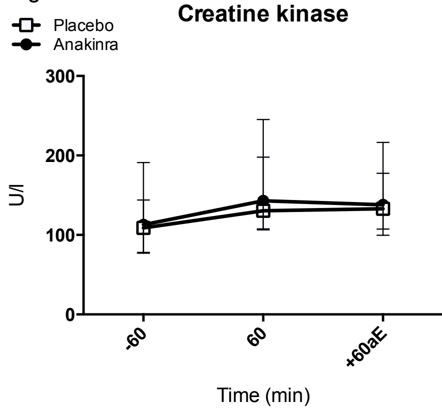

Fig. 9

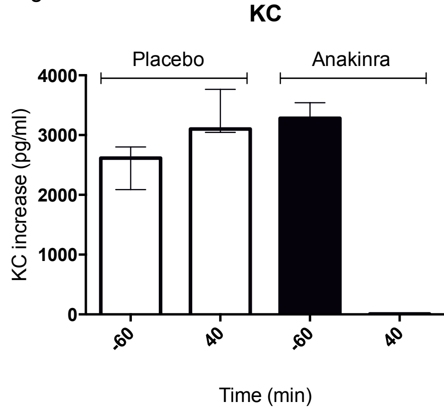

Tables

Table 1. Baseline characteristics of study participants. Data represent the median and interquartile range, n = 17 subjects.

Characteristics	
Age (years)	25 [23, 32]
Pulse (b/min.)	63 [54, 73]
Blood pressure systolic (mmHg)	125 [116, 134]
Blood pressure diastolic (mmHg)	72 [68, 78]
Body mass index (kg/m^2)	23 [21, 25]
Fat free mass (kg; n=13)	39 [35, 40]
Body cell mass (kg; n=13)	23 [20, 25]
Muscle mass (% weight; n=13)	65 [59, 74]
Fat mass (kg/m; n=13)	3 [1, 7]
Basal metabolic rate (kcal; n=13)	1930 [1830, 2035]
Creatinine (µmol/l)	77 [73, 81]
Aspartat aminotransferase (U/l)	24 [21, 29]
Alanine aminotransferase (U/l)	18 [16, 25]
High sensitive CRP (mg/l)	0.6 [0.3, 1]
Leucocytes (x10^9/l)	6 [5, 6]
Haemoglobin (g/l)	151 [143, 149]
Thrombocytes (x10^9/l)	249 [232, 296]

Table 2. Serum interleukin-1 receptor antagonist levels. Serum interleukin-1 receptor antagonist levels (pg/ml) before (-60 min.) and after (40 min.) placebo or anakinra administration. P = participant number.

	Placebo		Anakinra	
P	-60min	40min	-60min	40min
1	328.1	363.6	321.1	25842.5
2	326.6	288.4	360.9	24677.8
3	638.6	579.6	496.5	25780.5
4	339.1	291.5	220.1	20263.2
5	250.7	297.1	275.2	27390.5
6	321.0	364.3	1154.0	24124.1
7	267.4	357.9	254.5	24338.5
8	423.9	363.3	219.2	25185.1
10	232.9	371.5	222.2	27815.5
13	290.9	315.4	251.3	26980.4
14	294.7	387.0	325.9	19689.2
15	294.7	351.7	254.8	25932.2
16	532.4	801.1	456.3	20687.9
17	283.8	369.3	275.2	22316.0
19	209.8	340.0	265.4	20442.1
20	241.6	257.3	260.3	19574.7
21	315.9	468.9	321.0	22807.9

Supporting information

Supporting information can be found online (*doi: 10.1371/journal.pone.0139662)*

Acknowledgments

I would like to thank Prof. Marc Donath for giving me the opportunity to perform my PhD studies in his laboratories. I would like to thank Prof. Marc Donath and Dr. Marianne Böni-Schnetzler for supervising my thesis and for reviewing this this manuscript. Thirdly, I would like to thank the whole Donath Research group for the interesting research environment.

A special thank you goes to Prof. Ed Palmer. You are an inspiring scientist and a great and kind person. It was an honor to have you in my thesis committee. I wish you all the best for the days after "competitive science". May all your wishes be fulfilled.

Walking down this road would not have been possible without the endless help of Prof. Christoph Hess. You are an inspiring role model in both private and scientific matters and I truly hope that our paths will cross again. I cannot thank you enough.

The completion of this PhD thesis would not have been possible without the support of my loving parents. You mean the world to me.

The last word of acknowledgment goes to my wife Corinne and son Amit. Words cannot match the extent of my gratitude. You truly make me the luckiest person on earth.

References

[1] Fu Z, Gilbert ER, Liu D (2013) Regulation of insulin synthesis and secretion and pancreatic Beta-cell dysfunction in diabetes. Curr Diabetes Rev 9: 25-53
[2] De Vos A, Heimberg H, Quartier E, et al. (1995) Human and rat beta cells differ in glucose transporter but not in glucokinase gene expression. J Clin Invest 96: 2489-2495
[3] Ferrer J, Benito C, Gomis R (1995) Pancreatic islet GLUT2 glucose transporter mRNA and protein expression in humans with and without NIDDM. Diabetes 44: 1369-1374
[4] Iynedjian PB, Mobius G, Seitz HJ, Wollheim CB, Renold AE (1986) Tissue-specific expression of glucokinase: identification of the gene product in liver and pancreatic islets. Proc Natl Acad Sci U S A 83: 1998-2001
[5] Jetton TL, Liang Y, Pettepher CC, et al. (1994) Analysis of upstream glucokinase promoter activity in transgenic mice and identification of glucokinase in rare neuroendocrine cells in the brain and gut. J Biol Chem 269: 3641-3654
[6] McIntyre N, Holdsworth CD, Turner DS (1964) New Interpretation of Oral Glucose Tolerance. Lancet 2: 20-21
[7] Dupre J, Ross SA, Watson D, Brown JC (1973) Stimulation of insulin secretion by gastric inhibitory polypeptide in man. J Clin Endocrinol Metab 37: 826-828
[8] Kreymann B, Williams G, Ghatei MA, Bloom SR (1987) Glucagon-like peptide-1 7-36: a physiological incretin in man. Lancet 2: 1300-1304
[9] Ellingsgaard H, Hauselmann I, Schuler B, et al. (2011) Interleukin-6 enhances insulin secretion by increasing glucagon-like peptide-1 secretion from L cells and alpha cells. Nat Med 17: 1481-1489
[10] Sener A, Malaisse WJ (1980) L-leucine and a nonmetabolized analogue activate pancreatic islet glutamate dehydrogenase. Nature 288: 187-189
[11] Nolan CJ, Madiraju MS, Delghingaro-Augusto V, Peyot ML, Prentki M (2006) Fatty acid signaling in the beta-cell and insulin secretion. Diabetes 55 Suppl 2: S16-23
[12] Zhao FQ, Keating AF (2007) Functional properties and genomics of glucose transporters. Curr Genomics 8: 113-128
[13] Guo S (2014) Insulin signaling, resistance, and the metabolic syndrome: insights from mouse models into disease mechanisms. J Endocrinol 220: T1-T23
[14] Guo S, Rena G, Cichy S, He X, Cohen P, Unterman T (1999) Phosphorylation of serine 256 by protein kinase B disrupts transactivation by FKHR and mediates effects of insulin on insulin-like growth factor-binding protein-1 promoter activity through a conserved insulin response sequence. J Biol Chem 274: 17184-17192
[15] Gross DN, van den Heuvel AP, Birnbaum MJ (2008) The role of FoxO in the regulation of metabolism. Oncogene 27: 2320-2336
[16] Thorens B, Mueckler M (2010) Glucose transporters in the 21st Century. Am J Physiol Endocrinol Metab 298: E141-145

[17] Carruthers A, DeZutter J, Ganguly A, Devaskar SU (2009) Will the original glucose transporter isoform please stand up! Am J Physiol Endocrinol Metab 297: E836-848
[18] Thorens B, Guillam MT, Beermann F, Burcelin R, Jaquet M (2000) Transgenic reexpression of GLUT1 or GLUT2 in pancreatic beta cells rescues GLUT2-null mice from early death and restores normal glucose-stimulated insulin secretion. J Biol Chem 275: 23751-23758
[19] Bryant NJ, Govers R, James DE (2002) Regulated transport of the glucose transporter GLUT4. Nat Rev Mol Cell Biol 3: 267-277
[20] Organization WH (Accessed November 28, 2015) Fact sheet: obesity and overweight
[21] Pessin JE, Saltiel AR (2000) Signaling pathways in insulin action: molecular targets of insulin resistance. J Clin Invest 106: 165-169
[22] Cusi K, Maezono K, Osman A, et al. (2000) Insulin resistance differentially affects the PI 3-kinase- and MAP kinase-mediated signaling in human muscle. J Clin Invest 105: 311-320
[23] Aguirre V, Werner ED, Giraud J, Lee YH, Shoelson SE, White MF (2002) Phosphorylation of Ser307 in insulin receptor substrate-1 blocks interactions with the insulin receptor and inhibits insulin action. J Biol Chem 277: 1531-1537
[24] Asante-Appiah E, Kennedy BP (2003) Protein tyrosine phosphatases: the quest for negative regulators of insulin action. Am J Physiol Endocrinol Metab 284: E663-670
[25] Fraze E, Donner CC, Swislocki AL, Chiou YA, Chen YD, Reaven GM (1985) Ambient plasma free fatty acid concentrations in noninsulin-dependent diabetes mellitus: evidence for insulin resistance. J Clin Endocrinol Metab 61: 807-811
[26] Hotamisligil GS, Shargill NS, Spiegelman BM (1993) Adipose expression of tumor necrosis factor-alpha: direct role in obesity-linked insulin resistance. Science 259: 87-91
[27] Shoelson SE, Lee J, Goldfine AB (2006) Inflammation and insulin resistance. J Clin Invest 116: 1793-1801
[28] Weisberg SP, McCann D, Desai M, Rosenbaum M, Leibel RL, Ferrante AW, Jr. (2003) Obesity is associated with macrophage accumulation in adipose tissue. J Clin Invest 112: 1796-1808
[29] Yuan M, Konstantopoulos N, Lee J, et al. (2001) Reversal of obesity- and diet-induced insulin resistance with salicylates or targeted disruption of Ikkbeta. Science 293: 1673-1677
[30] Micossi P, Pontiroli AE, Baron SH, et al. (1978) Aspirin stimulates insulin and glucagon secretion and increases glucose tolerance in normal and diabetic subjects. Diabetes 27: 1196-1204
[31] Pal D, Dasgupta S, Kundu R, et al. (2012) Fetuin-A acts as an endogenous ligand of TLR4 to promote lipid-induced insulin resistance. Nat Med 18: 1279-1285
[32] Lee JY, Sohn KH, Rhee SH, Hwang D (2001) Saturated fatty acids, but not unsaturated fatty acids, induce the expression of cyclooxygenase-2 mediated through Toll-like receptor 4. J Biol Chem 276: 16683-16689
[33] Huh JY, Park YJ, Ham M, Kim JB (2014) Crosstalk between adipocytes and immune cells in adipose tissue inflammation and metabolic dysregulation in obesity. Mol Cells 37: 365-371

[34] Cinti S, Mitchell G, Barbatelli G, et al. (2005) Adipocyte death defines macrophage localization and function in adipose tissue of obese mice and humans. J Lipid Res 46: 2347-2355
[35] Nguyen MT, Favelyukis S, Nguyen AK, et al. (2007) A subpopulation of macrophages infiltrates hypertrophic adipose tissue and is activated by free fatty acids via Toll-like receptors 2 and 4 and JNK-dependent pathways. J Biol Chem 282: 35279-35292
[36] Hotamisligil GS (2010) Endoplasmic reticulum stress and the inflammatory basis of metabolic disease. Cell 140: 900-917
[37] Xu H, Barnes GT, Yang Q, et al. (2003) Chronic inflammation in fat plays a crucial role in the development of obesity-related insulin resistance. J Clin Invest 112: 1821-1830
[38] Nieto-Vazquez I, Fernandez-Veledo S, Kramer DK, Vila-Bedmar R, Garcia-Guerra L, Lorenzo M (2008) Insulin resistance associated to obesity: the link TNF-alpha. Arch Physiol Biochem 114: 183-194
[39] Fleischman A, Shoelson SE, Bernier R, Goldfine AB (2008) Salsalate improves glycemia and inflammatory parameters in obese young adults. Diabetes Care 31: 289-294
[40] Deodhar SD, McLeod MM, Dick WC, Buchanan WW (1977) A short-term comparative trial of salsalate and indomethacin in rheumatoid arthritis. Curr Med Res Opin 5: 185-188
[41] Jung TW, Choi HY, Lee SY, et al. (2013) Salsalate and Adiponectin Improve Palmitate-Induced Insulin Resistance via Inhibition of Selenoprotein P through the AMPK-FOXO1alpha Pathway. PLoS One 8: e66529
[42] Herrero L, Shapiro H, Nayer A, Lee J, Shoelson SE (2010) Inflammation and adipose tissue macrophages in lipodystrophic mice. Proc Natl Acad Sci U S A 107: 240-245
[43] Nixon M, Wake DJ, Livingstone DE, et al. (2012) Salicylate downregulates 11beta-HSD1 expression in adipose tissue in obese mice and in humans, mediating insulin sensitization. Diabetes 61: 790-796
[44] van Dam AD, Nahon KJ, Kooijman S, et al. (2015) Salsalate activates brown adipose tissue in mice. Diabetes 64: 1544-1554
[45] Hawley SA, Fullerton MD, Ross FA, et al. (2012) The ancient drug salicylate directly activates AMP-activated protein kinase. Science 336: 918-922
[46] Donath MY (2014) Targeting inflammation in the treatment of type 2 diabetes: time to start. Nat Rev Drug Discov 13: 465-476
[47] Fang F, Lu Y, Ma DL, Du TT, Shao SY, Yu XF (2013) A meta-analysis of salicylates for type 2 diabetes mellitus. J Huazhong Univ Sci Technolog Med Sci 33: 1-14
[48] Schmoldt A, Benthe HF, Haberland G (1975) Digitoxin metabolism by rat liver microsomes. Biochem Pharmacol 24: 1639-1641
[49] Uysal KT, Wiesbrock SM, Marino MW, Hotamisligil GS (1997) Protection from obesity-induced insulin resistance in mice lacking TNF-alpha function. Nature 389: 610-614
[50] Ofei F, Hurel S, Newkirk J, Sopwith M, Taylor R (1996) Effects of an engineered human anti-TNF-alpha antibody (CDP571) on insulin sensitivity and glycemic control in patients with NIDDM. Diabetes 45: 881-885
[51] Paquot N, Castillo MJ, Lefebvre PJ, Scheen AJ (2000) No increased insulin sensitivity after a single intravenous administration of a recombinant human

tumor necrosis factor receptor: Fc fusion protein in obese insulin-resistant patients. J Clin Endocrinol Metab 85: 1316-1319
[52] Dominguez H, Storgaard H, Rask-Madsen C, et al. (2005) Metabolic and vascular effects of tumor necrosis factor-alpha blockade with etanercept in obese patients with type 2 diabetes. J Vasc Res 42: 517-525
[53] Stanley TL, Zanni MV, Johnsen S, et al. (2011) TNF-alpha antagonism with etanercept decreases glucose and increases the proportion of high molecular weight adiponectin in obese subjects with features of the metabolic syndrome. J Clin Endocrinol Metab 96: E146-150
[54] Yazdani-Biuki B, Stelzl H, Brezinschek HP, et al. (2004) Improvement of insulin sensitivity in insulin resistant subjects during prolonged treatment with the anti-TNF-alpha antibody infliximab. Eur J Clin Invest 34: 641-642
[55] Marra M, Campanati A, Testa R, et al. (2007) Effect of etanercept on insulin sensitivity in nine patients with psoriasis. Int J Immunopathol Pharmacol 20: 731-736
[56] O'Rahilly SP, Nugent Z, Rudenski AS, et al. (1986) Beta-cell dysfunction, rather than insulin insensitivity, is the primary defect in familial type 2 diabetes. Lancet 2: 360-364
[57] Weyer C, Bogardus C, Mott DM, Pratley RE (1999) The natural history of insulin secretory dysfunction and insulin resistance in the pathogenesis of type 2 diabetes mellitus. J Clin Invest 104: 787-794
[58] Butler AE, Janson J, Bonner-Weir S, Ritzel R, Rizza RA, Butler PC (2003) Beta-cell deficit and increased beta-cell apoptosis in humans with type 2 diabetes. Diabetes 52: 102-110
[59] Sakuraba H, Mizukami H, Yagihashi N, Wada R, Hanyu C, Yagihashi S (2002) Reduced beta-cell mass and expression of oxidative stress-related DNA damage in the islet of Japanese Type II diabetic patients. Diabetologia 45: 85-96
[60] Yoon KH, Ko SH, Cho JH, et al. (2003) Selective beta-cell loss and alpha-cell expansion in patients with type 2 diabetes mellitus in Korea. J Clin Endocrinol Metab 88: 2300-2308
[61] Diabetes Genetics Initiative of Broad Institute of H, Mit LU, Novartis Institutes of BioMedical R, et al. (2007) Genome-wide association analysis identifies loci for type 2 diabetes and triglyceride levels. Science 316: 1331-1336
[62] Billings LK, Florez JC (2010) The genetics of type 2 diabetes: what have we learned from GWAS? Ann N Y Acad Sci 1212: 59-77
[63] Scott LJ, Mohlke KL, Bonnycastle LL, et al. (2007) A genome-wide association study of type 2 diabetes in Finns detects multiple susceptibility variants. Science 316: 1341-1345
[64] Sladek R, Rocheleau G, Rung J, et al. (2007) A genome-wide association study identifies novel risk loci for type 2 diabetes. Nature 445: 881-885
[65] Moltke I, Grarup N, Jorgensen ME, et al. (2014) A common Greenlandic TBC1D4 variant confers muscle insulin resistance and type 2 diabetes. Nature 512: 190-193
[66] Tabak AG, Jokela M, Akbaraly TN, Brunner EJ, Kivimaki M, Witte DR (2009) Trajectories of glycaemia, insulin sensitivity, and insulin secretion before diagnosis of type 2 diabetes: an analysis from the Whitehall II study. Lancet 373: 2215-2221

[67] Pick A, Clark J, Kubstrup C, et al. (1998) Role of apoptosis in failure of beta-cell mass compensation for insulin resistance and beta-cell defects in the male Zucker diabetic fatty rat. Diabetes 47: 358-364
[68] Dalboge LS, Almholt DL, Neerup TS, et al. (2013) Characterisation of age-dependent beta cell dynamics in the male db/db mice. PLoS One 8: e82813
[69] Talchai C, Xuan S, Lin HV, Sussel L, Accili D (2012) Pancreatic beta cell dedifferentiation as a mechanism of diabetic beta cell failure. Cell 150: 1223-1234
[70] Bernardo AS, Hay CW, Docherty K (2008) Pancreatic transcription factors and their role in the birth, life and survival of the pancreatic beta cell. Mol Cell Endocrinol 294: 1-9
[71] Lubaina S. Presswala BaJHS (2011) Intensive Insulin Therapy as the Primary Treatment for Type 2 Diabetes. Clinical Diabetes 29: 151-153
[72] Wang Z, York NW, Nichols CG, Remedi MS (2014) Pancreatic beta cell dedifferentiation in diabetes and redifferentiation following insulin therapy. Cell Metab 19: 872-882
[73] Guo S, Dai C, Guo M, et al. (2013) Inactivation of specific beta cell transcription factors in type 2 diabetes. J Clin Invest 123: 3305-3316
[74] Jonas JC, Sharma A, Hasenkamp W, et al. (1999) Chronic hyperglycemia triggers loss of pancreatic beta cell differentiation in an animal model of diabetes. J Biol Chem 274: 14112-14121
[75] Bonner-Weir S, Trent DF, Weir GC (1983) Partial pancreatectomy in the rat and subsequent defect in glucose-induced insulin release. J Clin Invest 71: 1544-1553
[76] Pi J, Bai Y, Zhang Q, et al. (2007) Reactive oxygen species as a signal in glucose-stimulated insulin secretion. Diabetes 56: 1783-1791
[77] Robertson RP (2004) Chronic oxidative stress as a central mechanism for glucose toxicity in pancreatic islet beta cells in diabetes. J Biol Chem 279: 42351-42354
[78] Grankvist K, Marklund SL, Taljedal IB (1981) CuZn-superoxide dismutase, Mn-superoxide dismutase, catalase and glutathione peroxidase in pancreatic islets and other tissues in the mouse. Biochem J 199: 393-398
[79] Tiedge M, Lortz S, Drinkgern J, Lenzen S (1997) Relation between antioxidant enzyme gene expression and antioxidative defense status of insulin-producing cells. Diabetes 46: 1733-1742
[80] Lee YE, Kim JW, Lee EM, et al. (2012) Chronic resveratrol treatment protects pancreatic islets against oxidative stress in db/db mice. PLoS One 7: e50412
[81] Kaneto H, Xu G, Song KH, et al. (2001) Activation of the hexosamine pathway leads to deterioration of pancreatic beta-cell function through the induction of oxidative stress. J Biol Chem 276: 31099-31104
[82] Harmon JS, Bogdani M, Parazzoli SD, et al. (2009) beta-Cell-specific overexpression of glutathione peroxidase preserves intranuclear MafA and reverses diabetes in db/db mice. Endocrinology 150: 4855-4862
[83] Chen H, Karne RJ, Hall G, et al. (2006) High-dose oral vitamin C partially replenishes vitamin C levels in patients with Type 2 diabetes and low vitamin C levels but does not improve endothelial dysfunction or insulin resistance. Am J Physiol Heart Circ Physiol 290: H137-145

[84] Paolisso G, Balbi V, Volpe C, et al. (1995) Metabolic benefits deriving from chronic vitamin C supplementation in aged non-insulin dependent diabetics. J Am Coll Nutr 14: 387-392
[85] Cnop M, Abdulkarim B, Bottu G, et al. (2014) RNA sequencing identifies dysregulation of the human pancreatic islet transcriptome by the saturated fatty acid palmitate. Diabetes 63: 1978-1993
[86] Gremlich S, Bonny C, Waeber G, Thorens B (1997) Fatty acids decrease IDX-1 expression in rat pancreatic islets and reduce GLUT2, glucokinase, insulin, and somatostatin levels. J Biol Chem 272: 30261-30269
[87] Eguchi K, Manabe I, Oishi-Tanaka Y, et al. (2012) Saturated fatty acid and TLR signaling link beta cell dysfunction and islet inflammation. Cell Metab 15: 518-533
[88] Shen X, Yang L, Yan S, et al. (2015) Fetuin A promotes lipotoxicity in beta cells through the TLR4 signaling pathway and the role of pioglitazone in anti-lipotoxicity. Mol Cell Endocrinol 412: 1-11
[89] Ling Z, In't Veld PA, Pipeleers DG (1993) Interaction of interleukin-1 with islet beta-cells. Distinction between indirect, aspecific cytotoxicity and direct, specific functional suppression. Diabetes 42: 56-65
[90] Ling Z, Van de Casteele M, Eizirik DL, Pipeleers DG (2000) Interleukin-1beta-induced alteration in a beta-cell phenotype can reduce cellular sensitivity to conditions that cause necrosis but not to cytokine-induced apoptosis. Diabetes 49: 340-345
[91] Cardozo AK, Heimberg H, Heremans Y, et al. (2001) A comprehensive analysis of cytokine-induced and nuclear factor-kappa B-dependent genes in primary rat pancreatic beta-cells. J Biol Chem 276: 48879-48886
[92] Ortis F, Naamane N, Flamez D, et al. (2010) Cytokines interleukin-1beta and tumor necrosis factor-alpha regulate different transcriptional and alternative splicing networks in primary beta-cells. Diabetes 59: 358-374
[93] Moore F, Naamane N, Colli ML, et al. (2011) STAT1 is a master regulator of pancreatic {beta}-cell apoptosis and islet inflammation. J Biol Chem 286: 929-941
[94] Blum B, Roose AN, Barrandon O, et al. (2014) Reversal of beta cell de-differentiation by a small molecule inhibitor of the TGFbeta pathway. Elife 3: e02809
[95] Negi S, Jetha A, Aikin R, Hasilo C, Sladek R, Paraskevas S (2012) Analysis of beta-cell gene expression reveals inflammatory signaling and evidence of dedifferentiation following human islet isolation and culture. PLoS One 7: e30415
[96] Larsen CM, Faulenbach M, Vaag A, et al. (2007) Interleukin-1-receptor antagonist in type 2 diabetes mellitus. N Engl J Med 356: 1517-1526
[97] Weber A, Wasiliew P, Kracht M (2010) Interleukin-1 (IL-1) pathway. Sci Signal 3: cm1
[98] Ortis F, Pirot P, Naamane N, et al. (2008) Induction of nuclear factor-kappaB and its downstream genes by TNF-alpha and IL-1beta has a pro-apoptotic role in pancreatic beta cells. Diabetologia 51: 1213-1225
[99] Maedler K, Sergeev P, Ris F, et al. (2002) Glucose-induced beta cell production of IL-1beta contributes to glucotoxicity in human pancreatic islets. J Clin Invest 110: 851-860

[100] Boni-Schnetzler M, Boller S, Debray S, et al. (2009) Free fatty acids induce a proinflammatory response in islets via the abundantly expressed interleukin-1 receptor I. Endocrinology 150: 5218-5229
[101] Oslowski CM, Hara T, O'Sullivan-Murphy B, et al. (2012) Thioredoxin-interacting protein mediates ER stress-induced beta cell death through initiation of the inflammasome. Cell Metab 16: 265-273
[102] Opie EL (1901) On the Relation of Chronic Interstitial Pancreatitis to the Islands of Langerhans and to Diabetes Melutus. J Exp Med 5: 397-428
[103] Westermark P, Andersson A, Westermark GT (2011) Islet amyloid polypeptide, islet amyloid, and diabetes mellitus. Physiol Rev 91: 795-826
[104] German MS, Moss LG, Wang J, Rutter WJ (1992) The insulin and islet amyloid polypeptide genes contain similar cell-specific promoter elements that bind identical beta-cell nuclear complexes. Mol Cell Biol 12: 1777-1788
[105] Masters SL, Dunne A, Subramanian SL, et al. (2010) Activation of the NLRP3 inflammasome by islet amyloid polypeptide provides a mechanism for enhanced IL-1beta in type 2 diabetes. Nat Immunol 11: 897-904
[106] Westwell-Roper CY, Ehses JA, Verchere CB (2014) Resident macrophages mediate islet amyloid polypeptide-induced islet IL-1beta production and beta-cell dysfunction. Diabetes 63: 1698-1711
[107] Larsen CM, Faulenbach M, Vaag A, Ehses JA, Donath MY, Mandrup-Poulsen T (2009) Sustained effects of interleukin-1 receptor antagonist treatment in type 2 diabetes. Diabetes Care 32: 1663-1668
[108] Cavelti-Weder C, Babians-Brunner A, Keller C, et al. (2012) Effects of gevokizumab on glycemia and inflammatory markers in type 2 diabetes. Diabetes Care 35: 1654-1662
[109] Rissanen A, Howard CP, Botha J, Thuren T, Global I (2012) Effect of anti-IL-1beta antibody (canakinumab) on insulin secretion rates in impaired glucose tolerance or type 2 diabetes: results of a randomized, placebo-controlled trial. Diabetes Obes Metab 14: 1088-1096
[110] Sloan-Lancaster J, Abu-Raddad E, Polzer J, et al. (2013) Double-blind, randomized study evaluating the glycemic and anti-inflammatory effects of subcutaneous LY2189102, a neutralizing IL-1beta antibody, in patients with type 2 diabetes. Diabetes Care 36: 2239-2246
[111] Cavelti-Weder C, Timper K, Seelig E, et al. (2015) Development of an interleukin-1beta vaccine in patients with type 2 diabetes. Mol Ther
[112] Spinas GA, Palmer JP, Mandrup-Poulsen T, Andersen H, Nielsen JH, Nerup J (1988) The bimodal effect of interleukin 1 on rat pancreatic beta-cells--stimulation followed by inhibition--depends upon dose, duration of exposure, and ambient glucose concentration. Acta Endocrinol (Copenh) 119: 307-311
[113] Auer VJ, Janas E, Ninichuk V, et al. (2012) Extracellular factors and immunosuppressive drugs influencing insulin secretion of murine islets. Clin Exp Immunol 170: 238-247
[114] Maedler K, Schumann DM, Sauter N, et al. (2006) Low concentration of interleukin-1beta induces FLICE-inhibitory protein-mediated beta-cell proliferation in human pancreatic islets. Diabetes 55: 2713-2722
[115] Scheller J, Chalaris A, Schmidt-Arras D, Rose-John S (2011) The pro- and anti-inflammatory properties of the cytokine interleukin-6. Biochim Biophys Acta 1813: 878-888

[116] Kishimoto T (2010) IL-6: from its discovery to clinical applications. Int Immunol 22: 347-352
[117] Pedersen BK, Febbraio MA (2012) Muscles, exercise and obesity: skeletal muscle as a secretory organ. Nat Rev Endocrinol 8: 457-465
[118] Benrick A, Wallenius V, Asterholm IW (2012) Interleukin-6 mediates exercise-induced increase in insulin sensitivity in mice. Experimental physiology 97: 1224-1235
[119] Geiger T, Towbin H, Cosenti-Vargas A, et al. (1993) Neutralization of interleukin-1 beta activity in vivo with a monoclonal antibody alleviates collagen-induced arthritis in DBA/1 mice and prevents the associated acute-phase response. Clin Exp Rheumatol 11: 515-522
[120] Nathan DM (2015) Diabetes: Advances in Diagnosis and Treatment. JAMA 314: 1052-1062
[121] Back SH, Kaufman RJ (2012) Endoplasmic reticulum stress and type 2 diabetes. Annu Rev Biochem 81: 767-793
[122] Sauter NS, Schulthess FT, Galasso R, Castellani LW, Maedler K (2008) The antiinflammatory cytokine interleukin-1 receptor antagonist protects from high-fat diet-induced hyperglycemia. Endocrinology 149: 2208-2218
[123] Butcher MJ, Hallinger D, Garcia E, et al. (2014) Association of proinflammatory cytokines and islet resident leucocytes with islet dysfunction in type 2 diabetes. Diabetologia 57: 491-501
[124] Chan JY, Luzuriaga J, Bensellam M, Biden TJ, Laybutt DR (2013) Failure of the adaptive unfolded protein response in islets of obese mice is linked with abnormalities in beta-cell gene expression and progression to diabetes. Diabetes 62: 1557-1568
[125] Kooptiwut S, Zraika S, Thorburn AW, et al. (2002) Comparison of insulin secretory function in two mouse models with different susceptibility to beta-cell failure. Endocrinology 143: 2085-2092
[126] Porta M, Curletto G, Cipullo D, et al. (2014) Estimating the delay between onset and diagnosis of type 2 diabetes from the time course of retinopathy prevalence. Diabetes Care 37: 1668-1674
[127] Harris MI, Klein R, Welborn TA, Knuiman MW (1992) Onset of NIDDM occurs at least 4-7 yr before clinical diagnosis. Diabetes Care 15: 815-819
[128] Venegas-Pont M, Manigrasso MB, Grifoni SC, et al. (2010) Tumor necrosis factor-alpha antagonist etanercept decreases blood pressure and protects the kidney in a mouse model of systemic lupus erythematosus. Hypertension 56: 643-649
[129] Omote K, Gohda T, Murakoshi M, et al. (2014) Role of the TNF pathway in the progression of diabetic nephropathy in KK-A(y) mice. Am J Physiol Renal Physiol 306: F1335-1347
[130] Chakravarthy H, Beli E, Navitskaya S, et al. (2016) Imbalances in Mobilization and Activation of Pro-Inflammatory and Vascular Reparative Bone Marrow-Derived Cells in Diabetic Retinopathy. PLoS One 11: e0146829
[131] Wada J, Makino H (2013) Inflammation and the pathogenesis of diabetic nephropathy. Clin Sci (Lond) 124: 139-152
[132] Herder C, Lankisch M, Ziegler D, et al. (2009) Subclinical inflammation and diabetic polyneuropathy: MONICA/KORA Survey F3 (Augsburg, Germany). Diabetes Care 32: 680-682

[133] Osborn O, Brownell SE, Sanchez-Alavez M, Salomon D, Gram H, Bartfai T (2008) Treatment with an Interleukin 1 beta antibody improves glycemic control in diet-induced obesity. Cytokine 44: 141-148
[134] Seok J, Warren HS, Cuenca AG, et al. (2013) Genomic responses in mouse models poorly mimic human inflammatory diseases. Proc Natl Acad Sci U S A 110: 3507-3512
[135] Eming SA, Krieg T, Davidson JM (2007) Inflammation in wound repair: molecular and cellular mechanisms. J Invest Dermatol 127: 514-525
[136] Gamelli RL, Liu H, He LK, Hofmann CA (1996) Augmentations of glucose uptake and glucose transporter-1 in macrophages following thermal injury and sepsis in mice. J Leukoc Biol 59: 639-647
[137] Norlin S, Ahlgren U, Edlund H (2005) Nuclear factor-{kappa}B activity in {beta}-cells is required for glucose-stimulated insulin secretion. Diabetes 54: 125-132
[138] Eckardt K, Gorgens SW, Raschke S, Eckel J (2014) Myokines in insulin resistance and type 2 diabetes. Diabetologia 57: 1087-1099
[139] Febbraio MA, Pedersen BK (2002) Muscle-derived interleukin-6: mechanisms for activation and possible biological roles. FASEB journal : official publication of the Federation of American Societies for Experimental Biology 16: 1335-1347
[140] Stienstra R, Joosten LA, Koenen T, et al. (2010) The inflammasome-mediated caspase-1 activation controls adipocyte differentiation and insulin sensitivity. Cell metabolism 12: 593-605
[141] Whitham M, Chan MH, Pal M, et al. (2012) Contraction-induced interleukin-6 gene transcription in skeletal muscle is regulated by c-Jun terminal kinase/activator protein-1. The Journal of biological chemistry 287: 10771-10779
[142] Cavelti-Weder C, Furrer R, Keller C, et al. (2011) Inhibition of IL-1beta improves fatigue in type 2 diabetes. Diabetes care 34: e158
[143] Cambronero JC, Rivas FJ, Borrell J, Guaza C (1992) Interleukin-1-beta induces pituitary adrenocorticotropin secretion: evidence for glucocorticoid modulation. Neuroendocrinology 55: 648-654
[144] Penner IK, Bechtel N, Raselli C, et al. (2007) Fatigue in multiple sclerosis: relation to depression, physical impairment, personality and action control. Mult Scler 13: 1161-1167
[145] Benedict RH, Duquin JA, Jurgensen S, et al. (2008) Repeated assessment of neuropsychological deficits in multiple sclerosis using the Symbol Digit Modalities Test and the MS Neuropsychological Screening Questionnaire. Mult Scler 14: 940-946
[146] Hung AM, Ellis CD, Shintani A, Booker C, Ikizler TA (2011) IL-1beta receptor antagonist reduces inflammation in hemodialysis patients. Journal of the American Society of Nephrology : JASN 22: 437-442
[147] Wallenius V, Wallenius K, Ahren B, et al. (2002) Interleukin-6-deficient mice develop mature-onset obesity. Nat Med 8: 75-79
[148] Pedersen BK, Hoffman-Goetz L (2000) Exercise and the immune system: regulation, integration, and adaptation. Physiological reviews 80: 1055-1081